BIOCHEMICAL FUNCTIONS OF C-TERMINAL BINDING PROTEINS: THEIR ROLE IN SHORT-RANGE REPRESSION AND DIMERIZATION

By

Damian Emil Curtis

A DISSERTATION

Presented to the Department of Biochemistry and Molecular Biology

and the Oregon Health and Sciences University

School of Medicine

in partial fulfillment of the requirements for the degree of

Doctor of Philosophy

April 26th 2011

School of Medicine

Oregon Health and Sciences University

CERTIFICATE OF APPROVAL

This is to certify that the Ph.D. thesis of

Damian Emil Curtis

has been approved

_____

Professor in charge of thesis

_____

Member

_____

Member

_____

Member

_____

Member

_____

Member

TABLE OF CONTENTS

List of Tables and Figures

Acknowledgements

None of the work that I present in the forthcoming thesis would have been possible without the support of Dr. James Lundblad. For more than five years he provided me with a lab, equipment, mentoring, and support. I am forever indebted to Jim for providing the opportunity to work with him and learn from him as I completed the work described in this thesis. Thank you Jim. I hope you understand that I did the very best job I could do given the circumstances.

I am also grateful to the other members of the Lundblad lab. To Dr. Dana Madison, who probably is happy that he no longer has to remember the dilution for random antibodies, I appreciate all the scientific help, the open office door, and sympathetic ear. To Dr. Sarah Smolik, who I hope will forgive me at some point for taking so damn long to write this, I am indebted for the hours in the fly lab with me, answering my many "stupid" fly cross questions, collecting virgins, talking politics and books (hopefully I'll now have time to read some of those), swapping Mailee and Collin stories for dog stories, and for serving as my genetics mentor even though no one ever asked her to and the benefits were few and far between. To Dr. Maureen Hoatlin without whom I would not be sitting here writing today. Maureen provided encouraging words, helpful ideas, pragmatism, and a genuine concern, which I am not sure I deserved, and for that I will always be indebted. Thank you to Dr. Ujwal Shinde for assistance with the homology modeling and Circular Dichroism experiments. To Dr.'s Matt Thayer and Dave Farrens, who not only serve on my committee but also took the time to care about me and the work that I've done, thank you. It means so very much and I will never forget any of you.

Also a huge Thank You to Aaron, Garth, George, Diana, Kiyoko, Mom, Annie, Kirsten, Christina, Abhinav, Judy, and Jackie P, you all helped in special ways and made this possible. From step one my best friend has been with me and I will never be able to explain how grateful I am for that. She was my constant companion, my "co-pilot", my sounding board, and my support. Thank you Misaki, you made it all possible and I hope you are happy to have done so. Along the way we picked up a couple hitchhikers and, though they do not understand it now, they too had an important role to play. In many ways this was all for Mailee and Collin, and I hope someday they will appreciate that.

Finally, I would like to dedicate this work to my father. The words don't exist to show my appreciation for all the support you've given me over the years. I truly would never have made it to this point without your love, honesty, support, and showing me what it means to work hard. Thank you and I love you Dad.

Abstract

This thesis examines the biochemical functions of the family of Carboxyl-terminal Binding Proteins (CtBP). CtBPs are co-repressors that exert their repressive effects by interacting with coenzymes, DNA-binding transcription factors, and chromatin interacting complexes. CtBPs are implicated in essential developmental processes and cancer biology and represent an important class of multifunctional biological molecules. This work employs two distinct biologically relevant *in vivo* assays utilizing the *Drosophila* form of CtBP to examine the essential requirements for coordinating short-range repression during embryogenesis. In addition, biochemical characterizations and in vitro assays increase the understanding of distinct biochemical domains within CtBP family members and the roles they play in transcriptional regulation and invertebrate development. . In order to address the ongoing issue of the relative importance of dinucleotide binding, putative dehydrogenase enzyme activity, and oligomeric state of an active CtBP protein, we examined wild type and mutant forms of the *Drosophila* CtBP in the *Drosophila* embryo where it normally plays a well understood biological function. Specifically we established an assay to monitor short-range repression at the *eve* locus by inserting DNA elements of our own making into a dCtBP null embryo. With these assays we determined that short-range repression is dependent on a CtBP which retains the ability to bind to dinucleotide but can still function in the absence of dehydrogenase activity. The requirement of dinucleotide binding is most likely due to an inability to form homodimers at the site of repression. The reliability of our *in vivo* data is high not only because of the system in which we evaluated activity, but each of our mutant

proteins was assessed for unwanted deleterious effects on the overall protein and/or disruption of biological activities associated with other CtBP functional domains.

Chapter 1. Introduction

Discovery of C-terminal Binding Protein Family

The general transcriptional co-repressor Carboxyl-terminal Binding Protein 1 (CtBP1) was originally identified as a binding partner for the adenoviral transforming protein E1A (1). DNA tumor viruses target cellular transcription factors, which disrupts normal cell cycle control mechanisms, leading to cellular transformation. E1A mutants that fail to sequester CtBP1 have enhanced oncogenicity, suggesting that the normal function of CtBP1 in mammalian cells is to repress the tumor suppressive activities of E1A targets such as CBP/P300 and the retinoblastoma (pRB) protein, and may also influence these processes by its role as a transcription factor. CtBP1 and other family members function as transcriptional co-repressors which mediate the activities of a number of cellular sequence-specific DNA-binding repressors and other proteins that function as silencers of transcription. In fact, many studies have linked CtBP1 to the repression of genes implicated in controlling cellular proliferation, apoptosis, cell-cell adhesion, and tumor invasiveness (2,3).

Shortly after the identification of CtBP1, a second mammalian CtBP isoform (CtBP2) was identified in a yeast two-hybrid screen for co-repressors of the E-box binding factor, δEF1/ZEB (4). Subsequently, CtBP homologues have been implicated as co-factors for a number of cellular transcriptional repressors, including DNA binding proteins involved in development, and also co-regulatory molecules such as C-terminal Interacting Protein (CtIP) and the nuclear hormone receptor co-repressor RIP140 (5,6). Vertebrates have two highly related but distinct genes that encode both isoforms, but the invertebrates *Drosophila melanogaster* and *Caenorhabtitus elegans* have only a single

CtBP gene (5). All known CtBP target proteins contain some form of the motif PxDLS (where x is any amino acid), and this is necessary for binding to CtBPs (Figure 1.1A and B). Removal or alteration of the PxDLS motif abrogates CtBP binding and, at least partially, the transcriptional repressive activities of these proteins.

CtBP proteins have some unusual characteristics; in particular, the family members lack common features found in other transcriptional regulatory proteins, and yet have striking primary sequence and structural similarity to the D-isomer specific 2-hydroxyacid dehydrogenase class of enzymes. In addition, CtBP homologs appear to have both cytoplasmic and nuclear functions. Cytoplasmic or non-nuclear functions are postulated based on the observation that the Brefeldin A ribosylation substrate (BARS-50) is nearly identical to CtBP1 (7). BARS-50 is a component of the Golgi tubule fission complex and has subsequently come to be known as CtBP3 or CtBP1-S since it is a shorter form of CtBP1 that is derived from the same genetic locus. Also, a splice variant of CtBP2 called RIBEYE has been found to be a component of the ribbon synapse, which resides outside the nucleus (8). Studies in mammalian cell lines aimed at comparing the two CtBP isoforms have not demonstrated consistent functional differences either in vitro or *in vivo*; however, studies of knockout animals indicated that CtBP1 and CtBP2 have different roles in development. As illustrated by CtBP1 null mice, which were viable but small, while CtBP2 null mice showed severe defects in axial patterning and a recessive embryonic lethal phenotype (9). CtBP1 and CtBP2 were shown to functionally overlap, because both proteins demonstrated ubiquitous and overlapping expression patterns during development (9); both equivalently influence transcription from responsive reporter constructs, and both appear to reside in the CtBP co-repressor complex purified

from HeLa (immortalized cervical cancer) cells (10). In addition, our laboratory and others have found that immunoprecipitation of each CtBP isoform individually co-purifies with the others, and that they heterodimerize in vitro (11,12, and our unpublished preliminary studies).

CtBP family members themselves exhibit striking similarities; however, there are important differences between each protein including evidence that posttranslational modifications such as phosphorylation and SUMOylation may determine CtBP1 localization (13,14) whereas acetylation of CtBP2 may be important for nuclear localization of CtBP2 (Figure 1.1A and 1.2). Unlike CtBP1, it has been shown that CtBP2 has a unique nuclear localization signal (NLS) located within its N-terminal region, and this contributes to its nuclear accumulation (12). CtBP2 appears to reside almost exclusively in the nucleus whereas CtBP1 is distributed between the cytoplasm and nuclear compartments (Figure 1.2) (12,13,15). The functional consequences of localization in different compartments are unclear, since in some cases cytoplasmic localization leads to inactivation (14), whilst in others activation of repressor activity (15). Unlike CtBP2, CtBP1 has no identified NLS, and its mode of nuclear translocation is currently unknown. Investigators have recently suggested that nuclear localization is mediated through interactions with targets such as the transcription factor BKLF as well as through heterodimerization with CtBP2 (12). CtBP1 has also been shown to interact with neuronal nitric oxide synthase (nNOS) through its PDZ domain, and in cells over expressing both nNOS and CtBP1 the localization becomes primarily cytoplasmic (16).

Transcriptional co-repression

The CtBP family of proteins functions as transcriptional co-repressors, and it is well established that many transcriptional co-repressors recruit CtBP through PxDLS like motifs in order to coordinate repression of target genes (6). It does remain unclear how that repression is mediated, and it is likely to be dependent on the co-repressor and target gene. Nevertheless there are two primary models supported by the current literature. In the recruitment model, CtBP acts as a scaffold for the recruitment of other co-regulatory proteins. Data supporting this model include associations with histone deacetylases (reviewed in ref. 6), and a macromolecular co-repressor complex comprised of CtBP in association with histone modifying enzymes has been purified from HeLa cells (10). The purified complex includes many of the common players found in histone modifying complexes, including HDAC1and HDAC2, and histone methyltransferases G9a and Eu-HMTase, as well as the first histone demethylase, LSD1 (10). In the second model CtBP has intrinsic enzymatic activity which accounts for CtBP-dependent repression events that are HDAC independent (17,18). These HDAC independent repressive functions include, but are not limited to, epigenetic silencing and DNA methylation of the E-cadherin promoter mediated by the ZEB family of repressors, known targets of CtBP1.

In addition to the two models described above, quite a bit is known about CtBP dependent repression in the developing *Drosophila* embryo. *Drosophila* Carboxyl-terminal Binding Protein (dCtBP) has been shown to interact with several key repressors and is essential for their repressive activity. dCtBP-dependent repression in the *Drosophila* embryo has been termed short-range repression due to the short distances (100 bp) between regulatory elements, and short-range repression is a histone deacetylase

independent process (19). The molecular mechanism of this short-range repression is yet to be fully understood. In addition to its role in short-range repression, dCtBP plays an essential role in repression mediated by polycomb group proteins (PcG) by modulating its DNA-binding ability (20,21).

Role of Dinucleotide (NAD(H)) Binding

Recently studies have implicated NAD^+ and the reduced form NADH in several nuclear transactions. These transactions include NAD^+ serving as a recipient or donor of reducing equivalents, regulating the DNA binding molecules Clock-BMAL1 and NPAS-BMAL1 (22,23), being consumed (breakage of the N-glycosidic bond between nicotinamide and ADP-ribose) as part of the DNA-damage response pathways (24), and serving as a coenzyme to the protein deacetylase Sir2 (25). The transcriptional regulatory activity of CtBPs appears to be regulated in part by the dinucleotide coenzyme NAD(H) as well. NAD(H) stimulate dimerization as well as interaction with PxDLS containing target proteins such as *Krüppel*, E-cadherin, and adenovirus E1A (19). Some researchers have proposed that CtBP proteins act as redox sensors based upon an enhanced affinity for NADH versus NAD^+ (26), but we and others (27,28) do not detect any difference in affinity for NAD^+ versus NADH.

It is clear that NAD(H) not only plays an important role in the coordination of transcriptional repression, but also plays important structural functions. Within the CtBP proteins is a NAD(H) binding motif which has been termed the Rossman fold. This is a conserved structural domain with a $\beta\alpha\beta\alpha\beta$ topology. The Rossman fold contains a variant of the G/AxGxxG(17x)D phosphate binding motif (19) which interacts with the phosphate moiety of NAD. Incubation of CtBPs with NAD(H) decrease sensitivity to

limited proteolysis (26,27), which implies altered three-dimensional confirmation. At this point in time all but one of the CtBP crystal structures contain a bound form of NAD which presents difficulties when trying to compare these structures to *apo* forms. It is likely that NAD binding leads to a "closed" conformation through intersubunit interactions at the dimerization interface which could explain the decreased sensitivity to proteolysis (19).

Binding to NAD(H) has structural implications for CtBP proteins, but what are the functional consequences. It appears to be dependent on the biological system and/or the manner in which one measures CtBP functions such as binding to targets and mediating repression. The work described here as well as by others (27,29) supports the model that NAD(H) binding stimulates binding to target proteins by some as yet unknown mechanism, and yet there are other published reports (30) indicating that CtBPs binds to E1A with high affinity in the absence of dinucleotide. NAD-dependent repression also appears to be context and experiment dependent. The fusion of CtBP proteins to GAL4 in a heterologous system, thus bypassing the NAD-dependent recruitment, show conflicting results depending on the biological system and dinucleotide-binding mutant proteins used. For example a dCtBP NAD-binding mutant constructed as a GAL4-fusion does not repress a reporter construct in the *Drosophila* embryo, whereas in transient mammalian cell based expression systems point mutations in the NAD binding fold do not alter repression mediated by GAL4-CtBP (19).

Homology to D-isomer specific 2-hydroxyacid dehydrogenase enzymes

As mentioned above, CtBPs are unique among transcriptional regulators because they do not contain structural hallmarks of DNA-binding proteins, but instead have

remarkable primary sequence and structural similarity to the D-isomer specific 2-hydroxyacid dehydrogenase class of enzymes (Figure 1.3). D-2-hydroxyacid dehydrogenase enzymes are well characterized and known to exhibit catalytic activity through a "proton shuttle" between a histidine and a carboxylic acid containing residue such as glutamate or asparagine, which coordinates the transfer of a hydride ion between the substrate and a coenzyme such as the dinucleotide NAD(H) (19). In all D-2-hydroxyacid dehydrogenases, these residues are conserved and all mammalian CtBP orthologs as well as invertebrate CtBPs, such as dCtBP, contain corresponding residues which indicate that CtBPs might have substrate specific enzymatic activity. To date no definitive substrates for the dehydrogenase activity of CtBP have been found, but some researchers have measured weak dehydrogenase activity of human CtBP1 using pyruvate as a substrate (27,28). In these experiments oxidation of NADH to NAD^+ is measured by the loss of absorbance at 340 nm, but in order to see activity these researchers used extraordinarily high concentrations of CtBP leading to questions about the biological significance of these results. Whether or not CtBP-dependent transcriptional regulation requires enzymatic activity is not clear and appears to be context dependent. For instance, catalytic residue mutants in CtBP1 abolish the RIP140/CtBP-dependent repression events (27), but dCtBP/*Knirps* mediated repression in the *Drosophila* embryo are unaffected by changes in the catalytic domain (31). It is clear that, in large part because of its uniqueness, the putative dehydrogenase activity question remains the most tantalizing and difficult area of CtBP research. It is likely that enzymatic activity is specific, tightly regulated, and requires a cleverly designed, highly sensitive *in vivo* experiment to fully examine.

Three Dimensional Structure of CtBP

Despite the amino acid sequence and two-dimensional similarities between CtBP homologues and the well understood D-isomer specific 2-hydroxyacid dehydrogenases, deriving crystal structures for CtBPs has proved rather challenging. Our own attempts to crystalize dCtBP failed despite very highly concentrated pure protein. However; there are six crystallographically determined structures of CtBP homologs reported. One of these is a small domain from *C. elegans* CtBP and provides little overall structure information. The structure for the core domain of human CtBP1, refined to 1.95 angstrom (Å) (Protein Data Bank entry 1MX3) (27), demonstrates overall structural similarity to core domains found in the D-2-hydroxyacid dehydrogenases. In addition there are four structures derived from the rat protein CtBP/BARS either in the wild type or mutant form or in complex with NAD and/or peptides, (Protein Data Bank entries 1HKU, 3GA0, 1HL3, and 2HU2 respectively). The rat CtBP/BARS is very similar (97%) to human and mouse CtBP1, and the primary differences between these vertebrate homologs is found at the carboxyl-terminal and amino terminal ends of the protein neither of which are present in these structures. Both the human and rat crystal structures contain structural motifs which are very similar to the substrate-binding domain and nucleotide-binding domain found in D-2-hydroxyacid dehydrogenases (Figure 1.3 and Figure 1.4) (19).

Even in the absence of experimental data, this high level of similarity allows one to make some relatively safe conclusions about CtBP structure-function relationships. CtBP proteins likely homodimerize through the formation of a hydrophobic dimerization interface around the nucleotide-binding domain in an NAD(H) dependent manner as do dehydrogenase enzymes. This has been shown experimentally in ours and other labs, but

recent crystal data of an NAD(H) free mutant CtBP shows this rather definitively (32). As a homodimer, CtBP forms an elongated structure with two PxDLS containing target binding sites at opposite ends of each monomer (Figure 1.4). The amino and carboxyl terminal ends of CtBPs are not conserved at the same level as the core of the protein, but they make up the majority of the substrate-binding domain. The substrate binding domain is comprised of a discontinuous peptide sequence from both the amino and carboxyl terminus of the protein. This domain contains the necessary elements for recruitment of PxDLS-containing targets coordinated at opposite ends of the dimer pole and this discontinuity with the rest of the protein complicates the interpretation of single amino acid deletions. It is unclear whether or not single point mutations in the substrate binding domain alter the overall structural organization of the CtBP dimer (19). It is likely that the ends of each monomer are structured in a manner which we do not fully understand, and the three-dimensional coordination is vital to the interaction with a variety of both PxDLS-like motif containing proteins (Krüppel, Knirps, E1A, etc.) and non-PxDLS proteins (HDACs, etc.). This loose structural topology is found in other dehydrogenases and has at least two functional consequences. First, CtBP homodimers can bind to two different target proteins (both PxDLS containing and non-PxDLS proteins simultaneously) and fulfill a scaffolding role by assembling co-repressor complexes in conjunction with DNA binding proteins exemplified by CtBP recruitment of CtIP and its associated binding partners (33). Second, CtBP homodimers can bind to two different DNA-binding proteins simultaneously or interact with DNA transcription factors which function as homo or hetero dimers. Three dimensional structures also illuminate a potential catalytic site between the substrate-binding lobe and nucleotide-binding region.

This is the active site of catalysis in the D-2-hydroxyacid dehydrogenase enzymes and its conservation within the CtBP family of proteins fuels the search for a CtBP specific substrate. There is a clear link between structure and function with virtually all proteins, but, given the diversity of functions, it is an especially important part of understanding CtBP biology.

***Drosophila melanogaster* CtBP co-repressor**

As outlined above, *Drosophila melanogaster* contains a member of the CtBP family, generally referred to as *dCtBP*, which plays essential roles in embryogenesis, acts as a general transcriptional co-repressor with several transcriptional co-regulators, and partakes in Polycomb-mediated repression. *dCtBP* was identified by yeast two-hybrid screen shortly after hCtBP1 was identified and cloned. *dCtBP* mRNA is expressed at all developmental stages in *Drosophila*. Maternally expressed *dCtBP* is evenly distributed throughout the *Drosophila* embryo and contributes to establishing patterning along with zygotic *dCtBP* (34,35), this will be discussed in detail below.

dCtBP genes, proteins, and targets

Unlike humans and mice, *Drosophila* has a single copy of the *dCtBP* gene which resides cytologically at 87D8-87D9. By analyzing both *dCtBP* expressed sequence tags (ESTs) and the genome sequence, gene prediction tools initially identified a 386 amino acid protein with four splicing variants which are different at the 5' end of the mRNA (36). At least four (383 aa, 386 aa, 479 aa, and 382 aa) proteins have been identified in yeast two-hybrid screens (19). Like other CtBP family members, *dCtBP* isoforms have been shown to be important transcriptional co-repressors, all contain the GxGxxG

NAD(H) binding motif, have high sequence and structural similarities to D-isomer-specific 2-hydroxy acid dehydrogenases, and have the catalytic triad (arginine, glutamic acid, and histidine residues) required for dehydrogenase activity. dCtBP binds to PxDLS containing targets which include the transcription factors Snail, Knirps, Krüppel, Teashirt, and Hairless (19). Unlike its vertebrate homologs, dCtBP can bind, in vitro, to motifs other than PxDLS including the BTB domain, and related sequences, of the DNA-binding factor Tramtrack69, Hairy, E(spl)m delta, and E-APC (37). Of the four known isoforms, isoform A (dCtBP(s)) and Isoform E (dCtBP(l)) are the most abundant proteins in the adult fly as well as larval and embryonic stages (38). The short and long form (s and l, respectively) of dCtBP are virtually identical through most of the protein with the long form differing due to a long carboxyl-terminal extension (39) (Figure 2.2). There are several labs actively working to dissect the relevant differences between these two proteins, and although it was not the main focus of this work, the data in Chapter 4 contributes to that research.

Drosophila melanogaster Embryogenesis

Drosophila melanogaster is one of the most powerful and accessible model systems for studying an array of genetic and biochemical systems. This model organism has helped scientists genetically dissect pathways, understand tumor suppressor proteins such as p53, examine signal transduction pathways, break down neuronal networks, comprehend developmental processes, and much much more. During early fruit fly embryogenesis, a hierarchy of gene networks consisting of both maternal and zygotic proteins coordinates the proper patterning across the embryo and direct embryogenesis (19).

Proper development of multicellular organisms, such as fruit flies, requires coordination of developmental decisions and some of these essential decisions are orchestrated by morphogen gradients (40). Morphogens provide cells information about their position within a patterning field. Specifically, a morphogen is a diffusible signal produced in one part of the embryo. This signal determines cell fates based upon the concentration of said morphogen at a specific time and place. At the source of the morphogen, the concentration is the highest and cells within that area of influence will respond differently from cells which are exposed to a lower concentration of a morphogen. There are many examples of morphogens in *Drosophila* embryogenesis and they establish not only the patterning of the embryo but also the adult structures which will be derived from embryonic structures (40).

Within the first three hours of development, complex gene networks which consist of both maternal and zygotic genes progressively divide the embryo into increasingly precise segments (19) (Figure 1.5). Segmentation genes, which are expressed in domains or stripes, coordinate the correct development within their region of the embryo and a hierarchy is established in four steps. Step one in this hierarchy is the establishment of early spatial information by maternally expressed genes. These are genes that are expressed during oogenesis and whose proteins are stored in the egg. These proteins initiate the genetic cascades and are localized to specific regions of the egg. Prior to fertilization of the egg, signaling events have begun as the egg and follicle cells coordinate the reorganization of the cytoskeleton scaffold of the oocyte. This process requires maternally deposited *bicoid* and *nanos* mRNA from which protein is translated and localizes the scaffold to the anterior and posterior poles (40). The nucleus migrates

along the cytoskeleton and leads to determination of the dorsal side of the embryo by inhibiting the ventral signal emanating from the follicle cells.

Just after fertilization of the egg, *bicoid* and *nanos* mRNAs are translated and the proteins travel throughout the syncytium (sack of nuclei) and form long-range gradients (40). These essential transcriptional regulators control the translation of other mRNAs, such as *hunchback* and *caudal,* within the embryo. Since mRNAs for *hunchback* and *caudal* are evenly distributed throughout the embryo, *nanos* and *bicoid* can generate a protein gradient across the embryo (Figure 1.5). This occurs because *nanos*, the posterior determinant, represses the translation of *hunchback,* which results in a gradient of Hunchback protein with high concentrations at the anterior end steadily decreasing as one travels towards the posterior end. *Bicoid* represses *caudal* translation in a similar manner and establishes a posterior caudal gradient.

Step two in the hierarchy of segmentation involves the gap genes which further subdivide the embryo into broader domains. Unlike the maternal genes, these are zygotic genes (mRNA transcribed by embryonic DNA), but their expression is controlled by the maternal genes discussed above. Important gap genes include *giant, hunchback, knirps,* and *krüppel*. Most importantly, gap genes regulate each other in space and time. An example of this is the gap gene *krüppel* which is expressed exclusively in the central domain of the embryo. Expression at the anterior end is negatively controlled by *hunchback* and *knirps* exerts a similar effect at the posterior domain (40). In *krüppel* mutant embryos, the *giant* domain expands to the center of the embryo and *hunchback* expands posteriorly. This crosstalk further refines gap gene expression patterns beyond maternal gene control and increases the preciseness of segmentation.

The next step in the hierarchy involves the pair rule genes, which organize segments in a double periodicity; hence they are expressed in seven stripes which is half the number of segments in a wild-type embryo. The pair rule genes are split into two groups with the primary pair rule genes, such as *even skipped* (*eve*), *runt*, and *hairy*, translating spatial information from maternal and gap proteins into a striped pattern (40). Specifically *eve* regulation is complex and requires specific concentrations of maternal and gap genes. For example *krüppel* and *giant* repress *eve* stripe 2 and 5 whereas stripes 3,4,6, and 7 are regulated by different concentrations of *knirps* and *hunchback* (Figure 1.6). Secondary pair rule genes, such as *fushi tarazu*, are regulated by the primary pair rule genes. The patterns established by the pair rule genes change over time, are dynamic in nature, and represent interactions between both primary and secondary pair rule genes. The final steps in the hierarchy include the segment polarity genes, which are expressed in 14 stripes at the onset of gastrulation. As expression of the gap genes and pair rule genes fade away, segment polarity genes refine the striped pattern. Finally, homeotic genes distinguish different segments from each other. These genes determine whether a segment will develop into a wing or some other adult structure, and as one would expect, different homeotic genes are active in different segments (40). Through the complex coordination of maternal, gap, pair ruled, segment polarity, and homeotic gene products and their respective targets the *Drosophila* embryo properly develops from an uncoordinated mass of cells to an organized embryo poised to become an active larva.

Short-range transcriptional repression

Short-range transcriptional repression occurs over distances of less than 100 base pairs unlike transcriptional repression in the context of chromatin which may occur

thousands of bases away from the site of repression. This means that short-range repressors are able to inhibit adjacent activators provided they interact with the DNA within 100 bps of the enhancer site (41). During *Drosophila* embryogenesis gap genes exert influence over pair-rule genes often through short-range repression. For example, *eve* transcription is regulated throughout the developing embryo in this manner. The *eve* locus contains 5 enhancer regions which determine expression of one or two of the 7 *eve* stripes (42). Each enhancer is usually 300bp to 1kb in length and has binding sites for activators and repressors. Enhancers turn on *eve* transcription, in the absence of all repressors *eve* would be expressed throughout the embryo; the binding of repressors and short-range repression of the enhancers are responsible for turning *eve* off and the formation of seven segments with *eve* on alternatively with seven segments with *eve* off (Figure 3.2A). Like much of the transcriptional regulation during embryogenesis, repression of *eve* transcription is attained through concentration thresholds of repressors and enhancers (Figure 1.6). For example, maternal Bicoid is an enhancer of *eve* stripe 2 transcription whose concentration is highest at the anterior end and lowest at the posterior end of the embryo, is unable to drive *eve* transcription beyond the borders of stripe 2 due to the high concentrations of the repressors Giant and Krüppel (Figure 1.6 and 1.7).

The Krüppel protein mediates repression of *eve* stripe 2 in two ways, direct competition with Bicoid for shared sites and via short-range repression due to binding within 100 bp of the Bicoid binding sites. The latter is a dCtBP dependent process. dCtBP serves as the co-repressor to Krüppel in regulating the borders of *eve* stripe 2 transcription (43) (Figure 1.7). Further distinguishing this as short-range repression is the observation that even though Krüppel expression overlaps with *eve* stripe 3, there is no

repression because the stripe 3 enhancer element is beyond the range of this repression. Short-range repression functions independently of histone modifying enzymes such as histone deacetylases and histone methyltransferases. Short-range repression is an HDAC independent process because it occurs in the absence of *dRpd3* (*dHDAC1*) and the repressors Knirps, Giant, and dCtBP are insensitive to the histone deacetylase inhibitor trichostatin A (19). This makes sense because chromatin is unlikely to play a role over such short distances, but it begs the question "In the absence of these remodeling enzymes, how does dCtBP mediate repression?". It has been shown that short-range repression mediated by Krüppel at the *eve* locus requires dCtBP and disruption of the NAD(H) binding motif abrogates the repression activity (34), but mutants in the catalytic residues still have repressive activity. However, it remains unclear whether or not the mutants used in these studies disrupt overall function of dCtBP and researchers have used artificial, overexpression systems to study the effects of these mutants. The work described here evaluates mutant forms of dCtBP, transcribed at "normal" levels, which only disrupt one function while all others remain intact in a biologically relevant *in vivo* assay.

CtBP: Roles in Oncogenesis

When CtBPs were discovered based upon their interactions with the human adenoviral protein E1A, researchers almost immediately began to appreciate the role that CtBPs play in the regulation of essential cellular processes. Much research has been committed to looking at roles in signaling pathways and transcriptional repression, but another very important area of study is how CtBP modulates the activities of oncogenes,

apoptotic genes, and tumor progression pathways. E1A is an adenoviral transforming protein, proposed to mediate transformation by binding and sequestering essential cellular gene products including Rb and CBP/p300. Important effects on oncogenesis were inferred from early experiments showing that E1A proteins, mutant for CtBP binding, demonstrated enhanced oncogenicity of transformed primary rodent epithelial cells (19). This phenomenon occurs in the presence of activated *Ras* oncogene and transformed cells became highly tumorigenic and metastatic in transplantation experiments. Through binding CtBP, E1A has a mechanism for sequestering CtBP away from its normal transcriptional functions, and when unbound to E1A normal cellular CtBP functions make cells more amenable to transformation. In addition, oncogenic pathway proteins are miss-regulated in CtBP knockout cells. One can conclude that an important normal CtBPs normal function is to regulate pathways hijacked during transformation and tumorigenesis. This presents a challenge when one thinks about CtBP as a therapeutic target something which will be elaborated on in chapter 5.

Regulator of Epithelial-to-Mesenchymal transition and apoptosis

Two essential pathways which CtBP family members have been shown to regulate are the epithelial-to-mesenchymal transition (EMT) and apoptosis. Apoptosis, or programed cell death, is a well understood phenomenon which occurs in normal cells but fails or is shut down in tumor cells. EMT, the process by which a cell alters physical characteristics and the switch from epithelial to a fibroblastic phenotype (19), has been appreciated as an essential feature of embryonic development and more recently as part of the evolution of carcinoma cells. These two pathways have more recently become linked based upon the observation that carcinoma cells often lose several key apoptotic

pathways. For example, apoptosis due to detachment from the cellular matrix or attachment to the wrong matrix, anoikis, is almost always lost (44). As carcinomas transition between epithelial-like cells, which exhibit anoikis, and mesenchymal-like cells, which generally do not exhibit anoikis, the cells become more invasive and tumor progression is promoted. The interplay of these two pathways is clearly at work as tumor cells detach from their native cell matrix, survive due to disruption of normal apoptotic pathways, travel to a new location within the body, re-attach, and proliferate, i.e. metastasize.

CtBP was linked to these processes based upon the observation that through binding to CtBP, the E1A protein sensitizes the cell to apoptosis and induces the expression of epithelial cell adhesion and cytoskeletal genes in several tumor cell lines and mouse embryo fibroblasts which lack CtBP1 and CtBP2 (19). In order to understand this connection, we must first accept that despite E1A 243 oncogenic activity in rodent cell lines this protein is clearly acts like a tumor suppressor in human tumor cells and that these activities are mediated through interactions with many proteins (45). In tumor cell lines derived from melanoma, fibrosarcoma, and others, expression of E1A leads to increased production of cytoskeletal genes, epithelial-specific cell adhesion genes, and increased susceptibility to anoikis. E1A mutants, which have lost the ability to bind to CtBP proteins, lose some of the ability to activate these pathways (46). This indicates that CtBP normally represses epithelial-specific genes and apoptosis promoting genes. Microarray studies looking at CtBP1/2 knockout mouse cells indicate that this is the case. In these studies, genes that were up regulated included cytokerins and cell junction proteins as well as the pro-apoptotic genes (19). The interplay between apoptosis,

specifically anoikis, and EMT within cancer cells has become better understood and more greatly appreciated as an important convergence of gene pathways. Is it possible that CtBP proteins play an essential central role as regulator of these two programs?

A very important cellular adhesion molecule and hallmark of epithelial cells is E-cadherin, and E-cadherin expression is inversely correlated with tumor invasiveness and grade (2). Loss of expression of E-cadherin is a common finding in many human epithelial cancers, contributing to tumor invasion, metastasis, and progression of malignancies (3). Dr. Dana Madison has shown that mouse embryo fibroblasts derived from CtBP1/2 knockout mice express E-cadherin at very high levels (unpublished data). Using a lentiviral delivery system, when Dr. Madison adds back wild type CtBP1 and CtBP2 E-cadherin mRNA expression levels drop. Conversely, in tumor cell lines which contain CtBP1 and CtBP2, but do not express e-cadherin, CtBP knockdown with siRNA, induces E-cadherin mRNA and protein. CtBP proteins clearly repress the transcription of the E-cadherin gene, thus confirming its role as a regulator of an essential cell-adhesion molecule and important player in the EMT transition. Our lab has also looked at the mechanism by which CtBP is repressing E-cadherin transcription and Dr. Lundblad shows CtBP-dependent changes in the DNA methylation pattern within the E-cadherin promoter. Methylation changes occur depending on the presence or absence of CtBP1 and/or CtBP2 in the cell.

Studies using cells derived from CtBP1/2-knockout mouse fibroblasts have also been informative for understanding CtBP roles in EMT transition and related pathways. Not only does EMT appear to be defective or non-existent in knock-out embryos, but cells derived from these mice are hypersensitive to apoptosis (47). The hypersensitivity

seems to occur due to de-repression of several pro-apoptotic genes in the absence of mouse CtBP proteins. These results clearly implicate CtBP proteins as regulators in two key oncogenic pathways. There are a number of experiments one could perform to examine *Drosophila* CtBP's role in regulating apoptosis in the fly eye through the interaction with *armadillo* (β-catenin).

Hematopoiesis and Leukemogenesis

In addition to important roles in apoptosis and EMT pathways, CtBP also has important roles in hematopoiesis, the process of blood lineage development, and leukemogenesis. In gene expression studies using CtBP1/2 knock-out cells similar to those described above, several hematopoetic genes are up regulated in the absence of CtBPs. These include the iron storage protein ferritin light chain 1, the negative regulator of hematopoiesis, TGFβ3, Krüppel like factor 3 (KLF3/BKLF), and the zinc finger protein multitype 1 (FOG-1) (19). A number of these genes are targets of the erythroid transcription factor GATA-1 and are normally up regulated during eythroid differentiation (48). Two important GATA1 cofactors, FOG and FOG-2, bind CtBP through a PxDLS motif and research has shown that when FOG proteins function as repressors, CtBP is likely to contribute (49,50). Further analysis of this interaction in *Xenopus* embryos suggests that CtBP tempers FOG protein driven erythropoiesis (51), and in FOG-1 -/- mouse cell lines rescued with a CtBP binding deficient FOG mutant, erythropoiesis is enhanced compared to cells rescued with FOG-1 wild type. As this complex regulation becomes better understood, it is clear that cell type, space, time, and transcription factor/cofactor concentration levels regulate this essential maturation

process in much the same way that CtBP modulates functions in the developing *Drosophila* embryo.

Other important hematopoetic transcription factors include the large and diverse family of Krüppel-Like Factors (KLF) and the Ikaros family of zinc finger DNA binding proteins. KLF proteins are abundant in erythroid cells and repress several important target genes (49). Homology is limited between these family members but these factors contain a conserved CtBP binding motif and disruption of that motif leads to a reduction of their repressive activity (52). Ikaros and its family members are thought to regulate specification, differentiation, and function of lymphocytes, and a homozygous knockout of mouse Ikaros leads to complete loss of lymphocytes and lymphocyte precursors (53). Ikaros is a strong repressor which interacts with HDACs at chromatin, but it can also repress genes in an HDAC-independent mechanism (17). This HDAC-independent repression is dependent on CtBP, and other Ikaros family members also require CtBP for repression. The Ikaros/CtBP interaction appears to be an essential mechanism during lymphocyte production and maturation (19).

As discussed above, CtBP, through its interaction with E1A, is implicated in the regulation of key oncogenic pathways such as EMT and apoptosis. CtBP's normal functions are taken advantage of by foreign (E1A and EBV) and native oncogenes. This theme reappears as researchers examine CtBP's role in leukemia. Leukemia is a cancer of the blood or bone marrow characterized by an abnormal increase of blood cells, usually leukocytes (white blood cells) and a common player in myeloid leukemias is the oncogenic transcription factor ectopic viral integration site-1 (Evi-1). Evi-1 contains two CtBP binding motifs within its repression domain and mutations in these motifs lessen

repressive activity and Evi-1 mediated transformation of rat fibroblasts in vitro (54,55). In addition to inherent oncogenic activity, Evi-1 appears to be a hot-spot for translocations and specifically a fusion of AML1 with Evi-1 causes malignant transformation of hematopoietic stem cells (56). A model for CtBP's role in AML/Evi-1 mediated transformation is the aberrant repression of AML target genes through the unnatural recruitment of a repressor complex (Evi-1 + CtBP + HDAC) to AML target loci (19). This model fits with the related observation that AML1/FOG-2 fusions are found in patients with myelodysplasia (57). The AML1-FOG-2 fusion recruits a repressor complex containing CtBP which could lead to altered transcription of both GATA-1 and AML1 gene targets independently. Although less well studied, CtBP binds to the repression domain of the common translocation partner transcription factor MLL (mixed myeloid leukemia), is overexpressed in chronic myelogenous leukemia K-562 and lymphoblastic leukemia MOLT-4 cell lines (19), and is a critical member of the Polycomb-group protein complex which is aberrantly active in Hodgkin's lymphoma (58).

CtBP proteins are clearly important cofactors in the production, maturation, and disruption of healthy blood cells. As with the essential roles that CtBP plays in EMT and apoptosis, further understanding of the part that CtBPs play in hematopoietic growth will lead to a greater understanding of the underlying mechanisms of these malignancies and could potentially lead to better, more specific treatments of leukemia and other cancers.

<u>CtBP: Therapeutic drug target</u>

Based upon the roles that CtBP plays in cancer pathways, we have proposed the idea that CtBP might be a good target for inhibition and by blocking its repressive

activity one could slow cancer initiation, progression, and metastasis. Despite the identification of a CtBP specific substrate, we believe that CtBP is an enzyme and thus is amenable to modulation by small molecules. There are several ways that one could target CtBP proteins with a small molecule or other type of inhibitor. One method is to screen through small molecule libraries for chemicals that bind to CtBP, and this would be a good starting point. A combination of high throughput screening incorporated with the structure/function information we already have about CtBP would be even better. Much like companies, researchers who have used small molecules which resemble adenosine tri-phosphate (ATP) to search for inhibitors of kinase enzymes, a screen using small molecules which resemble NAD(H) in shape, molecular make-up, and redox state could yield molecules which interact with CtBP and alter its function. An even more elegant and possibly effective option could be inhibition via a peptide or antibody. It's been speculated that simply using the C-terminal region (exon 2) of E1A could relieve the repressive effects on tumor-restraining genes (19) and researchers have identified the endogenous protein Pinin/DRS which appears to relieve CtBP-mediated repression of E-cadherin (59).

An essential, missing, and controversial component of CtBP research is a detailed understanding of the mechanism of action of repression. How exactly does CtBP mediate repression at so many different loci? Precise understanding of the mechanism of repression at a variety of loci is essential not only for understanding CtBP biology but also for designing any kind of inhibitor. An obvious method for blocking CtBP-mediated repression would be to inhibit interactions with all targets; i.e. a small molecule or protein that binds to or occludes the N-terminal region which is known to interact with PxDLS

containing proteins. This is likely to have unexpected off target effects and lead to disruption of normal functions. In fact, there is evidence that CtBP proteins act as tumor suppressors in the colon via the protein adenomatous polyposis coli (APC) (60) which could be a deadly unwanted effect of blocking all CtBP target binding. If one concludes that this type of approach is not specific enough, then one could block NAD(H) binding, inhibit potential enzymatic activity, disrupt oligomeric forms of CtBP proteins, or target interactions with specific binding partners. All of these methods of attenuating CtBP activities require clear understanding of the essential biochemical structure/functions which mediate HDAC-dependent repression, HDAC-independent repression, short-range repression, tumor-restraining gene repression, tumor-suppressor activities, pro-apoptotic gene repression, EMT regulation, and hematopoietic gene control.

The experiments described in the forthcoming chapters of this thesis are an attempt to clarify the biochemical determinants of CtBP biology through the use of a relevant biological system and establish an in vitro assay to study CtBP function while monitoring dimerization. In order to address the ongoing issue of the relative importance of dinucleotide binding, putative dehydrogenase enzyme activity, and oligomeric state of an active CtBP protein, we examined wild type and mutant forms of the *Drosophila* CtBP in the *Drosophila* embryo where it normally plays a well understood biological function. Specifically we established an assay to monitor short-range repression at the *eve* locus by inserting DNA elements of our own making into a dCtBP null embryo. With these assays we determined that short-range repression is dependent on a CtBP which retains the ability to bind to dinucleotide but can still function in the absence of dehydrogenase activity. The requirement of dinucleotide binding is most likely due to an inability to

form homodimers at the site of repression. The reliability of our *in vivo* data is high not only because of the system in which we evaluated activity, but each of our mutant proteins was assessed for unwanted deleterious effects on the overall protein and/or disruption of biological activities associated with other CtBP functional domains. Finally we embarked on experiments to create a fluorescent assay to screen for small molecules which block dimerization of CtBP proteins.

Tables and Figures

Figure 1.1A Two-Dimensional layout of CtBP1 protein, functional domains: PxDLS containing target binding occurs at the N-terminus, dinucleotide binding occurs through the GxGxxG motif, and putative dehydrogenase domain outlined. Phosphorylation and SUMOylation sites identified.

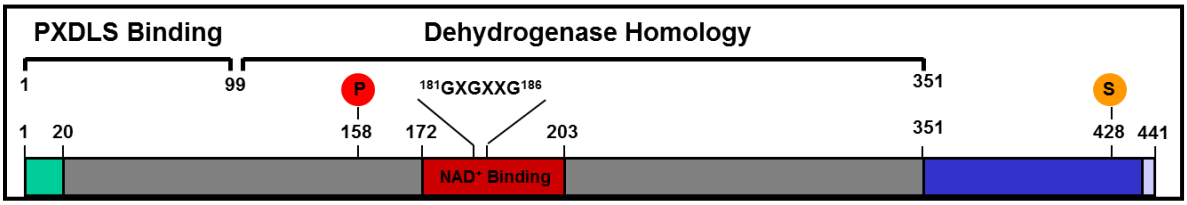

Figure 1.1B Adapted from Nardini 2003; Figure 4 – Three dimensional model of the consensus PIDLSKK peptide (yellow) bound to the N-terminal region of t-CtBP/BARS.

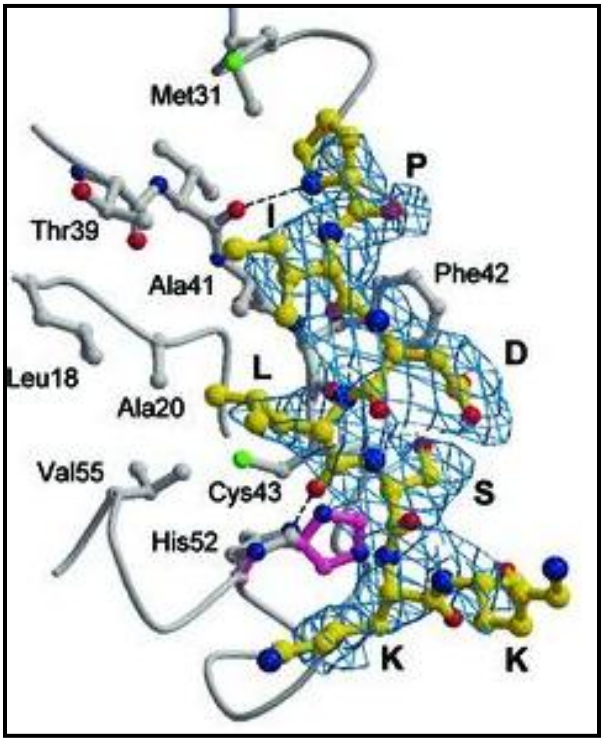

Figure 1.2 Nuclear localization of CtBP proteins

CtBP2 localizes into the nucleus of the cells, CtBP1-L is distributed throughout the nucleus and the cytoplasm, and CtBP1-S is predominantly cytoplasmic. Cos-1 cells transfected with expression vectors, and the expressed proteins were visualized by confocal microscopy. Graph depicts the quantitative data obtained from three independent experiments. N, exclusive nuclear staining; NC, cytoplasmic and/or nuclear staining.

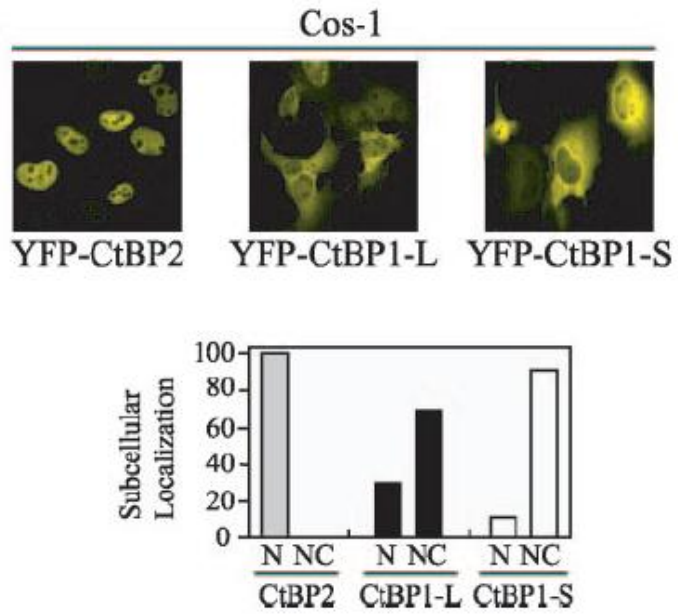

Figure 1.3 Amino Acid Sequence and structural alignment between CtBP proteins and *E. coli* 3-Phosphoglyceraldehyde Dehydrogenase; a D-isomer specific 2-hydroxyacid dehydrogenase enzyme. Residues in black boxes are absolutely conserved; yellow boxes indicate essential residues for catalytic activity in dehydrogenase enzymes. Helical and β-sheet secondary structures highlighted with red and blue boxes, respectively.

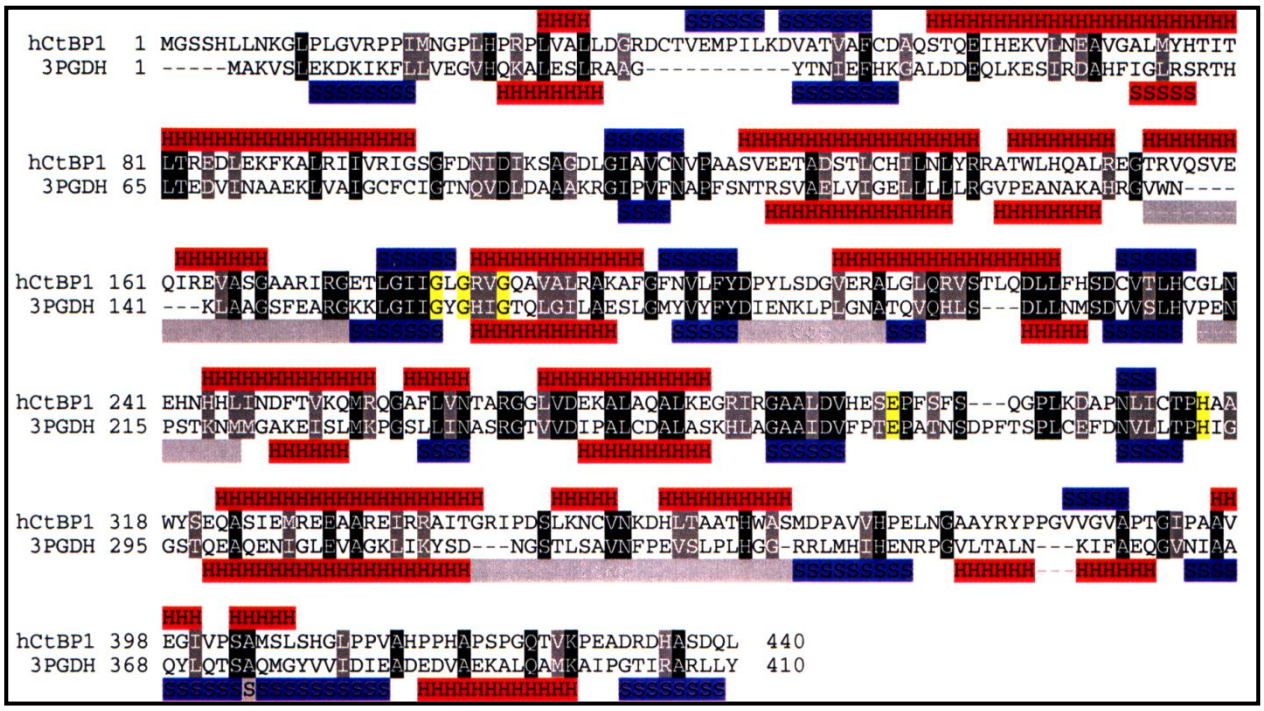

Figure 1.4 Adapted from J. Lundblad, 2006 – Model of CtBP1 dimer bound to PxDLS peptide and NAD dinucleotide; dimers shown in gold and red/blue for clarity. Structure does not include C-terminal portion of the protein; PxDLS peptide binds at substrate binding domain (SBD); NAD binds at nucleotide binding domain (NBD); dimer forms through NBD.

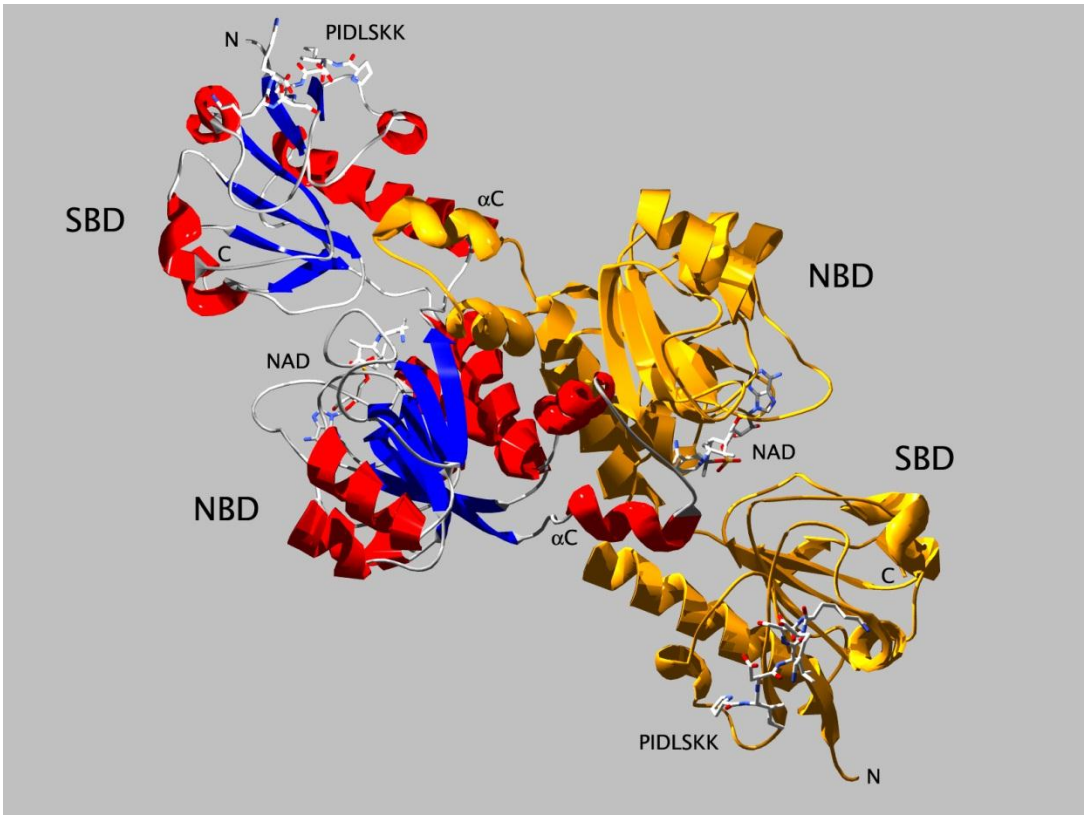

Figure 1.5 Image provided by Dr. Sarah Smolik – *Drosophila* embryogenesis – graphical description of the coordination of maternally deposited mRNAs; the establishment of polarity within the embryo; the concentration dependent expression of gap genes; the interaction between maternal genes and zygotic genes; coordinated steps to proper segmentation.

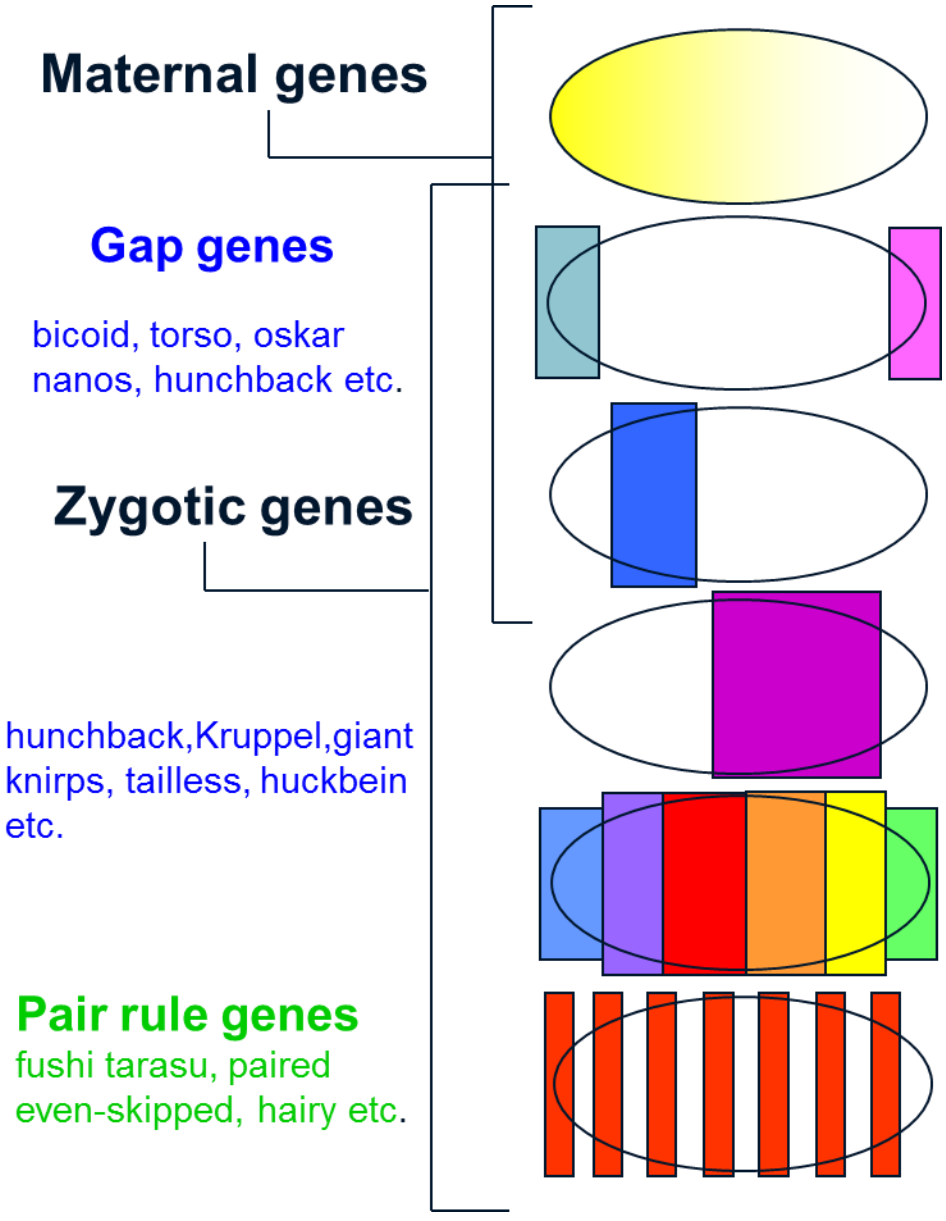

Figure 1.6 Modified from Alberts, Molcular Biology of the Cell, 4th Ed. and J. Lundblad 2006 – *eve* locus and transcriptional regulation (top): *eve* locus coding region in red bordered by control regions shown in yellow

Graphical representation of embryo, *eve* stripes 2 – 5 with anterior on left (Bottom): colored lines indicate relative expression of each gap protein; grey bands indicated *eve* stripes of expression

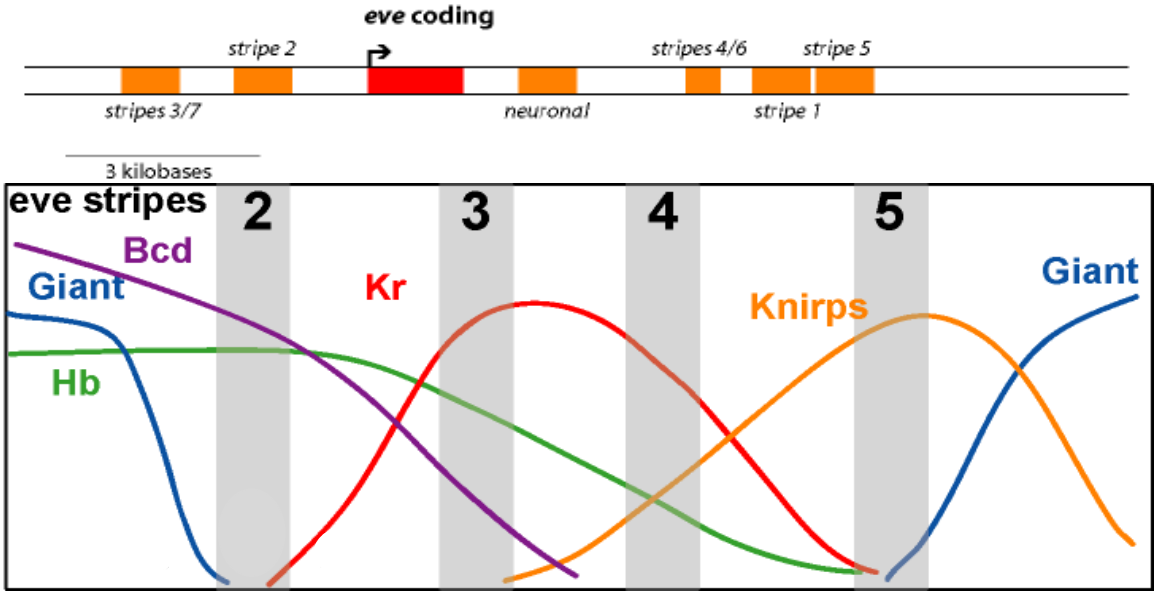

Figure 1.7 Modified from J. Lundblad 2006 – Protein occupancy and regulation at *eve* stripe 2 enhancer: Giant (Gt) and Bicoid (Bcd) activate *eve* transcription at anterior border of stripe 2; Krüppel (Kr) blocks activation by Gt and Bcd at posterior border by competition and short-range C-terminal Binding Protein (CtBP) dependent repression

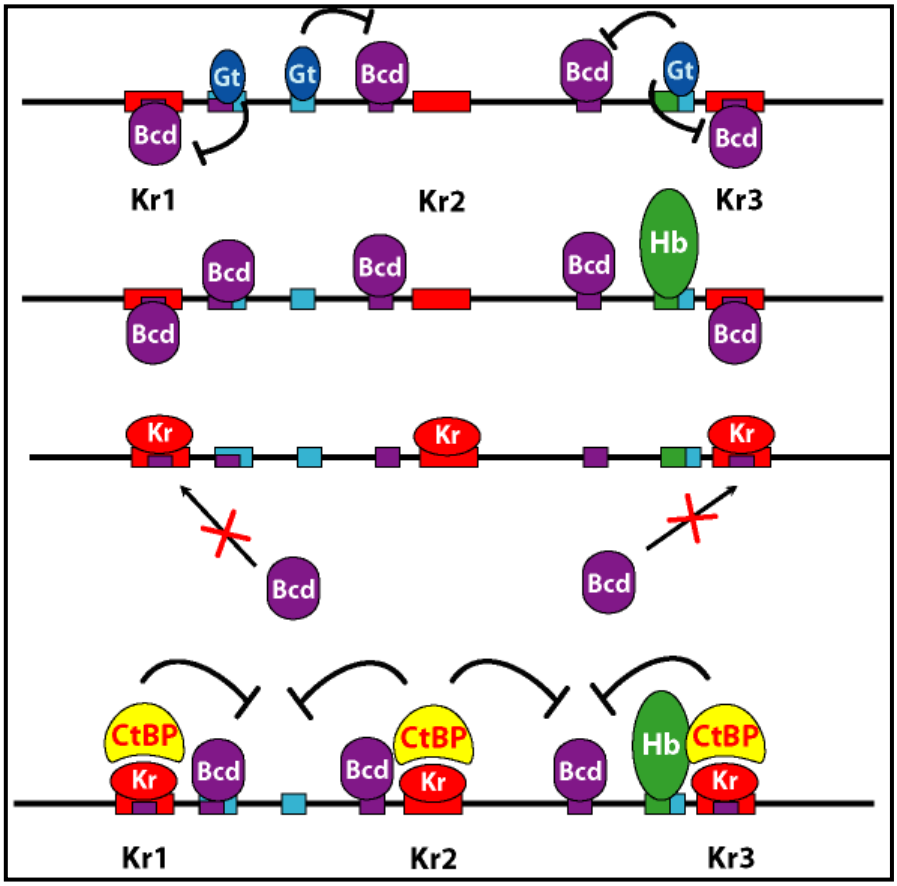

Figure 1.8 – Adapted from J. Lundblad, 2006 – Model of the Rossman fold of CtBP: essential residues for direct interaction with NAD(H) shown as well as conserved residues from dehydrogenase enzymes

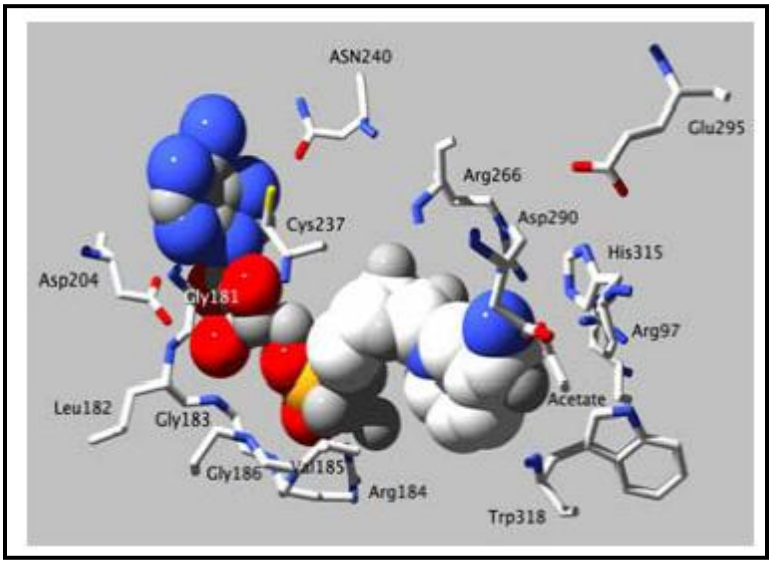

Chapter 2. *Drosophila* C-terminal Binding Protein – Biochemical analysis of wild type and mutant proteins

Damian E. Curtis[1], Ujwal Shinde[1], and James R. Lundblad[2]

[1]*Dept. of Biochemistry and Molecular Biology, Oregon Health Sciences University*

[2]*Dept. of Medicine, Oregon Health and Sciences University*

Abstract

Drosophila Carboxyl-terminal Binding Protein (dCtBP) is a member of the CtBP family of biologically essential transcriptional co-repressors. It is highly homologous to the human and other vertebrate members of the CtBP family. Like other members it bears striking similarity to a specific class of dehydrogenase enzymes. Here we focus on the dCtBP protein; its secondary and tertiary structures, oligomerization state, target binding activities, and coenzyme binding. We examine the wild type protein as well as a series of mutants which abolish distinct biochemical functions as a prelude to examining these functional mutants in an *in vivo* model for dCtBP activity. We determine that single amino acid substitutions do not disrupt the overall structure of the protein and we are able to remove distinct dCtBP functions while keeping others intact. Each of the individual mutants are examined using *in vivo* assays described in future chapters.

Introduction

Unlike vertebrates which have two highly related but distinct genes that encode both CtBP isoforms, the invertebrate *Drosophila melanogaster* has only a single CtBP gene, known as *dCtBP* (6). CtBP family members exhibit a high level of sequence similarity (Figure 2.2) and all known CtBP-dependent repressors and binding partners contain some form of the motif PxDLS (where x is any amino acid). Removal or alteration of the PxDLS motif abrogates CtBP binding and, at least partially, the transcriptional repressive activities of these proteins.

CtBP proteins have some unusual characteristics; in particular, the family members lack common features found in other transcriptional regulatory proteins, and yet have striking primary sequence and structural similarity to the D-isomer specific 2-hydroxyacid dehydrogenase class of enzymes (a family including D-lactate dehydrogenase, and 3 phosphoglycerate dehydrogenase). In addition, our laboratory and others have found that immunoprecipitation of each CtBP isoform individually co-purifies with others, and that they heterodimerize in vitro (12, 29, and our unpublished preliminary studies).

The CtBP family of proteins act as transcriptional co-repressors, but it remains unclear how that repression is mediated. There are two models supported by the current data. In the recruitment model, CtBP acts as a scaffold for the recruitment of other co-regulatory proteins and is independent of any intrinsic enzymatic activity. Data supporting this model include associations with histone deacetylases (reviewed in ref. 6), and a macromolecular co-repressor complex comprised of CtBP in association with histone modifying enzymes has been purified from HeLa cells (10). The purified

complex includes many of the common players found in histone modifying complexes, including HDAC1and HDAC2, and histone methyltransferases G9a and Eu-HMTase. In the second model CtBP has intrinsic enzymatic activity, which accounts for CtBP-dependent repression events that are HDAC independent (17,18). These HDAC independent repressive functions include epigenetic silencing of the E-cadherin promoter, and the mechanism of short-range repression observed in the *Drosophila* embryo.

CtBP contains a NAD-binding motif termed the Rossmann fold. This is an evolutionarily conserved structural domain comprised of repeated βαβαβ structural components (61) found in D-2-hydroxyacid dehydrogenases, to which CtBP bears striking structural similarity. Proteins containing the Rossmann fold have a glycine-rich loop, G/AxGxxG(17x)D that interacts with the pyrophosphate moiety of NAD (Figure 1.4). CtBP has been proposed to use NAD as a co-regulatory small molecule. D-2-hydroxyacid dehydrogenases are a heavily studied class of enzymes and their reliance on NAD as a co-enzyme is well understood. In these enzymes, mutations in the G/AxGxxG loop result in loss of co-enzyme binding; whereas mutations which coordinate the enzymatic activity of the protein, see Figure 1.3 Histidine and Glutamic Acid highlighted in yellow, retain co-enzyme binding but lose enzymatic activity. Given the striking similarities between CtBP proteins and D-2-hydroxyacid dehydrogenases, we expect these mutations to selectively abrogate specific funtions of CtBP. NAD has well defined roles in metabolism as a carrier of reducing equivalents, cellular signaling, as a substrate for protein modifications, and precursor to the synthesis of calcium mobilizing second messenger molecules (62). The role of NAD in CtBP-dependent repression remains controversial and has not been investigated *in vivo*.

Dehydrogenase enzymes containing the Rossmann fold have catalytic activity through a "proton shuttle" between a histidine and a carboxylic acid residue (i.e., glutamate or aspartate) with the transfer of a hydride ion between the substrate coenzyme, and an arginine residue in the active site interacts with the substrate carboxylic acid during catalysis (63). All of these catalytic residues are conserved in all mammalian CtBP orthologs as well as *Drosophila* which strongly argues that CtBP retains oxo-reductase enzymatic activity. The role of these conserved residues in CtBP function remains controversial (27, 28). Other labs have measured some nominal activity using pyruvate as a substrate, but the activity found in these in vitro assays with recombinant protein could be due to contamination by lactate dehydrogenase. A *bona fide* substrate for CtBPs has not been identified. The current hypothesis for CtBP dependent transcriptional repression suggest that CtBP acts as a cellular redox-dependent transcriptional co-repressor, and it is sensitive to the ratio of reduced to oxidized NAD (NADH:NAD^+). This model proposes that binding to NADH is preferred over binding to NAD and the resulting conformational changes increase association with target. Although one prominent lab has reported large differences between NADH and NAD^+ binding and association with E1A (26), our lab and others have found little or no difference in affinity for the two NAD redox states (27, 28). For most of these studies, researchers use CtBP protein expressed and purified in *E. coli*, and evidence of CtBP requiring NAD binding for co-repressor activity comes from studies of CtBP proteins with mutations in the NAD binding glycine-rich loop motif (31). We find that *Drosophila* CtBP proteins with some of these mutations misfold, and thus we must consider whether the loss of co-repressor function of these mutants is due to global disruption of protein folding.

Finally, binding to PxDLS-containing targets is accomplished via determinants located in the N-terminal domain, and target binding is structurally and thermodynamically separable from NAD binding. The experiments outlined in this chapter, as well as Chapters 3 and 4, aim to determine the biological roles of these biochemical functions through the examination of mutant proteins that selectively disrupt target binding, NAD(H) binding, and putative dehydrogenase functions of dCtBP in a relevant biological setting.

This chapter is dedicated to understanding wild type dCtBP protein as well as each individual mutant protein in vitro, and this allowed us to contextualize the *in vivo* experiments in forthcoming chapters. We began by utilizing homology modeling and structure prediction software to propose the first three dimensional structure of the 386 amino acid dCtBP isoform (A or *dCtBP(S)*) and consider the nature of this model, the information gleaned, and provided new insight into the poorly understood C-terminal domain location and secondary structure. dCtBP proteins mutated at a single residue in order to disrupt one, and only one, of the distinct dCtBP functions were evaluated for overall disruption of the protein and found not to cause drastic changes in the secondary structure when compared to the wild type protein. Each individual mutant protein was characterized for target binding and coenzyme binding. Finally, we compare the effect of removing each biochemical function has on self-association and discuss the implications of these results.

Materials and Methods

Cloning of dCtBP and creation of Mutant cDNAs; subcloning

dCtBP isoform A coding sequence PCR amplified using VENT polymerase from an mRNA pool (4 ul) derived from adult flies and ligated to a modified pBSKS vector by Dr. James Lundblad (Table 3.1 for list of primers used). PCR conditions: denaturation at 95ºC for 1 minute; 35 cycles of 94ºC for 30 seconds, annealing at 55ºC for 1 minute, extension at 72ºC for 1 minute, finishing at 72ºC for five minutes. PCR run out on 1% Agarose gel with ethidium bromide, visualized on UV light box, and excised from gel. DNA purified away from agarose by adding 500 ul of TE buffer 8.0, melting gel at 65ºC, adding 350 ul of pre-warmed phenol, mixing, and centrifuging for 5 minutes at 13,000 rpm. The aqueous (upper) phase removed and phenol extraction repeated. Aqueous removed again and added to an equal volume of Chloroform:Isoamyl alcohol (24:1), mixed, and centrifuged for 5 minutes at 13,000 rpm. The aqueous phase removed, 3M sodium acetate (NaOAc) added to a final concentration of 0.3M, and 500 ul of ice cold 100% ethanol. This mixture stored at -20ºC for no less than 20 minutes and centrifuged for 20 minutes at 13000 rpm. The DNA pellet washed with cold 70% ethanol, centrifuged at 13,000 rpm for 5 minutes, air dried, and resuspended in TE ph 8.0.

The PCR amplicon was digested with Asp718I and XbaI restriction enzymes at 37ºC along pBSKS plasmid vector cut with the same enzymes. DNA fragments analyzed on agarose gel and purified as described above. Digested, cleaned PCR fragment ligated to digested, cleaned pBSKS vector using T4 DNA ligase overnight at 20ºC. Ligated PCR and vector transformed into DH5α competent *E. coli* by mixing 1 ul of ligation mix with 50 ul of DH5α cells on ice for several hours, heat shocking at 42ºC for 30 seconds,

incubating on ice for 5 minutes, rescuing cells for 1 hour with 500 ul of SOC (20 g Bacto Tryptone, 5 g Bacto Yeast extract, 2 ml of 5M NaCl, 2.5 ml of 1M KCl, 10 ml of 1M $MgCl_2$, 10 ml $MgSO_4$, 20 ml 1M glucose, adjusted to 1 L of diH_2O) media at 37ºC with 230 rpm shaking. 100 ul of transformation mix plated onto Luria Broth agar (LB – 10 g Bacto-tryptone, 5 g Yeast extract, 19 g NaCl, 15 g bacto-agar, adjust volume to 1 L of diH_2O, autoclaved to sterility, cooled to 55ºC, 10 cm petri dishes filled) plates with 100 ug/ml Ampicillin (LB-AMP100) and incubated overnight at 37ºC in an upright incubator. Single colonies picked from LB-AMP100 plates, grown in 4 ml of LB plus 100 ug/ml ampicillin overnight at 37ºC with 250 rpm shaking. One ml of culture set aside for glycerol stock (pellet cells, resuspend in 500 ul fresh LB and 500 ul of sterile 50% glycerol, frozen at -80ºC) and remaining cells pelleted by centrifugation, plasmid DNA purified using Qiagen QIAprep Spin Miniprep Kit (QIAGEN Valencia, CA 91355), DNA eluted in 40 ul of elution buffer and stored at 4ºC.

dCtBP insert was confirmed and shown to be free of PCR inserted errors by Sanger sequencing at the OHSU MMI DNA services core facility using BSKS top and -20 sequencing primers (Table 3.1). Nucleic acid sequence retrieved from MMI core database and analyzed using Accelrys dsGENE desktop DNA analysis software. Nucleic acid and translated amino acid sequence were compared manually to published *dCtBP* cDNA sequences (34) using EMBOSS pairwise alignment tool. PCR, gel extraction, ligation, transformation, plasmid DNA purification, and insert sequencing/confirmation protocols were performed as described above in all other experiments within this document unless otherwise noted.

Site-directed mutagenesis using Stratagene Quick-Change protocol (64) used to insert nucleic acid changes in the wild type *dCtBP* gene which conferred the following point amino acid mutations (Figure 3.1i - Right); Alanine 52 to Aspartic Acid (A52D), Valine 66 to Arginine (V66R), Glycine 183 to Alanine (G183A), Isoleucine 185 to Aspartic Acid (I185D), Cysteine 237 to Methionine (C237M), Arginine 266 to Glutamine (R266Q), and Histidine 315 to Alanine (H315A) (Table 3.1). In addition to changing the amino acid sequence, these primers inserted new restriction enzyme sites for easy screening for successful mutagenesis: A52D inserted a SalI site, V66R eliminated a EcoNI site, G183A inserted a BssHII site, I185D removed the BssHII inserted by G183A when G183A plasmid DNA was used as the mutagenesis template, C237M inserted an NdeI site, and H315A inserted an EagI site. R266Q mutagenesis was confirmed by Sanger sequencing as no suitable restriction enzyme site could be constructed.

Site-directed mutagenesis protocol: 500 – 1000 ng of purified plasmid DNA mixed with 250 – 1000 ng of primer top and 250 – 1000 ng of primer bottom, 1 ul 25 mM dNTPs, 10 ul of 10x PFU Ultra buffer, 1 ul of 2.5 U/ul PFU Ultra HF DNA polymerize enzyme (Stratagene), and molecular biology grade H_2O to 100 ul. Mutagenesis reactions performed overnight on ABI Thermocyler using the following conditions: denaturation at 95ºC for 3 minutes, 18 cycles of 94ºC for 30 seconds, 58ºC primer anneal for 2 minutes, extension at 68ºC for 10 minutes, and finishing for 10 minutes at 68ºC. DH5α *E. coli* transformed, rescued, plated, and incubated. Single colonies grown and plasmid DNA isolated. Mutations confirmed either by restriction enzyme digest or Sanger sequencing.

Wild type and mutant *dCtBP* constructs subcloned into pCDNA3 vector containing an in-frame C-terminal 2xFLAG epitope tag (pCDNA3_Ct_2xFLAG) via Asp718I and XbaI restriction enzyme sites, and pET23d HIS-6 tagged vector via NcoI and XhoI restriction enzyme sites for expression and purification of proteins in *E. coli* expression system for Equilibrium Dialysis, Circular Dichroism, and GST pull down experiments. Wild type and mutant cDNA constructs excised out of pCDNA3_Ct_2xFLAG with Asp718I and XbaI restriction enzymes and subcloned into the P-element containing pUAST vector downstream of the UAS elements for construction of transgenic flies (Figure 3.1ii – Right). All plasmid constructs confirmed by Sanger sequencing and stored as glycerol stocks at -80ºC.

Expression and purification of His-6 tagged wild type and mutant dCtBP protein

E. coli BL21 competent cells transformed with plasmid DNA from wild type and mutant *dCtBP* constructs cloned into pET23d plasmid vectors described above.

Protein expression protocol: 100 ml LB with 200 ug/ml ampicillin inoculated with a single colony from LB-AMP100 plate, grown in 250 ml flask at 37ºC, 250 rpm overnight. 25 ml of overnight culture used to inoculate 1 L of LB with 200 ug/ml ampicillin and 0.2% glucose, shaken at 37ºC until OD600 reaches 0.5-0.6 (approximately 3 hours). Culture cooled and induced with 1 ml of 0.4 mM Isopropyl β-D-1-thiogalactopyranoside (IPTG) and an additional 500 ul of ampicillin, shaken for 16 - 24 hours at 12ºC. Cells pelleted by centrifugation at 6000 rpm for 10 minutes at 4ºC in 250 ml bottles (multiple spins to collected entire 1L culture). Cell pellets resuspended in 35

ml of cold 1X PBS and transferred to 50 ml screw cap tubes. Cells centrifuged at 4000 rpm for 45 minutes at 4ºC, supernatant removed and pellets stored at 4ºC overnight

Protein purification protocol: Cells resuspended in 27 ml of Nickel-NTA Buffer A (50mM Tris, 300mM NaCl, ph 7.5, 5% Glycerol filter sterilized) and 3 ml of Nickel-NTA Buffer B (50mM Tris, 300mM NaCl, .5 M Imidazole, pH 7.5, 5% Glycerol, filter sterilized) by vortexing and pipetting. Just prior to cell lysis by French Press, 1mM final concentration of PMSF and 50 mM final concentration β-mercaptoethanol added to the samples. Cells lysed using French pressure cell press 2 times at 1500 psi. Samples centrifuged for 40 minutes at 16000 rpm at 4ºC. Supernatant is collected, bound to pre equilibrated Ni-NTA column using FPLC instrument at 2.50 ml/min. Column washed with 10 column volumes of 90% Ni-NTA buffer A and 10% Ni-NTA buffer B. Protein eluted off the Ni-NTA column with increasing concentrations of Ni-NTA Buffer B (10% - 100% over 125 ml) and collected in 5 ml fractions using an automated fraction collector. Fractions visualized on a 10% SDS-PAGE gels followed by Coomassie Blue (0.25 g Coomassie Blue, 75 ml Glacial Acetic Acid, 500 ml Methanol, bring to 1 L with dH_20) staining overnight, and destained (100 ml Glacial Acetic acid, 900 ml dH_2O:Methanol (1:1)) the following day. 10% SDS-Polyacrylamide Electrophoresis gel with 5% SDS-Polyacrylamide stacking gel constructed according to the following protocol: 10% gel: 1.5 ml of 40% Acrylamide, 1.25 ml 4X Tris-HCL-SDS, 2.2 ml H_2O, 2.5 ul Temed, and 50 ul of 10% ammonium persulfate. 5% stacking gel: 0.25 ml of 40% Acrylamide, 0.50 ml 4X Tris-HCL-SDS (pH6.8), 1.3 ml H_2O, 2 ul Temed, and 20 ul 10% ammonium persulfate. 10% gel poured into glass plate gel assembly apparatus followed by 1 ml H_2O, and after gel solidifies H_2O removed and 5% stacking gel is poured on top

of 12% gel. Gel comb inserted and after stacking gel solidified gel ready for use or storage at 4ºC.

Based upon analysis of destained SDS-PAGE gel, fractions containing desired protein pooled, sealed in dialysis tubing with 10,000 MW cut-off, and dialyzed overnight at 4ºC in 4 L of dialysis buffer (25 mM Tris, 1mM EDTA pH 7.5, 5% glycerol, 1mM DTT added just before fractions) with constant mixing. Dialyzed fractions collected and purified a second time on a Q-sepharose HiTrap ion exchange column. Ion exchange column is equilibrated with Q column Buffer A (25 mM Tris, 1mM EDTA, pH 7.5, 5% glycerol, filter sterilized), fractions loaded onto column at 5 ml/min, washed with 25 ml of Buffer A plus 5% Q column Buffer B (25 mM Tris, 1mM EDTA, 1M NaCl, pH 7.5, 5% glycerol, filter sterilized), eluted off with increasing concentrations of Buffer B (5% - 100% over 125 ml), collected in 5 ml fractions using automated fraction collector. Fractions visualized on 10% SDS-PAGE gels stained with Coomasie Blue overnight and destained. Fractions containing desired protein combined into dialysis tubing and dialyzed into storage buffer (25 M Tris, 1mM EDTA, 100mM NaCl, pH 7.5, 5% glycerol, 1mM DTT added just before use) at 4ºC overnight with slow mixing.

Wild type and all mutant (A52D, V66R, G183A, I185D, C237M, R266Q, H315A) dCtBP His-6 tagged protein was expressed and purified according to the protocols described above, and fractionated on 10% SDS-PAGE gel, stained with Coomassie Blue, destained, and visualized on Oydssey (Li-COR) imaging system (Figure 2.1) All other proteins described in future sections also expressed and purified according to this protocol unless stated otherwise. Protein quantified using spectrophotometer by

measuring absorbance at 280 nm, subtracting background absorbance and dividing by the molar absorption coefficient for the protein (76). See equation below:

uM concentration = (280 nm abs – 300 nm abs)/molar absorption coefficient

All proteins stored at -80ºC until needed for Equilibrium Dialysis, Circular Dichroism, or GST pulldown experiments.

Construction, expression, and purification of GST-dCtBP protein

Digested pCDNA3_*dCtBP* with restriction enzymes NcoI and XhoI, purified, and ligated to NcoI/XhoI prepared pGEX-KG vector upstream and in frame with a GST protein tag. GST-dCtBP protein expression and purification: pGEX-KG_GST-dCtBP plasmid transformed into *E. coli* DH5α chemical competent cells, single colony grown according to protein expression and purification protocols above. Following centrifugation of cells, pellet resuspended in lysis buffer (1xPBS, 1mM EDTA, 0.1% Triton-X100, 0.4 mM PMSF), cells lysed by French Press, and cell debris pelleted at 16000 rpm for 30 minutes at 4ºC. Supernatant loaded onto equilibrated GST column, washed, and eluted off the column (50 mM Tris-HCl pH 8, 10 mM reduced G1utathione) into 20 fractions. Fractions analyzed on 10% SDS-PAGE gel, dialyzed into storage buffer overnight, and stored at -80ºC until used in GST pulldown experiments.

Construction and purification of GST-Krüppel and GST-Krüppel DLAS mutant

BAC RP98, used to construct the *Krüppel*-GAL4 driver fly construct in Chapter 3 Materials and Methods, used as a template for PCR amplification of 300 base pairs of the *Krüppel* gene containing the PxDLS domain. The region of interest PCR amplified, digested with BamHI and HindIII (restriction sites contained in 5' end of PCR primers), and ligated to BamHI/HindIII prepared pBSKS prepared vector (Table 3.1). Inserts confirmed by Sanger sequencing and free of nucleic acid changes inserted during PCR amplification. pBSKS_Krüppel_PxDLS plasmid DNA used as a template for site directed mutagenesis to mutate the PxDLS domain to PxASS. Mutations confirmed by Sanger sequencing. pBSKS_Krüppel_PxDLS and pBSKS_ Krüppel_PxASS digested with BamHI and HindIII, insert purified, and ligated to BamHI/HindIII prepared pGEX-KG vector upstream and in frame with a GST protein tag. pGEX-KG_GST-Krüppel_PxDLS and pGEX-KG_GST- Krüppel_PxASS used to generate GST-Kr and GST-Kr* protein, respectively. Proteins expressed and purified in the same manner as GST-dCtBP protocol described above.

GST pulldowns

Histidine-6 tagged, purified, wild type and mutant *dCtBP* protein were dialyzed into GST binding buffer (20 mM HEPES, 1mM EDTA, 250 mM NaCl, 10% Glycerol, 0.1% NP-40, 25 ug/ml Bovine Serum Albumin (BSA), 1mM DTT, filter sterilized), quantified (as described above), and used in GST-pulldown experiments. 10 nm, 25 nm, 50 nm, and 100 nm concentrations of wild type dCtBP or mutant proteins mixed with GST-Kr protein (100 amino acids of the *Drosophilia Krüppel* protein containing the PxDLS motif fused to GST), GST-Kr* (GST-*Kr* with PxDLS mutated to PxASS), or

GST protein only for two hours at 4°C with slow rocking in the presence and absence of 10 um NAD. A fifty percent slurry of Glutathione-Sepharose was equilibrated with GST binding buffer added to the proteins, mixed, and rocked for an additional hour. Samples centrifuged at 4ºC at 1000 rpm, supernatant removed, and sepharose washed 5 times in the same manner with 500ul GST buffer (with or without 10uM NAD). Protein-bound sepharose beads resuspended in 20 ul of 2x SDS loading buffer (0.2M Tris-HCL pH 6.8, 4% SDS, 20% glycerol, B-mercaptoethanol, 0.4 mg/ml Bromophenol blue), heated in 95ºC water bath for 5 minutes, and loaded onto 10% SDS-PAGE gel along with input control.

Western blot performed by transferring SDS-PAGE gels onto PVDF (Millipore) membrane according to the following protocol: transfer apparatus assembled, Whatman blotting paper wetted in 1X transfer buffer (10X transfer buffer – 30.3 g Tris base, 144.1 g glycine, brought to 1 L with H_2O; 1X transfer buffer; 1X – 100 ml 10X buffer stock, 700 ml H_2O, 200 ml methanol), laid out onto transfer apparatus. PVDF membrane wetted in methanol for 1 minute, transferred to 1X transfer buffer, laid out onto Whatman blotting paper. SDS-PAGE gel placed on top of PVDF membrane and covered with pre-wetted Whatman blotting paper. Entire transfer apparatus reassembled and protein transferred to PVDF membrane at 21 volts for 1 hour. Following transfer, apparatus disassembled, membrane blocked for 15 minutes with cold Blocking Buffer (Li-COR Odyssey®) mixed 1:1 with TBST (10X TBS – 24.23 g Tris-HCL, 80.06 g NaCl, 1 L H_2O, pH to 7.6; TBST – 100 ml of TBS 10X, 1 ml Tween20, 900 ml H_2O) for 15 minutes with gentle rocking. PVDF membrane probed with mouse anti-His6 primary antibody diluted 1:6000 in 1:1 TBST and Blocking Buffer overnight at 4ºC overnight with gentle

rocking. Primary antibody was collected, PVDF membrane washed at least 4 times for 15 minutes with TBST, probed with anti-mouse Alexa Fluor 680 diluted 1:6000 in 1:1 TBST and Blocking Buffer for 2 hours at room temperature with gentle rocking followed by at least 4 washes for 15 minutes with TBST. Membrane was visualized on Odyssey infrared imaging instrument (Li-COR).

GST pulldowns and Western blots with GST-dCtBP were performed in the same manner.

Equilibrium dialysis

His-6 tagged, purified, wild type or mutant *dCtBP* protein added to Harvard Apparatus Micro-Equilibrium Dialyzer as described in (65). Using a single 10,000 MWCO membrane, 250 ul of protein (10uM concentration in binding buffer (25mM Tris, 100uM NaCl, 1mM EDTA, 5% glycerol, 1mM DTT)) added to one side of all 10 vessels without disturbing the membrane. To the other side of the vessel, 250 ul of NAD, at the following concentrations 50uM, 20uM, 10uM, 7.5uM, 5uM, 2uM, 1uM, 0.5uM, 0.1 uM, and 12nM, added along with 1 ul of the stock of tritiated NAD. Following forty-eight hours of gentle rocking at 4°C, samples collected from each side of the membrane with the protein containing side labeled as 'bound + free' and the side with no protein is the labeled 'free'. One fifth of the volume collected from the sides diluted ten-fold in scintillation fluid and radioactive counts measured on scintillation counter.

In order to determine bound versus free NAD for each concentration the equations below are used:

Bound+Free = (b+f/(free + b+f) * [NAD]

Free = (free/b+f + free) * [NAD]

Bound = B+F - Free

The calculated Bound and Free NAD were graphed using GraphPad Prism by fitting the data to the following equation by nonlinear regression:

Y=Bmax*X/(Kd+X).

This equation describes the binding of a ligand to a protein that follows the rules of mass action. Bmax is the maximal binding and Kd is the concentration of NAD required to reach half-maximal binding. The raw binding data for wild type and mutant proteins are entered into the calculation and that data is plotted (Figure 2.4A)

Circular Dichroism

His-6 tagged, purified, wild type and mutant *dCtBP* protein circular dichroism spectra were taken as described in (66). Using an automated AVIV 60DS spectrophotometer maintained at 4C, the spectra were taken from 260 to 190 nm and represents an average of three independent scans. The protein concentration was 0.3 mg/ml in storage buffer (25 M Tris, 1mM EDTA, 100mM NaCl, pH 7.5, 5% glycerol, 1mM DTT) and a path length of 0.1 cm was used. Background spectra were subtracted from the raw data; subtracted data was transformed and graphed using GraphPad Prism (Figure 2.4B)

Three-dimensional model of dCtBP

The amino acid sequence of wild type *dCtBP* isoform A was separated into three domains. The amino acid sequence for each of these domains was used for homology

modeling versus human CtBP1 using the Robetta server (http://robetta.bakerlab.org). Structure prediction using the Robetta server is described in detail in (67. Briefly; sequences are submitted and parsed into putative domains and models are generated using comparative modeling or de-novo prediction methods. Three-dimensional structure modeled and displayed using Swiss PDB Viewer (Figure 2.3).

Results

The 383 amino acid sequence of dCtBP isoform A (dCtBP(s)) (see page 12 for description of *Drosophila* CtBP isoforms) was divided into three amino acid sequence segments; segment 1 contains amino acids 1 to 123; segment 2 contains amino acids 124 to 296; segment 3 contains amino acids 297 to 383. Each of the segments was individually uploaded into the full-chain protein structure prediction program Robetta. Homology modeling, using the human CtBP1, and iterative *ab initio* modeling was performed on each of the three individual predicted structures to generate the final structure (Figure 2.3). One of the hallmarks of the CtBP family of proteins is the level of conservation even across vertebrates and invertebrates. This was illustrated in an alignment of amino acid sequences (Figure 2.2) which shows stretches of complete conservation (grey shading) between human CtBP1 and dCtBP isoforms A and E throughout the core of the protein with greater variation at the amino and carboxyl termini. Within these regions of complete conservation are amino acids, which are indispensable for interacting with CtBP targets (A52 and V66) (68), binding to dinucleotide cofactors (G183 and I185) (27,28), and putative dehydrogenase activity (C237, R266, and H315) (27,28).

Our model of dCtBP predicts a largely alpha-helical structure with the dinucleotide binding Rossman fold. The bi-lobed structure is separated by a flexible linker region with target binding elements positioned on the outer edge of the substrate binding domain (SBD) of the protein. Nucleotide binding domain (NBD) elements are proximal to the interface of the two lobes which has been shown in previous reports (30,32) to be the site of cofactor binding. Putative dehydrogenase elements are positioned

across from the NBD elements on opposite sides of the interface of the two lobes. It has been hypothesized, by us as well as others (19), that the coordination of NAD(H) in close proximity to residues essential for the catalytic activity of D-2-hydroxy acid dehydrogenase enzymes indicates that CtBP proteins are enzymes with specific substrates. Unlike other CtBP protein structures, our model predicts that the poorly conserved C-terminal region of the protein is alpha-helical in nature and wraps back around the target-binding lobe. The implications of this are discussed below.

In order to properly evaluate target binding, dinucleotide binding, and dehydrogenase mutants of dCtBP proteins *in vivo* it was essential that we first show that these functional mutants retain all other normal dCtBP functions in vitro. We began by assessing the overall secondary structure content of the wild type and mutant dCtBP proteins using circular dichroism (CD) as described in Materials and Methods. His-6 tagged wild type and mutant dCtBP protein was purified (Figure 2.1) and CD spectra (average of 3 replicates) taken as described in (66). The wild type protein is largely alpha-helical in nature and none of the mutants grossly disrupt the overall structure of the protein or alter the percentage of helical or β-sheet secondary structures across the protein when compared to the wild type protein (Figure 2.4B).

Dinucleotide binding is an essential function of all known CtBP family members, and it appears to play an important structural and functional role. In order to show that only the dinucleotide binding mutants failed to bind to NAD^+, we performed Equilibrium Dialysis (ED) as described in the Materials and Methods portion of this chapter. All mutant proteins, except for dinucleotide binding mutants G183A, I185D, and C237M, bind to radiolabeled NAD^+ with similar affinity as the wild type protein which has a Kd

of approximately 0.44 μM in my experiments. Most single amino acid residue changes in other functional domains had little or no effect on dinucleotide binding in vitro (Figure 2.4A) with the exception of the V66R mutant protein which has a 10-fold lower affinity for NAD.

GST-pull down experiments were performed, as described in the Materials and Methods section of this chapter, to assess target binding using the PxDLS region of the endogenous dCtBP target protein Krüppel, C-terminally fused to Glutathione-S-transferase (GST). Only dCtBP proteins mutated at A52 and V66 lose the ability to bind to target proteins. Dinucleotide binding mutants (G183A, I185D, and C237M) bind to target protein, and protein mutated at conserved catalytic residues (R266 and H315) behave much like the wild type protein (Figure 2.5). Not only do these proteins retain target-binding capabilities, but the catalytic mutants bind with slightly higher binding in the presence of the cofactor NAD^+ much like the wild type dCtBP protein. This increased affinity is lost with mutants which no longer bind to NAD(H) (Figure 2.5). The interaction with the Krüppel protein is dependent on the presence of an intact PxDLS domain; as mutating the domain to PxASS abrogates binding to wild type dCtBP protein as well as any of the mutants which bound to the PxDLS containing protein; none of the proteins interact with GST alone (Figure 2.5).

Many researchers have proposed that CtBP proteins may function as dimers at the site of repression (19). In order to determine whether dCtBP can self-associate and to evaluate the role that biochemical mutants play in this, we constructed a full-length *dCtBP* cDNA C-terminally fused to GST, expressed and purified protein (GST-dCtBP), and performed GST pull down experiments with purified wild type and mutant proteins.

Wild type dCtBP binds to GST-dCtBP in a concentration dependent manner (Figure 2.6) whereas protein that is mutated at G183, I185, and C237, which are essential dinucleotide binding residues, do not self-associate. The target binding and catalytic mutant proteins self-associate much like the wild type protein (Figure 2.6). Surprisingly, there was no increase in self-association in the presence of NAD^+ the implications of this will be discussed below.

Discussion

The results of our in vitro biochemical analysis of wild type and mutant dCtBP proteins contextualize our *in vivo* findings, confirm that our mutants abrogated only one specific function without causing gross disruptions in the overall structure of the protein thus confounding our *in vivo* data, and determine how removal of one biochemical function ultimately affects the essential biological activity of dCtBP. We've dissected individual biochemical functions to determine how these changes affect biological function.

Comparison of our predicted model of dCtBP to published CtBP structures (27, 30, 32) shows conservation of a bi-lobed structure with SBD and NBD domains creating a cleft proximal to the site of nucleotide binding and coordination of target binding by residues in the N-terminal region. Not only are these overall features similar to those found in other CtBP homologs, but, not surprisingly, the predicted locations of essential residues common to CtBP proteins as well D-2-hydroxy acid dehydrogenase enzymes are conserved. Our model also fits with the hypothesis that CtBP proteins form homodimers, and by comparing Figures 2.3 and 1.4 one can envision two dCtBP monomers coming together in an anti-parallel stoichiometry as predicted for the human protein.

One interesting observation about the dCtBP protein is that, unlike the human forms, it does not seem to form homomultimeric (tetramers) molecules. That is to say that human CtBP1 and CtBP2 purified proteins both form large molecular weight complexes in an NAD^+ dependent manner and dCtBP does not appear to do this (Figure 2.7 A and B). Removal of the C-terminal tail of the human proteins abrogates this phenomenon which implicates it in the regulation of this process (Data not shown). The C-terminal

portion of the human and rat proteins are removed from all crystals structures, but our model of dCtBP indicates that the C-terminal tail is ordered and forms an alpha-helical secondary structure and appears to wrap back around the N-terminal SBD. The ordered nature of the C-terminus may indicate that it does not coordinate higher order CtBP oligomers as has been found with vertebrate CtBPs whose C-terminal tail is thought to be disordered in the monomeric state and whose presence clearly causes crystallization obstacles. An alternative explanation is that higher order oligomerization is lost in *dCtBP* isoform A, but is present in *dCtBP* isoform E which has a long C-terminal extension. It would be interesting to evaluate dCtBP(l) protein for oligomerization.

A number of studies aimed at evaluating the distinct biochemical functions of CtBP proteins utilize multiple mutations or strings of very disruptive amino acid changes to remove specific functions. We made single amino acid changes which not only block functions such as target binding (A52D and V66R), dinucleotide binding (G183A, I185D, and C237M), and putative dehydrogenase activity (R266Q and H315A), but do not disrupt the overall integrity of the protein. We showed this using CD (Figure 2.4B) with proteins which were expressed 16ºC over a longer time period in *E. coli* as opposed to the more commonly used 37ºC induction over a few hours. This was crucial for purifying soluble protein (Figure 2.1). Producing any non-microbial protein in *E. coli* is fraught with challenges but it makes sense from a biological standpoint that *Drosophila* protein produced more slowly at a lower temp would be less prone to problems such as improper folding and precipitation. Our CD studies showed that wild type dCtBP, as well as all the mutants, are mostly alpha-helical in nature with some β-sheet regions which correlates nicely with our three dimensional model.

As we examined disruption of specific functions and how they would play out in an *in vivo* assay, we found that the dinucleotide binding mutants G183A and I185D, which directly interact with NAD(H), and C237M, which is a bulky insertion proximal to the Rossman fold (Figure 1.8), no longer bound NAD^+ (Figure 2.4A). The wild type, A52D, R266Q, and H315A bind NAD^+ with similar affinity, but V66R did exhibit a ten-fold lower affinity. We hypothesized that these disruptions would be replicated *in vivo* as well as other in vitro activity assays. We found this to be true upon examination of dCtBP's ability to bind to the endogenous, PxDLS containing, target Krüppel protein (Figure 2.5). As expected the target binding mutants A52D and V66R did not associate with Krüppel in vitro whereas wild type and all other mutants retained target binding function. Interestingly, although the dinucleotide binding mutants bind target proteins similar to wild type, we did not see an increase in bound target protein with the addition of NAD^+(Figure 2.5: compare wild type, R266Q, or H315A +/- NAD^+ versus G183A, I185D, or C237M +/- NAD^+). Based upon our own observations and those in the literature, we concluded that dinucleotide binding impacts the stoichiometry of binding due to the formation of dCtBP dimers, and proteins that cannot form homodimers bind target proteins in a 1:1 ratio. In order to test this, we performed in vitro self-association studies using our wild type and mutant proteins along with a tagged full-length version of dCtBP. In line with our hypothesis, the dinucleotide mutants no longer bind to wild type dCtBP protein. Also, based upon the observation that addition of NAD^+ to this reaction does not increase self-association in the wild type or mutant proteins; more evidence that dCtBP do not form higher order oligomers like their vertebrate homologs. If NAD(H) is

required for self-association, Why does dCtBP self-associate in binding experiments without NAD(H)?

In conclusion, we generated a three-dimensional structure of the dCtBP Isoform A protein, functionally specific mutants whose overall protein structure is very similar to the wild type protein and retain all other "normal" functions. In forthcoming chapters, these mutants are evaluated for their effect on transcriptional repression in a biologically relevant, non-overexpression, *in vivo* assay.

Tables and Figures

Figure 2.1 – Coomassie stained SDS-PAGE gel: His-6 tagged wild type and mutant dCtBP protein expressed in *E. coli*, purified on Ni-NTA column, followed by Ion Exchange purification, concentrated, and normalized to one another

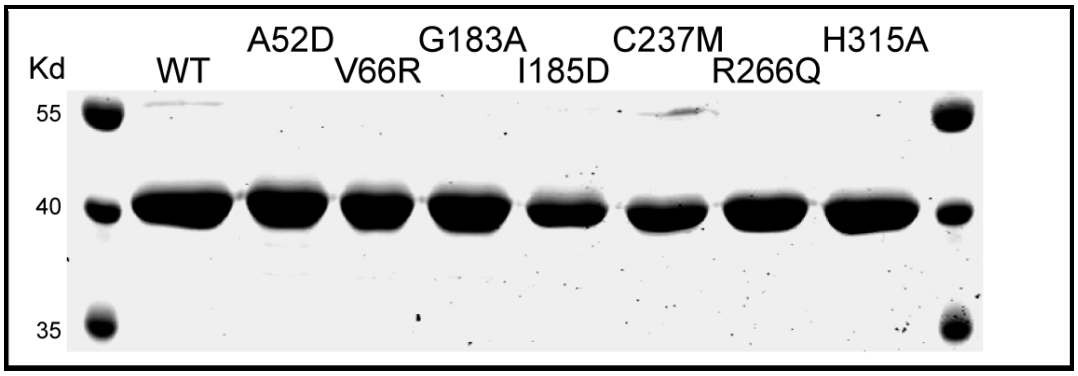

Figure 2.2 – Amino Acid sequence alignment of human CtBP1 (hCtBP1), dCtBP isoforms A and E: Conserved residues highlighted, target binding residues and corresponding mutants (red), NAD binding residues and mutants (green), and putative enzyme residues and mutants (blue)

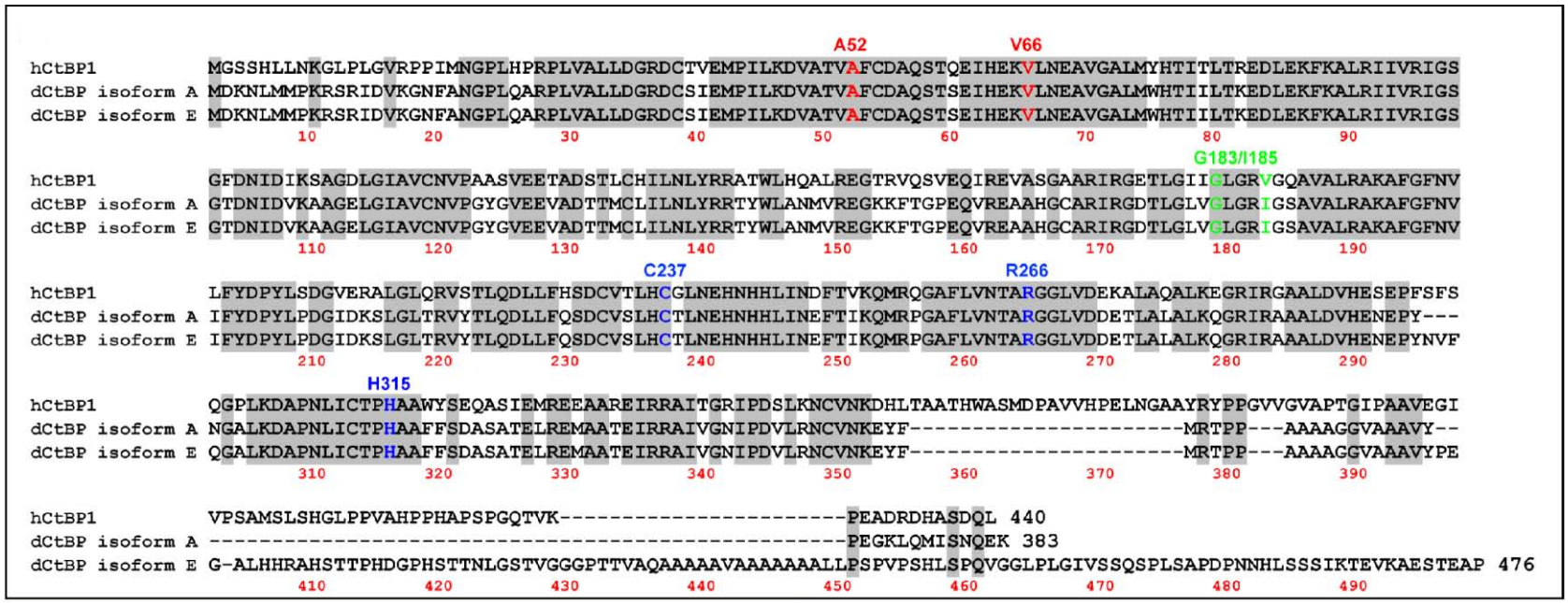
A52
V66
hCtBP1 MGSSHLLNKGLPLGVRPPIMNGPLHPRPLVALLDGRDCTVEMPILKDVATVAFCDAQSTQEIHEKVLNEAVGALMYHTITLTREDLEKFKALRIIVRIGS
dCtBP isoform A MDKNLMMPKRSRIDVKGNFANGPLQARPLVALLDGRDCSIEMPILKDVATVAFCDAQSTSEIHEKVLNEAVGALMWHTIILTKEDLEKFKALRIIVRIGS
dCtBP isoform E MDKNLMMPKRSRIDVKGNFANGPLQARPLVALLDGRDCSIEMPILKDVATVAFCDAQSTSEIHEKVLNEAVGALMWHTIILTKEDLEKFKALRIIVRIGS
10 20 30 40 50 60 70 80 90
G183/I185
hCtBP1 GFDNIDIKSAGDLGIAVCNVPAASVEETADSTLCHILNLYRRATWLHQALREGTRVQSVEQIREVASGAARIRGETLGIIGLGRVGQAVALRAKAFGFNV
dCtBP isoform A GTDNIDVKAAGELGIAVCNVPGYGVEEVADTTMCLILNLYRRTYWLANMVREGKKFTGPEQVREAAHGCARIRGDTLGLVGLGRIGSAVALRAKAFGFNV
dCtBP isoform E GTDNIDVKAAGELGIAVCNVPGYGVEEVADTTMCLILNLYRRTYWLANMVREGKKFTGPEQVREAAHGCARIRGDTLGLVGLGRIGSAVALRAKAFGFNV
110 120 130 140 150 160 170 180 190
C237
R266
hCtBP1 LFYDPYLSDGVERALGLQRVSTLQDLLFHSDCVTLHCGLNEHNHHLINDFTVKQMRQGAFLVNTARGGLVDEKALAQALKEGRIRGAALDVHESEPFSFS
dCtBP isoform A IFYDPYLPDGIDKSLGLTRVYTLQDLLFQSDCVSLHCTLNEHNHHLINEFTIKQMRPGAFLVNTARGGLVDDETLALALKQGRIRAAALDVHENEPY---
dCtBP isoform E IFYDPYLPDGIDKSLGLTRVYTLQDLLFQSDCVSLHCTLNEHNHHLINEFTIKQMRPGAFLVNTARGGLVDDETLALALKQGRIRAAALDVHENEPYNVF
210 220 230 240 250 260 270 280 290
H315
hCtBP1 QGPLKDAPNLICTPHAAWYSEQASIEMREEAAREIRRAITGRIPDSLKNCVNKDHLTAATHWASMDPAVVHPELNGAAYRYPPGVVGVAPTGIPAAVEGI
dCtBP isoform A NGALKDAPNLICTPHAAFFSDASATELREMAATEIRRAIVGNIPDVLRNCVNKEYF----------MRTPP---AAAAGGVAAAVY--
dCtBP isoform E QGALKDAPNLICTPHAAFFSDASATELREMAATEIRRAIVGNIPDVLRNCVNKEYF----------MRTPP---AAAAGGVAAAVYPE
310 320 330 340 350 360 370 380 390
hCtBP1 VPSAMSLSHGLPPVAHPPHAPSPGQTVK----------PEADRDHASDQL 440
dCtBP isoform A ----------PEGKLQMISNQEK 383
dCtBP isoform E G-ALHHRAHSTTPHDGPHSTTNLGSTVGGGPTTVAQAAAAAVAAAAAAALLPSPVPSHLSPQVGGLPLGIVSSQSPLSAPDPNNHLSSSIKTEVKAESTEAP 476
410 420 430 440 450 460 470 480 490

Figure 2.3 – Three dimensional model of dCtBP – Model derived using homology modeling and *ab initio* prediction, mutant forms of the protein shown in red (target binding), green (dinucleotide binding), and blue (catalytic mutants)

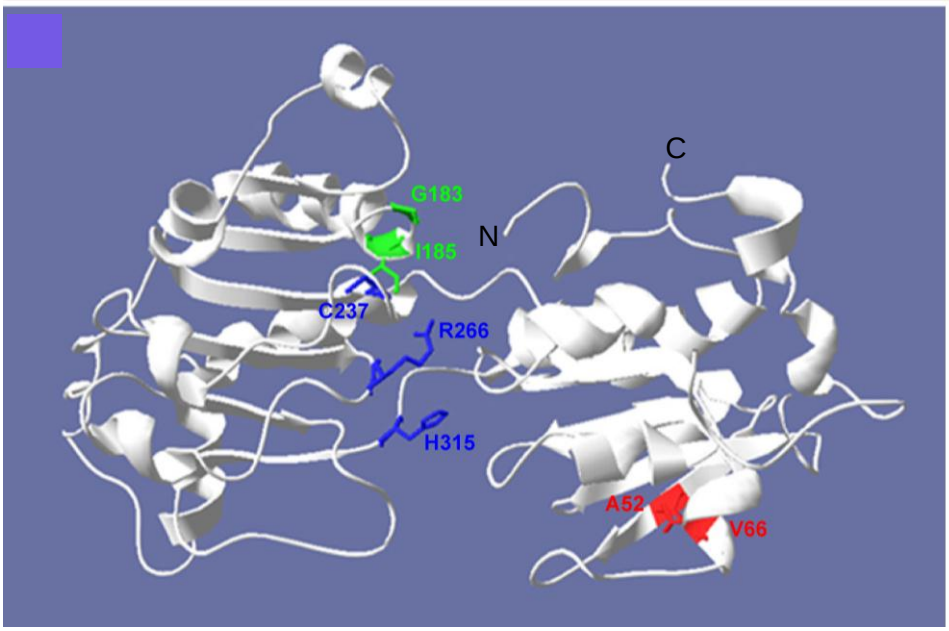

Figure 2.4 – Structure/Function assay of wild type and mutant proteins: (A) Equilibrium Dialysis (ED) binding data from purified wild-type and mutant dCtBP proteins – all units are µM: Single amino acid changes at residues essential for co-factor binding abrogate binding to labeled NAD^+; (B) Circular Dichroism (CD) data for wild-type and mutant proteins. Single amino acid changes do not disrupt the overall structure of dCtBP.

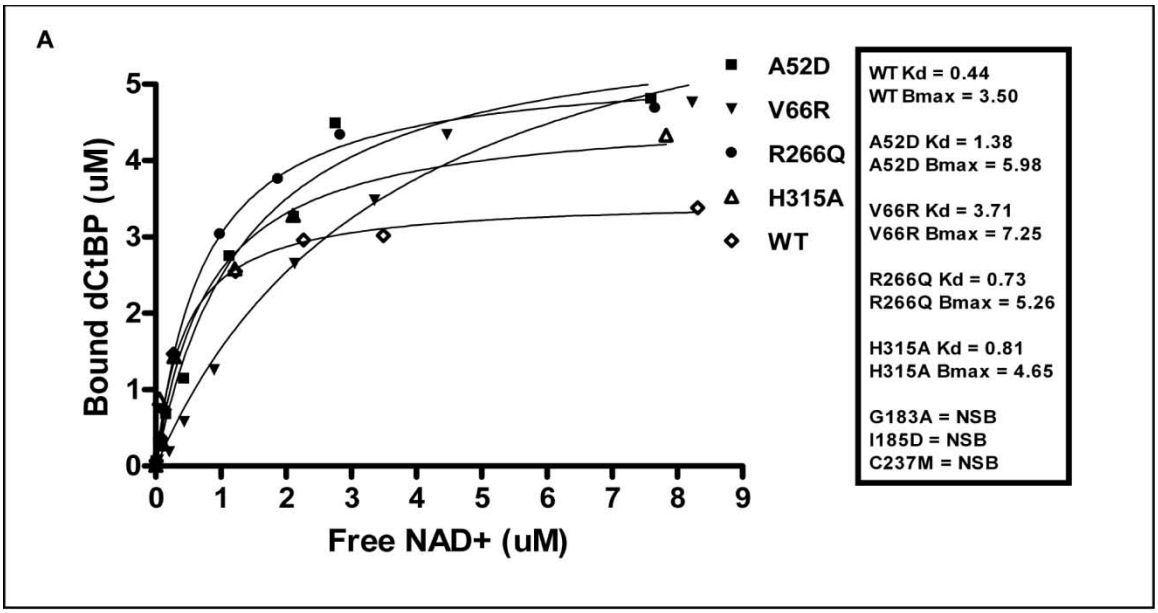

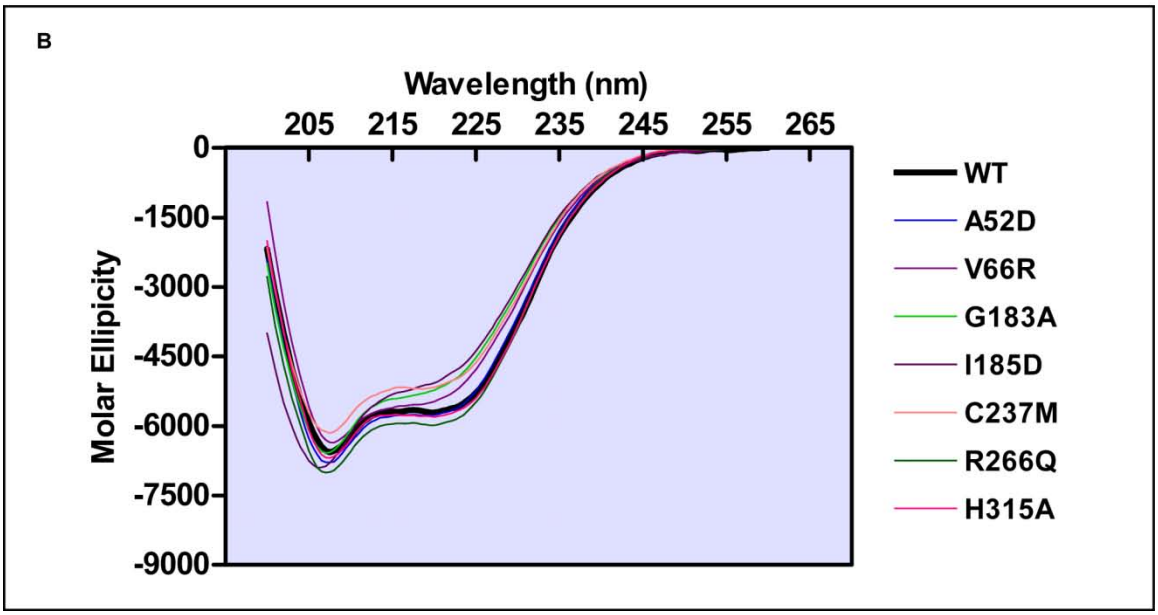

Figure 2.5 – GST-Kr target binding pulldown experiment: Increasing concentrations of wild-type and mutant His6 tagged dCtBP proteins bind to the PxDLS containing region of the Krüppel protein fused to a GST construct (GST-Kr). Co-repressor binding mutants no longer bind to GST-Kr. GST-Kr* (PxASS mutant) no longer interacts with wild-type or mutant dCtBP proteins. Addition of 5uM NAD^+ slightly enhances this interaction

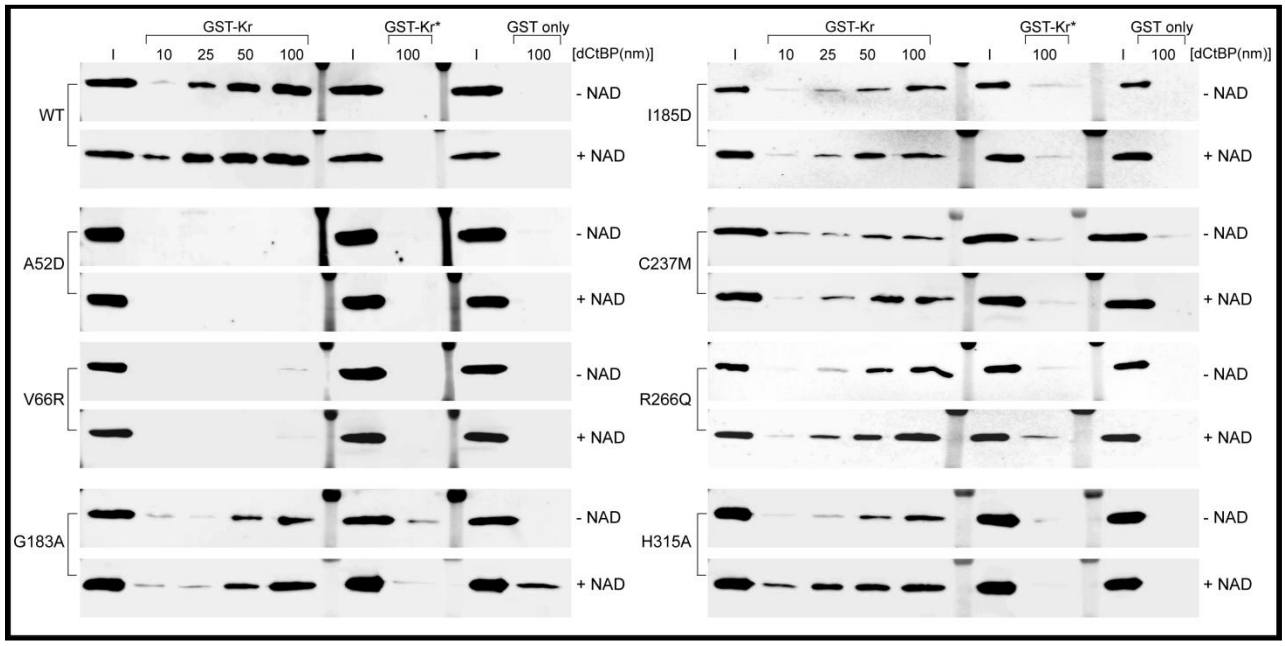

Figure 2.6 – GST-dCtBP pulldown experiments with wild type and mutant proteins: α-His6 western blot of GST-dCtBP pulldown experiment; wild type and mutant proteins that retain NAD^+ binding can self-assemble

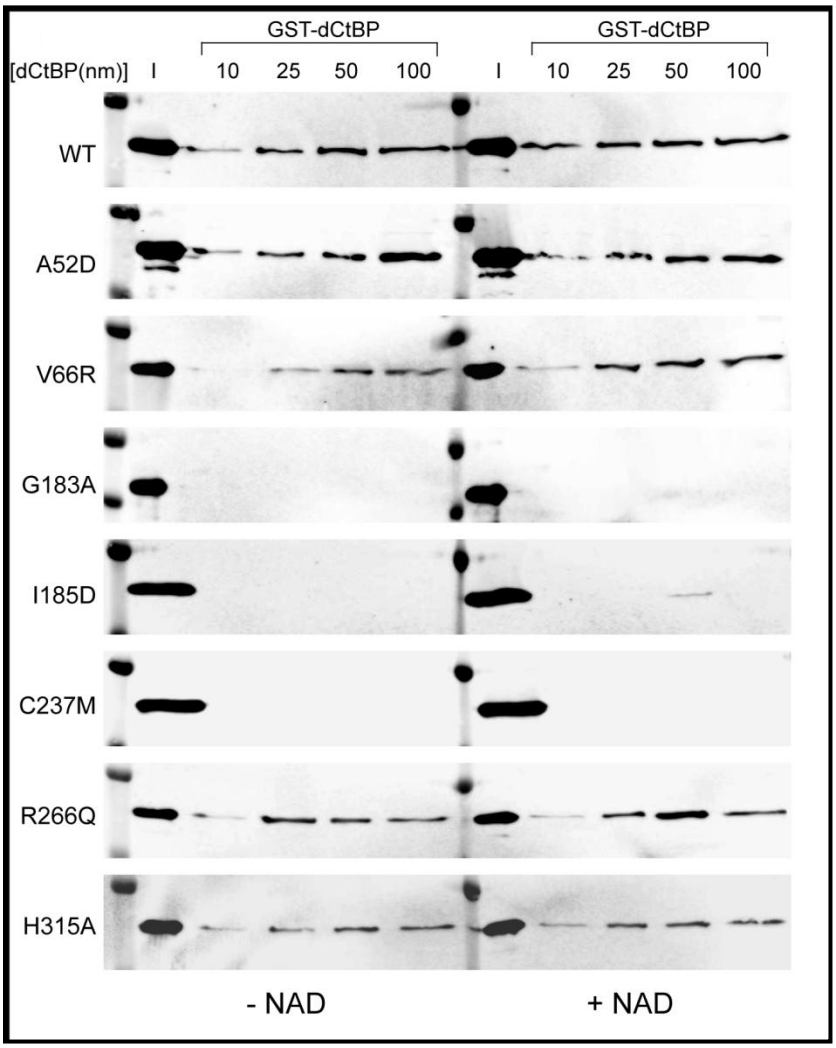

Figure 2.7 – Size fractionation of wild type dCtBP and hCtBP1 proteins:

A – Purified dCtBP protein run on S-200 column +/- NAD^+ compared to size markers

B – Purified hCtBP1 protein run on S-200 column +/- NAD^+ compared to size markers

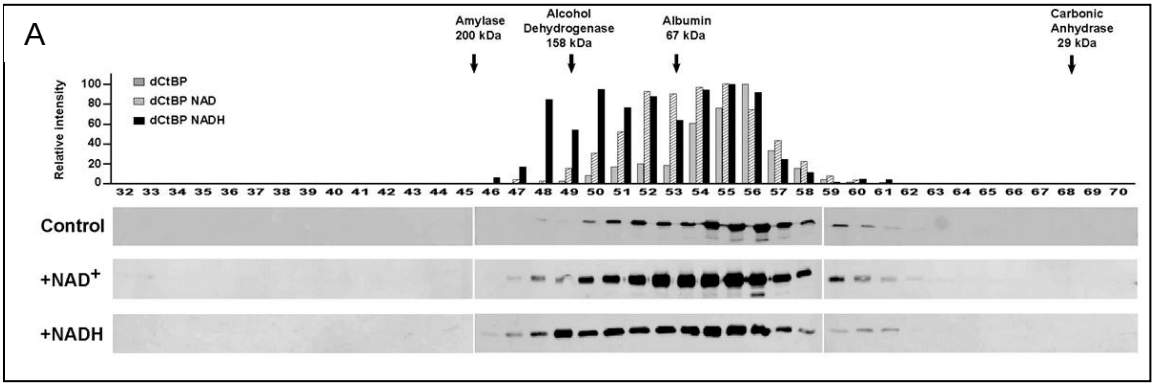

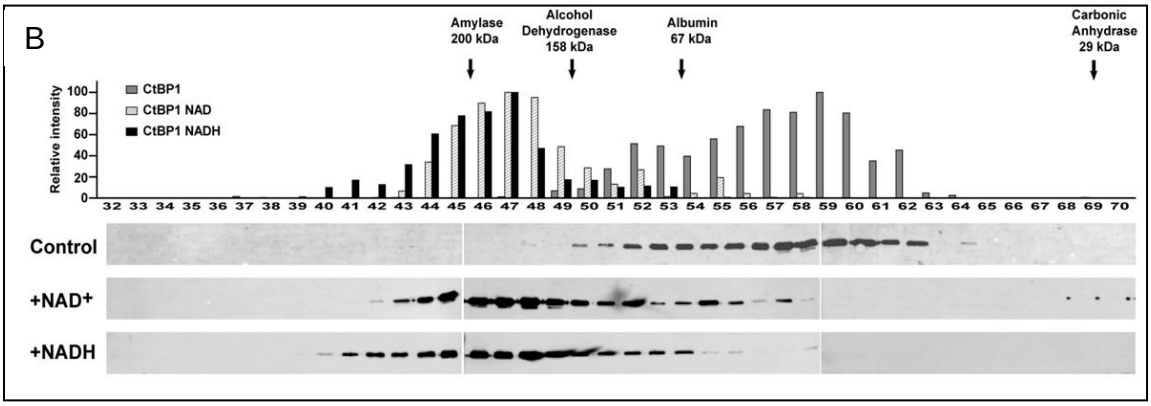

Chapter 3. The role *Drosophila* C-terminal Binding Protein functional domains play in short-range transcriptional repression – GAL4/UAS system

Damian E. Curtis[1], Sarah M. Smolik[2], and James R. Lundblad[3]

[1]*Dept. of Biochemistry and Molecular Biology, Oregon Health Sciences University*

[2]*Dept. of Cell and Developmental Biology, Oregon Health Sciences University*

[3]*Dept. of Medicine, Oregon Health and Sciences University*

Abstract

Drosophila Carboxyl-terminal Binding Protein (dCtBP) is an essential transcriptional repressor during normal embryogenesis. dCtBP's role is to help coordinate the segmentation patterning through interactions with several transcription factors in a concentration dependent manner. Disruption of either dCtBP or its binding partners causes massive changes in the complex signal cascades which, when undisturbed, lead to proper intracellular and cell-cell signaling to achieve normal embryogenesis. Due to the careful dissection of this pathway and fairly clear understanding of dCtBP's role, we were able to establish an *in vivo* assay for dissection of distinct CtBP functions. The work described in this chapter examines the roles of target binding, dinucleotide binding, and dehydrogenase activity in short-range repression of the *eve* locus by ectopically expressing exogenous dCtBP in a null background. Through these experiments we determined that dinucleotide binding is essential for this process and dehydrogenase activity is likely to not play a role in short-range repression.

Introduction

In spite of considerable knowledge of the transcriptional targets of CtBP proteins, the biochemical mechanism of CtBP-dependent co-repression of target genes remains elusive and controversial. In previous chapters we discussed, in detail, the unique characteristics of CtBP family members such as their remarkable similarity to the D-2-hydroxyacid dehydrogenase class of enzymes and the challenge to determine the relevance of this similarity. The close homology of CtBP to dehydrogenases suggests NAD may participate in the function of CtBPs, but the role of the dehydrogenase domain in CtBP function is inconclusive. One has to consider whether or not an intrinsic oxido-reductase enzymatic activity of CtBP is necessary for function; data are conflicting due to the use of artificial, ex-vivo experimental methods.

In this chapter we investigate the distinct CtBP functions in a well-studied, biologically relevant, and CtBP dependent assay. The role of *dCtBP* as a co-repressor for short-range repression, which establish the initial steps for dividing the *Drosophila* embryo into defined body segments, is the best understood biological function of CtBPs. *dCtBP* is an essential co-repressor for the repressive activity of the short-range (<100 base pairs away) repressors in the developing embryo; Knirps, Krüppel, and Snail (34,35,69). Each of these transcription factors contain PxDLS-related sequences, and mutations in this motif cause a loss of some of their respective repressive capabilities. The transcriptional repressors Knirps and Krüppel, termed gap-genes, inhibit nearby activators and repress promoter elements of the pair-rule gene *even-skipped (eve)*. The specific and tightly controlled interactions between these proteins establishes anterior to posterior embryonic segmentation.

The *eve* gene is expressed in a series of 7 stripes of cells (Figure 3.2 A), and this pattern is established by concentration gradients of transcriptional activators and repressors (Figure 1.5 and 1.6). The actual *eve* coding sequence is quite small, but large regulatory regions surround it, both upstream and downstream. Upon binding to a regulatory region, activators such as Bicoid (Bcd) and Hunchback (Hb) drive *eve* expression in a precise region of the embryo. For example, if Bcd is bound to the stripe 2 regulatory region (in the absence of short-range repressors) (Figure 1.7), *eve* expression is on in those cells. However, in the presence of a short-range repressor like Krüppel, activation by Bcd is blocked and *eve* expression is lost. This is the exact process which occurs in cells at the border of *eve* expression. In embryos null for the short-range repressors Krüppel or Knirps, *eve* expression is completely disrupted and the precise formation of the seven stripes is lost. A key observation for our work was that in CtBP null embryos the pattern of *eve* expression mimics the missexpression found in both Knirps and Krüppel mutants (Figure 3.2 B) (35,69). This suggested that CtBP regulates transcription of *eve* via the Knirps and Krüppel transcription factors. Researchers have gone on to show this definitively as well as examine a number of the essential interactions between enhancers and repressors at the *eve* locus. Our understanding of this highly regulated and CtBP-dependent developmental process provides us an opportunity to evaluate *dCtBP's* role in the regulation of *eve* transcription.

In the experiments described in this chapter as well as chapter 4, we use genetic tools to reconstitute *dCtBP* expression in *Drosophila* embryos which are completely null for *dCtBP*. The challenge in studying *dCtBP* in embryos is creating a CtBP null embryo as there is maternally deposited mRNA. We generated maternal and zygotic null embryos

through the construction of germ line clones, and assayed *dCtBP* function in those null embryos. Germ line clones are constructed by forcing recombination on the third chromosome in developing female larvae through a heat-controlled flipase gene. Recombination on the third chromosome results in a female fly with germ cells which are either homozygous for a p-element insertion at the dCtBP locus or have one or 2 copies of a dominant sterile marker. When these female flies are mated to male flies containing a second chromosome homozygous for a GAL4 driver line and the dCtBP p-element insertion, one third of the resulting embryos will be both maternal and zygotic dCtBP nulls. Since both the female and male flies have a UAS-*dCtBP* transgene on the second chromosome, the only dCtBP protein transcribed and translated will be from this transgene. Using this GAL4-UAS system, we express exogenous UAS-*dCtBP* in the null embryo; specifically within the central domain of *Krüppel* embryonic expression using the *Krüppel* promoter region fused to the GAL4 protein. The *Krüppel* promoter region is ideal because it is unaffected by the absence of *dCtBP*, it is tightly regulated, and it eliminates the pitfalls of overexpression systems that have plagued CtBP research. By expressing exogenous dCtBP protein (wild type and mutant forms described in Chapter 2), we determine the functional roles of dinucleotide binding, and the dehydrogenase domain in the short-range repression of *eve* transcription in an *in vivo* setting.

Materials and Methods

Purification of plasmid DNA for construction of transgenic flies

DNA for wild type and mutant pUAST_*dCtBP* constructs were purified using ultracentrifugation in a cesium chloride density gradient for creation of transgenic fly lines by embryo injection at BestGene Inc. (2918 Rustic Bridge, Chino Hills, CA 91709). Cesium Chloride plasmid DNA purification protocol (70): 2 ml of LB plus ampicillin inoculated with single *E. coli* colonies containing wild type and mutant *dCtBP* constructs in pUAST vector, grown at 37ºC for 4 hours with shaking, inoculated 1 L of Terrific Broth (TB) (950 ml diH_2O, 12 g Tryptone, 24 g Yeast extract, 4 ml glycerol, sterilize by autoclaving, cool to room temp, add 50 ml of 2x Potassium Phosphate solution - final concentration is 0.17M KH_2PO_4 and 0.72M K_2HPO_4), added ampicillin to 100 ug/ml, and incubated at 37ºC overnight with shaking. Pelleted cells at 6000 rpm for 15 minutes, resuspended pellet in 60 ml of Solution 1 (25mM Tris-HCl pH8, 10mM EDTA pH8, 15% glucose) by vortexing and pipetting, added 120 ml of Solution 2 (0.5M NaOH, 1% SDS), mixed and placed on ice for 5 minutes, 90 ml of Solution 3 (3M Potassium Acetate pH 5.0) added and mixed, placed on ice for 1 hour. Cellular debris pelleted by centrifugation at 6000 rpm at 4ºC for 20 minutes, and supernatant filtered through sterile cheese cloth, 100 ml of room temperature Isopropanol added, incubated for 30 minutes at room temperature. Centrifuged for 40 minutes at 6000 rpm at 4ºC, supernatant carefully removed, and pellet dried. Pellet resuspended in 7 ml of TE through gentle rocking (several hours), transferred to 14 ml snap cap tube, brought to 10 ml with TE, 1 g CsCl added, 800 ul ethidium bromide stock added, and tubes centrifuged for 20 minutes at 5000 rpm. Supernatant transferred to ultracentrifuge tubes using sterile syringe and 18

gauge needle, entire tube volume filled by adding additional 1g/ml CsCl solution, tubes sealed with metal caps by heating, and spun for at least 20 hours in ultracentrifuge rotor Ti-88 at 55,000 rpm.

After 20 hour spin, tubes removed and main DNA band extracted using sterile syringe and 16 gauge needle, transferred to new ultracentrifuge tube, topped off with 1 g/ml CsCl solution, resealed, and spun at 55000 rpm for another 20 hours. Following second centrifugation step, ethidium bromide labeled DNA bands transferred to a 50 ml screw cap tube using sterile syringe and needle and DNA washed at least 5 times with 15 ml of Butanol saturated with H_2O. All ethidium bromide removed from DNA for successful creation of transgenic flies. Phenol chloroform extraction performed as described in Chapter 2 Materials and Methods and DNA precipitated with 100% ethanol and 0.3M NaOAc. DNA washed with 70% ethanol, dried, and resuspended in 2 ml of TE buffer ph 8.0.

Integrity of plasmid DNA determined by visualization on agarose gel, and DNA quantified using spectrophotometer by measuring optical density (OD) at 260 and 280 nm. The OD 280 nm measurement indicates the amount of protein in the sample and the OD 260 nm reading can be used to calculate the concentration of nucleic acid in the sample. An OD 260 of 1 = 50 ng/ul of dsDNA and protein free samples will have an OD260/OD280 ratio of 1.8 – 2.0. CsCl purified pUAST_*dCtBP* wild type and mutant plasmids re-precipitated, dried, and resuspended in molecular grade H_2O to ~ 1.0 ug/ul concentration, frozen, and sent to BestGene Inc.

Construction of even-skipped in situ RNA probe

One kilobase piece of *eve* coding region PCR amplified from *Drosophila* genomic DNA, generously provided by Kristen Jones in the Forte lab, using F1 and R2 primer pair (Table 3.1). Amplicon digested with Asp718I and NotI restriction enzymes, run out on agarose gel, purified, and ligated to Asp718I/NotI prepared pBSKS vector. Insert Sanger sequenced to confirm identity and absence of PCR inserted nucleic acid changes. Purified plasmid DNA used to generate DIG-labeled RNA probe using the following conditions: 10 ul plasmid DNA,3.2 ul 10X T7 polymerase buffer, 3 ul 1M DTT, 1 ul RNAsin, 3 ul rATP, rCTP, and rGTP, 1.8 ul rUTP, 1.2 ul rDIG-UTP, 2 ul of T7 RNA polymerase enzyme. Polymerase reaction incubated for 2 hours at 37ºC, 3 ul 2X carbonate buffer (120 mM Na_2CO_3, 80 mM $NaHCO_3$, pH solution to 10.2 with NaOH) added, reaction heated to 65ºC for 20 minutes, 65 ul stop solution (0.2 M Sodium Acetate, pH to 6.0 with acetic acid) added. Probe precipitated over night at -20ºC with 19.5 ul 4M LiCl, 13 ul of 20 mg/ml tRNA, 400 ul 100% EtOH. Prode centrifuged at 13,000 rpm for 30 minutes at 4ºC, washed with 70% EtOH (in DEPC H_2O), and resuspended in Hybridization buffer (50% formamide, 5x SSC, 0.05 mg/ml tRNA, 1% SDS, and 0.05 mg/ml heparin) buffer. *Eve* probe (1ul) tested on wild type embryos according to protocol described below (Figure 3.2A) stored at -20ºC until used in embryo staining procedure.

Fly stocks

dCtBP wild type and mutant cDNA lines, *dCtBP* wild type and mutant locus lines, and *Krüppel*-GAL4 transgenic lines were constructed by injection of plasmid DNA purified from CsCl gradient into embryos of strain *yw* by BestGene Inc. using standard procedures (71). Upon receipt of pupae from BestGene Inc., male and females collected

as they eclosed and separated for crosses described below. Multiply-marked fly stock *(+/+; sp/cyo;TM-2/MKRS)* generously provided by Dr. Sarah Smolik. *dCtBP* P-element (*dCtBP*^{03463}) insertion line kindly provided by Dr. Norbert Perrimon (Harvard Medical School, Department of Genetics, New Research Building/RM 339, 77 Avenue Louis Pasteur, Boston, MA 02115). Bloomington stocks 1929 *(P{hsFLP}12, y w*$^{'}$*; sna*^{Sco}*/CyO)* and 2149 *(w*$^{'}$*; P{neoFRT}82B P{ovoD1-18}3R/ TM3, Sb)* purchased from the stock center and used as described below.

Construction of dCtBP^{03463}*, UAS-dCtBP wild type and mutant fly stocks*

Males and female flies from injected embryos provided by BestGene Inc. were crossed to multiply-marked flies *(+/+; Sp/CyO;TM-2/MKRS)* with the presence of red eyes in the F1 population indicating successful insertion of the transgene. Using *yw* (+/+;+/+) males and females, the transgenes were mapped to a chromosome. Red eyed flies containing *UAS-dCtBP*, wild type and mutant, insertions residing on chromosome II *(w'/w;UAS-dCtBP/UAS-dCtBP;+/+)* were crossed with multiply-marked white eyed flies (*w/y*; *Sp/CyO;MKRS/TM-2).* Red-eyed F1s with the genotype (*w'/w;UAS-dCtBP*/*CyO*;+/*TM-2)* collected and crossed to white-eyed males (*w/y;Sp/CyO;dCtBP*^{03463}*/MKRS)* which were constructed in the same manner using the *dCtBP*^{03463} P-element insertion stock and the multiply-marked stock. Through sibling mating, stocks for wild type and mutant *UAS-dCtBP* transgenes *(w'/w;UAS-dCtBP/UAS-dCtBP;dCtBP*^{03463}*/TM-2)* were constructed and maintained. All wild type and mutant *UAS-dCtBP* lines confirmed as inducible by GAL4 protein by crossing to *prd*-GAL4

(provided by Dr. Sarah Smolik), collecting staged embryos as described below, and staining for FLAG epitope tag (data not shown).

Construction of Krüppel-GAL4 fly stock

Six kilobases of the promoter region from the *Krüppel* locus was cloned into plasmid vector pCDNA3 by digesting the Bacterial Artificial Chromosome (BAC) RP98 (Children's Hospital and Research Center at Oakland) with the restriction enzymes SalI, XbaI, and Asp718I and ligating fragment to a SalI/Asp718I prepped plasmid vector pBSKS. Digests performed for several hours and run on a 0.4% low melting point agarose gel at 25 volts alongside a High Molecular Weight DNA ladder and a 1 kb DNA ladder. DNA restriction fragments between 5 and 7 kb were excised from the agarose gel and eluted, by electrophoresis, into 0.5x TBE (1X TBE – 10.8 g Tris Base, 5.5 g Boric acid, and .93 g EDTA in 1 L H_2O) and bromophenol blue (to visualize the collection tube on gel elution apparatus). Eluted DNA was ethanol precipitated, dried, washed, and resuspended in TE pH 8.0.

Separately a 1.2 kb portion of the endogenous promoter region between the 3' SalI site of the Asp718I/SalI fragment, described above, and the start of *Krüppel* transcription was PCR amplified, cleaned, digested, and ligated into SalI/NotI prepared plasmid vector pBSKS using the endogenous 3' SalI site and a unique 5' NotI site inserted during PCR amplification (Table 3.1). Identity of insert and absence of PCR introduced mutations were confirmed by Sanger sequencing the purified plasmid with BSKS top and -20 primers. Finally the 6 kb Asp718I/SalI and 1.2 kb SalI/NotI fragments were three-way ligated with a modified, Asp718I/NotI prepared P-element pC3G4 vector

upstream of the GAL4 gene to complete the *Krüppel*-GAL4 driver line, (Figure 3.1i – Left and 3.1ii - Left) The original pC3G4 (Drosophila Genomics Resource Center catalog #1224) multiple-cloning-site (MCS) was modified by digestion with SacII and BamHI and ligation with a double stranded oligo with a SacII compatible 5' end and a BamHI compatible 3' end. Successful modification was determined by Sanger sequencing of the purified plasmid DNA using pC3G4 sequencing primers (Table 3.1). The MCS oligo which included Asp718I, NotI, SbfI, KpnI, SacI, and EcoRI restriction sites was induced to form a double stranded DNA oligo by combining the top and bottom oligos together in TE buffer, heating to 95ºC for 2 minutes, and cooling slowly at room temperature.

Circular plasmid DNA of high concentration and purity purified using cesium chloride protocols and sent to BestGene Inc. to make transgenic flies as described above. Flies containing the *Krüppel*-GAL4 transgene were mapped to chromosome II as described above and crossed to the *dCtBP* P-element insertion on chromosome III (*w'/w*;*Krüppel*-GAL4/ *Krüppel*-GAL4; $dCtBP^{03463}$/*TM-2)* using the same crossing scheme as used for the *UAS-dCtBP* fly stocks. Endogenous promoter activity was confirmed by crossing transgenic *Krüppel*-GAL4 males with transgenic UAS-*dCtBP* wild type females, collecting staged embryos, staining for FLAG epitope tag, and visualizing as described below (Figure 3.1iii).

Construction of Heat-Shock Flipase stock

Heat shock flipase *(P{hsFLP}12, yw';Sp/CyO;TM-2/MKRS)* stock was generated in the following manner. Bloomington stock 1929 *(P{hsFLP}12, y w'; sna^{Sco}/CyO)* crossed to multiple marked females (*w'/w'*; *Sp/CyO;MKRS/TM-2)* and female F1s

marked with *sp* on the second and *TM-2* or *MKRS* on the third chromosome were collected *(P{hsFLP}12,yw/w'; Sp/CyO;+/TM-2 or MKRS)* and crossed to make *(P{hsFLP}12, yw';Sp/CyO;TM-2/MKRS)* fly stock.

Creation of maternal and zygotic dCtBP null germline clones

P{hsFLP}12, yw';Sp/CyO;TM-2/MKRS virgins collected and crossed to Bloomington stock 2149 *(w';P{neoFRT}82B P{ovoD1-18}3R/ TM3, Sb)* males. Male *P{hsFLP}12, yw';Sp or CyO/+; P{neoFRT}82B P{ovoD1-18}3R /TM-2 or MKRS* flies collected and crossed to virgin *w'/w;UAS-dCtBP/UAS-dCtBP; dCtBP^{03463}/TM-2* flies. Males and females combined for 3 days at 25ºC and, when vials contained mostly first instar larvae (2-3 days at 25ºC), all flies removed and vials heat shocked in a 37°C water bath for one hour twice a day for 3 days to induce heat shock-FLPase gene. Adult flies as collected as they eclose and virgin *P{hsFLP}12, yw';* UAS-*dCtBP/+; P{neoFRT}82B P{ovoD1-18}3R / dCtBP^{03463}* crossed to male *Krüppel*-GAL4 driver (*w'/y*;GAL4-*Krüppel*/GAL4-*Krüppel*;*dCtBP^{03463}*/*TM-2*).

Embryo collection and fixing

Fifty or more virgin female flies (*P{hsFLP}12, yw';* UAS-*dCtBP/+; P{neoFRT}82B P{ovoD1-18}3R / dCtBP^{03463})* combined with ten to fifteen males (*w'/y*;GAL4-*Krüppel*/GAL4-*Krüppel*;*dCtBP^{03463}*/*TM-2*) and after 2-3 days stage 5 embryos collected from females laying at 30°C. Embryo collections were performed by placing males and females in an empty black fly collection bottles on top of apple juice/agar egg laying plates (200 ml dH_2O, 4 g Bacto-Agar, 6.6 g Sucrose, boiled, mixed,

cooled; 66 ml Apple Juice, 0.7 g Mold Inhibitor (Methyl 4-hydroxybenzoate - Sigma cat# H6654) dissolved in 2.8 ml 100 % Ethanol, poured into 20 cm petri dishes, cooled) spotted with bread yeast paste. Females allowed to lay for one hour at 30ºC, flies removed, plates stored at 30ºC for approximately 3 more hours. Plates removed, embryos collected, and fixed. Embryos washed off egg-laying plates with dH_2O into collection screens, rinsed with copious amounts of dH_2O, dechorionated in 50% bleach solution for 2 minutes, washed with copious amounts of dH_2O, transferred to a 2 ml eppendorf tube containing 500 ul 4% paraformaldehyde and 500 ul heptane. Embryos fixed for 30-40 minutes at room temperature with constant, aggressive back-and-forth mixing. Paraformaldehyde removed and 500 ul of methanol added to the embryos and heptane. Tubes mixed vigorously heptane and methanol removed, embryos washed two times with methanol, and stored at -20ºC. Embryo collections performed 3 times a day until the females stop laying at a high rate, approximately 10 days. Embryos stable when stored at -20ºC in methanol for months.

Embryo in situ, immunohistochemistry and fluorescent staining

Brief staining protocol: embryos prepared for two-stage fluorescent labeling using standard protocols (72). Visualization of *eve* mRNA transcript performed using in situ digoxigenin (DIG) labeled RNA probe followed by an anti-DIG-HRP primary antibody and fluorescent labeling, and FLAG tagged UAS-*dCtBP* transgenes visualized with a mouse anti-FLAG primary antibody, anti-mouse secondary antibody, and fluorescent labeling. Sequential staining of embryos was accomplished using Tyramide Signal Amplification (TSA) reagents from Invitrogen (73). The TSA kit protocol was used with

the following modifications. Embryos hybridized for approximately 20 hours at 60°C with DIG-labeled *eve* RNA probe. After removal of the *eve* probe, embryos probed overnight at 4°C with sheep anti-DIG-HRP (Roche) and mouse anti-FLAG antibodies (Sigma). TSA reaction fluorescently labels the *eve* probe with Tyramide 488 Alexa Fluor followed by probing with anti-mouse-HRP secondary antibody and a second tyramide signal amplification reaction to label the FLAG tagged transgene with Tyramide 568 Alexa Fluor.

Detailed three day staining protocol:

Day one: embryos removed from -20ºC storage, washed three times with methanol, incubated for 1 hour at room temperature in 1000 ul of xylene mixed with 500 ul of ethanol followed by 5 washes with ethanol, two washes with methanol, and three washes with 1X phosphate buffer solution + 0.1% triton-X (PBT). Embryos re-fixed in 4% paraformaldehyde + PBT for 20 minutes with gentle rocking at room temperature followed by three five minute washes in PBT. Embryos mixed for 5 minutes in 500 ul of PBT and 500 ul of Hybridization followed by three washes with hybridization buffer over the course of one hour at 60ºC. DIG labeled RNA probe (see above for construction) heated for 3 minutes at 80ºC, cooled on ice for 3 minutes, added to embryos, and incubated over night at 60ºC.

Day two: embryos washed at 60ºC with 400 ul of pre-warmed hybridization buffer twice for 15 minutes, once for 15 minutes with 600 ul of 3:1 Hyb:PBT, one time for 15 minutes with 600 ul of 1:1 Hyb:PBT, and one time for 15 fifteen minutes with 1:3 Hyb:PBT. Embryos washed 2 more times with 60ºC PBT only for 15 minutes and 3 times for 10 minutes with room temperature PBT. All room temperature wash steps carried out

with gentle rocking. Embryos gently rocked in 500 ul of blocking reagent from TSA Kit (Invitrogen Catalog #T20912) for 1 hour at 4ºC. Embryos incubated overnight at 4ºC with gentle rocking in PBT + blocking reagent and mouse anti-FLAG primary antibody diluted 1:7000 and sheep anti-DIG-HRP diluted 1:500.

Day three: embryos washed 6 times for 10 minutes with PBT at room temp with gentle rocking. Tyramide labeled Alexa Fluor 488 probe diluted to 1:50 and incubated with embryos for 1 hour at room temperature. All washes use 500 ul and are performed in the dark with gentle rocking from this point forward. Embryos washed for 1 minute 4 times with PBT and 2 times with phosphate buffer solution (PBS) alone. HRP activity of the Tyramide-488 is quenched in a 1% hydrogen peroxide solution in PBS for 15 minutes. Embryos washed 3 times in PBT for 10 minutes per wash. A 1:200 dilution of anti-mouse-HRP secondary is made (Invitrogen TSA kit T20914) and embryos incubated for 2 hours at room temperature. Embryos washed 3 times in PBT and 3 times in PBS, 10 minutes each. A 1:100 dilution of Tyramide labeled 569 Alexa Fluor made and embryos incubated for 1 hour at room temperature. Embryos washed 3 times with PBT and 3 times with PBS, 10 minutes each. Embryos transferred to slow fade mounting solution (Invitrogen) and stored overnight at 4ºC prior to mounting onto microscope slides.

Confocal Microscopy: Image capture and analysis

Embryos are mounted in anti-fade mounting media and visualized on a Zeiss LSM710 laser scanning confocal microscope. All confocal microscopy performed at the Oregon Health and Sciences Advanced Light Microscopy Core (http://www.ohsu.edu/xd/research/research-cores/almc/) located in the fourth floor of the

Biomedical Research Building. The LSM710 is mounted on a fully motorized AxioObserver Z1 inverted microscope stand with a motorized stage. This system allows one to acquire images of large areas using two or three lasers simultaneously. For all embryo images collected, the 457/488/514nm Argon laser was used to capture the Alexa Fluor 488 emission signal and the 561nm DPSS laser used to capture the Alexa Fluor 568 emission signal. Desired embryos identified using ocular lens, briefly scanned for positioning, signal optimization, and Z-stack setup; followed by automated scan of entire embryo with 30 individual Z-stacks per embryo. Images saved, analyzed, and compressed into 2-dimensional image using Zeiss Zen Light imaging software.

Western blot of UAS-dCtBP transgenic embryos

Approximately 25 dechorionated embryos from GAL4-UAS and *yw* embryo collection washed 5 times for 10 minutes with PBT. PBT removed and 20 ul of 2X Tris-glycine SDS-Polyacrylamide Gel loading buffer added to embryos. Samples heated at 95ºC for 10 minutes, embryos ground up using mortar and briefly centrifuged. Lysed embryo samples (10 ul) loaded into gel lanes along with protein ladder and FLAG positive control, run out on two 10% SDS-PAGE gel, transferred and western blot performed as described in Chapter 2 Materials and Methods. PVDF membrane probed with either mouse anti-FLAG primary antibody or anti-β-actin primary antibody diluted 1:8000 in 1:1 TBST and Blocking Buffer overnight at 4ºC overnight with gentle rocking. Primary antibody collected, PVDF membrane washed at least 4 times for 15 minutes with TBST, probed with anti-mouse Alexa Fluor 680 diluted 1:6000 in 1:1 TBST and Blocking Buffer for 2 hours at room temperature with gentle rocking followed by at least

4 washes for 15 minutes with TBST. Membrane visualized on Odyssey infrared imaging instrument (Li-COR) (Figure 3.3).

Results

In order to develop an *in vivo* assay to assess whether or not regulation of short-range repression of *eve* transcription by *dCtBP* requires cofactor binding, dehydrogenase activity, or both, we constructed FLAG-epitope tagged transgenic flies as described in the materials and methods which contain a GAL4 responsive UAS-*dCtBP* insertion on Chromosome II for the wild type protein as well as Alanine 52 to Aspartic Acid (A52D), Valine 66 to Arginine (V66R), Glycine 183 to Alanine (G183A), Isoleucine 185 to Aspartic Acid (I185D), Cysteine 237 to Methionine (C237M), Arginine 266 to Glutamine (R266Q), and Histidine 315 to Alanine (H315A) (Figure 3.1 i – right). We also constructed a GAL4 transgenic fly which contains the essential, for proper embryonic expression, promoter regions from the *Drosophila* gap gene *Krüppel* upstream of the GAL4 protein (Figure 3.1 i – left). By combining these two transgenes into one fly (Figure 3.1 ii), we "drove" the expression of the UAS-transgene in a tightly controlled region of the developing embryo (Figure 3.1 iii). This *in vivo* assay allows for monitoring distinct *dCtBP* functional domains in a well understood and relevant biological system. We monitor *dCtBP* activities by evaluating *eve* transcription in our *in vivo* assay. *Eve* transcription is measured by in situ hybridization using a DIG-labeled RNA probe, see Materials and Methods for construction, which hybridizes to *eve* mRNA in the embryo (Figure 3.2 A, B).

Proper experimentation of exogenous dCtBP wild type and mutant forms in the developing embryo requires removal of both maternal and zygotic dCtBP protein. We generated maternal and zygotic *dCtBP* null germ line clones as described in the Materials and Methods portion of this chapter. Heat shock activation of the FLP recombinase

induces mitotic recombination in the ovaries; only eggs that have had a recombination event induced in them and have lost the dominant female sterile (DFS) mutation, *ovoD1,* and with it the normal CtBP allele present on the same chromosome arm will survive. Within these germ line clones, the only dCtBP protein made is derived from the transgene which we've inserted and by utilizing the GAL4-UAS system the region of dCtBP transcription/translation is restricted to cells which are actively making GAL4 protein. The fusion of the *Krüppel* promoter region to the GAL4 gene ensures tightly regulated GAL4 production only in the central domain of stage 5 (~2.75 hours post fertilization) embryos. With these two transgenes in a *dCtBP* null embryo we express wild type or mutant dCtBP protein function in the central domain of the embryo while evaluating regulation of *eve* transcription (Figure 3.1 ii, iii, and Figure 3.4).

Embryos collected from crossing UAS-transgene containing flies, which have been induced to form germ line clones, with our *Krüppel*-GAL4 transgene express FLAG-tagged dCtBP. Embryos from wild type, A52D, V66R, G183A, I185D, C237M, R266Q, and H315A crosses were lysed and run out on an SDS-PAGE gel. Western blot for FLAG identified dCtBP-FLAG specific bands at the appropriate size when compared to embryos collected from *yw* females (Figure 3.3). One third of the embryos collected from each (wild type or mutant) screen are null for zygotic and maternal dCtBP and they will not express any dCtBP due to the absence of the *Krüppel*-GAL4 driver line. The presence of these embryos indicates that germ line clones have been created in each individual cross and assay. These null embryos also exhibit the well-characterized disruption of the normal seven-stripe *eve* transcription pattern; we, like others (38),

observe fusion of stripes 2 and 3, loss of stripes 4 and 5, and fusion of stripes 6 and 7 (Figure 3.2 A, B).

Embryos collected from the germ line clone protocol were probed for FLAG-tagged protein and *eve* transcription is monitored. The Materials and Methods describes this labor intensive process in detail; embryos processed this way have FLAG-tagged protein labeled with a red fluorescent probe (Alexa Fluor 568) and *eve* mRNA is labeled with a green fluorescent probe (Alexa Fluor 488). *dCtBP* null embryos expressing a wild type *dCtBP*-transgene exhibit partial rescue of *eve* stripes 4 and 5 (Figure 3.4A – see arrows) when compared to null embryos collected from the same screen (Figure 3.4I). Embryos expressing A52D and V66R mutant transgenes exhibit *eve* transcription which is similarly disrupted as the null embryo (Figure 3.4B, C). Embryos expressing the dinucleotide binding mutant transgenes (G183A, I185D, and C237M) exhibit *eve* transcription which is also quite similar to the null embryo (Figure 3.4 D, E, F). Embryos expressing the putative dehydrogenase mutants exhibit partial *eve* rescue similar to the wild type transgenes in both level of activity and specificity (Figure 3.4G, H, J). All *dCtBP* mutants were evaluated with two distinct transgenes from separate insertion events to eliminate genomic positional affects.

Discussion

In this chapter we established a biologically relevant *in vivo* assay for evaluating the roles that dinucleotide binding and the dehydrogenase domain play in short-range transcriptional repression at the *eve* locus in the developing embryo. Our *in vivo* model specifically expressed exogenous *dCtBP* wild type and mutant proteins, in null embryos, within the tightly controlled *Krüppel* expression domain (Figure 3.1 ii and iii). It is well established that repression of *eve* enhancers by *Krüppel* at the posterior border of *eve* stripe 2 is accomplished through short-range repression and is a dCtBP-dependent phenomenon. Our expectation based upon this previous knowledge was that the wild type UAS-*dCtBP* transgene would "rescue" *Krüppel* mediated *eve* repression within the domain of *dCtBP* production. Surprisingly this is not what we found. Instead we found that our wild type transgene rescued, albeit at low levels, proper *eve* transcription at stripes 4 and 5 with little noticeable effect on *eve* stripes 2 or 3 as they appear to be fused into one large band similar to *dCtBP* null embryos.

Another gap protein, Knirps, also regulates *eve* transcription via dCtBP-dependent short-range repression. Knirps concentration within the developing embryo is very tightly regulated, much like Krüppel, and at the time when *eve* is transcribed in its classic 7 stripe pattern Knirps levels are highest in the embryonic region around *eve* stripes 4 and 5 (Figure 1.6). In *dCtBP* null embryos, stripes 4, 5, and 6 are either very diffuse and nearly invisible or fused into one large bright band (compare Figure 3.2 B and 64 Figure 6Aii). The differences between the *eve* levels in these embryos may be due to the staining procedure or slight differences in the stage of the embryo. Whether through proper repression or a concentration of signal effect, the addition of exogenous wild type *dCtBP*

in a null background rescues Knirps mediated repression of the posterior borders of stripes 4 and 5 (Figure 3.4A). We know this is a dCtBP-target mediated event because UAS transgenes which do not bind to target are unable to rescue *eve* transcription in stripes 4 and 5. In addition, this is dependent upon dinucleotide binding, but independent of dehydrogenase activity as these mutants look the same as the wild type rescue experiments. This is an important finding and when coupled with the results from Chapter 2, dinucleotide binding clearly plays a very important role in *dCtBP* function. One can conclude from this data that short-range repression requires dCtBP protein that binds NAD(H). A reasonable explanation of this is that in order for dCtBP to function properly in this biological context, it has to be able to self-associate as dinucleotide mutants no longer are able to do so.

Why did the wild type UAS-*dCtBP* transgene fail to rescue Krüppel dependent *eve* repression at the posterior border of stripe 2? There are at least two potential explanations for this result. As outlined in Chapter 1, coordination of embryogenesis is absolutely dependent upon the proper regulation of protein concentrations in space and time. Our assay simply may not replicate the "normal" concentration of dCtBP thus Krüppel is unable to repress Giant and Bicoid activation of *eve.* This hypothesis is supported by the fact that in order to visualize our FLAG epitope tagged transgenes, we had to enzymatically amplify the fluorescent signal, as describe in the Materials and Methods section of this chapter. In addition, careful examination of the stained embryos shows that the *Krüppel*-GAL4 driver line is behaving as it should, and the domain of activation is centrally located within the embryo with the highest concentration right in the middle of the embryo. This high concentration of *Krüppel*-GAL4 driven UAS-

transgene protein falls right on top of the partial rescue of stripes 4 and 5 observed. It is also well known that due to both maternal and zygotic mRNA, dCtBP protein is normally present throughout the entire embryo. It is not clear what the normal concentration of dCtBP is, and quite possibly it is in much higher concentration relative to the Krüppel protein. As Krüppel levels rise around stripe 2 in a wild type embryo, there may be an abundant supply of dCtBP which is not the case in our GAL4-UAS system.

An alternative explanation is that there are separate and distinct functions of each *dCtBP* isoform in the developing embryo. It has been shown that *dCtBP* isoform A and E (dCtBP(s) and dCtBP(l)) are found in the embryo as well as the adult fly (38) but it is unclear what each isoform is doing in the embryo. It is possible that dCtBP-dependent short range repression of *eve* is isoform specific, and since our assay only expressed *dCtBP* isoform A we were unable to rescue *eve* transcription in other regions of the embryo and/or through other co-repressors.

Despite the unexpected result, the *in vivo* assay for dissecting distinct *dCtBP* biochemical functions answered the key question: Does dCtBP-dependent short-range transcriptional repression require dCtBP dehydrogenase residues? It seems rather clear that the answer is no. These residues are clearly dispensable for this important *dCtBP* function. Chapter 4 examines some of the same questions in a different manner, and sheds some light on the new questions which arose from the data in Chapter 3.

Tables and figures

Table 3.1 – Primer list

dCtBP_F2	AATCTGATGATGCCGGCGGTACCGGATCCACGCCACCATGGACAAA
dCtBP_R	GCTCTAGACTACTCGAGCTTTTCTTGATTTGATATCATTTGTAG
dCtBP_A52D_top	TAAAGGATGTGGCCACGGTCGACTTTTGCGATGCACAAAGCACC
dCtBP_A52D_bot	TGCTTTGTGCATCGCAAAAGTCGACCGTGGCCACATCCTTTAGG
dCtBP_V66R_top	ACCTCCGAAATACACGAGAAGAGGCTCAACGAGGCAGTGGGAGC
dCtBP_V66R_bot	TCCCACTGCCTCGTTGAGCCTCTTCTCGTGTATTTCGGAGGTGC
dCtBP_G183A_top	TTGGGTCTGGTGGGACTGGCGCGCATTGGTAGCGCCGTGG
dCtBP_G183A_bot	ACGGCGCTACCAATGCGCGCCAGTCCCACCAGACCCAAGG
dCtBP_I185D_top	ACCTTGGGTCTGGTGGGACTGGGCCGCGATGGTAGCGCCGTGGC
dCtBP_I185D_bot	GCCACGGCGCTACCATCGCGGCCCAGTCCCACCAGACCCAAGG
dCtBP_C237M_top	TCCGATTGCGTCTCACTGCATATGACGCTCAACGAGCACAACC
dCtBP_C237M_bot	TGTGCTCGTTGAGCGTCATATGCAGTGAGACGCAATCGGACTGG
dCtBP_R266Q_top	CATTTCTGGTGAACACTGCACAAGGCGGTCTGGTCGATGACG
dCtBP_R266Q_bot	CGTCATCGACCAGACCGCCTTGTGCAGTGTTCAGGAGAAAT
dCtBP_H315A_top	AAATCTGATTTGCACACCGGCCGCCGCCTTCTTCAGCGACG
dCtBP_H315A_bot	CGTCGCTGAAGAAGGCGGCGGCCGGTGTGCAAATCAGATTTGG
dCtBP_E295A_top	CCTGGACGTTCACGAAAACGCGCCTTACAATGTATTTCAAGT
dCtBP_E295A_bot	ACTTGAAATACATTGTAAGGCGCGTTTTCGTGAACGTCCAGG
Kr_SalI_NotI_F1	TCTTTGAGACTTTGCTCAACAG
Kr_SalI_NotI_F2	AAACTGAACTTCCACGTCTTTG
Kr_SalI_NotI_R1	GTGCTCCTAATTTTGTGCTCGCACGGCGGCCGCATAGCT
Kr_SalI_NotI_R2	ACACCTATAATATTCGCCTTCGAGGGCGGCGCGATAGCT
pC3G4_MCS_seqF	CAGGTACCTGAGCTCCACG
pC3G4_MCS_seqR	ATCCACTGAATTCGAGCGG
PC3G4_MCS_bot	GATCCACTGAATTCGAGCGGCCGCCGTGGAGCTCAGGTACCTGTCCTGCAGGGCGC
BSKS_20	GTAAAACGACGGCCAGT
BSKS_top	GGAAACAGCTATGACCATG
Kr_GST_F1	ACGGATCCGTGGCAATCTCCGCAATTGCTA
Kr_GST_F2	GTTCTAGACGTGGCAATCTCCGCAATTGCTA
Kr_GST_R1	TGAAGCTTCTAATGTTGTTGATGGCCCATATA
Kr_DLAS_top	AGGACGATGGTCCATTGGCTTCGTCTGAAGATGGAGCCAG
Kr_DLAS_bottom	CTGGCTCCATCTTCAGACGAAGCCAATGGACCATCGTCCT
eve_probeF1	ACTGCGGCCGCACCGAACCTACAACATGGAG
eve_probeR1	CTAGGTACCATGCATATGAGGACCAGCG
eve_probeF2	ACTGCGGCCGCCGGATAACTCCTTGAACGGC
eve_probeR2	CTAGGTACCTTGAAGAGCTTCGGCTTGG

Table 3.2 – Primer list

dCtBPloc_Frag1_for	TTCCTGCAAAATCGCCTGGACAAGCTATCC
dCtBPloc_Frag1_rev1	TCGAATCTCTTTCTGTTGCTGGAATGCCTG
dCtBPloc_Frag1_rev2	CCCCCTGACAATGGCAAGCGTACTATAAAC
dCtBPloc_Frag2_for1	GTCGGCTTGTACGGCATCAGAATCGGAATC
dCtBPloc_Frag2_for2	ATCTGTTAGATACGCGACCGCGACTTACTG
dCtBPloc_Frag2_rev1	GCGACGTAGTTTGGAAACTCGCCGAAAACG
dCtBPloc_Frag2_rev2	TTCCTTGCTGTTTGCCTGTTTGTTGTAGCC
dCtBPloc_Frag3_for1	CCATACCATAGCACACCCACACAAGCACAC
dCtBPloc_Frag3_for2	TTTTGCTACAGATGCGACCTGGTGCATTTC
dCtBPloc_Frag3_rev	CCGATAGCGGCCGCGTGCATCCTGTTCCCTCTGTTGGATTTTATCATTCCC
dCtBPloc_Asp718_top	AACCAGATGTGAGTGGGTACGGTACCTTGCTCTTCTGTGTTCC
dCtBPloc_Asp718_bot	CACAGAAGAGCAAGGTACCGTACCCACTCACATCTGGTTTG
2xFLAG_oligo_top	TCGACTACAAGGACGACGATGACAAGGACTACAAGGACGACGATGACAAGTGA
2xFLAG_oligo_bot	GATCTCACTTGTCATCGTCGTCCTTGTAGTCCTTGTCATCGTCGTCCTTGTAG
C38A-Top	CTGGATGGCCGGGACGCCACAGTGGAGATGCCCATC
C38A-Bottom	GATGGGCATCTCCACTGTGGCGTCCCGGCCATCCAG
C54A_Top	CACTGTGGCCTTCGCCGACGCGCAGTCCAC
C54A_Bottom	GTGGACTGCGCGTCGGCGAAGGCCACAGTG
C118A_Top	GATTTAGGCATTGCCGTCGCCAACGTGCCCGCGGCG
C118A_Bottom	CGCCGCGGGCACGTTGGCGACGGCAATGCCTAAATC
C232A_Top	CTCTTCCACAGCGACGCCGTGACCCTGCACGCC
C232A_Bottom	GGCGTGCAGGGTCACGGCGTCGCTGTGGAAGAG
C312A_Top	GCACCCAACCTCATCGCCACCCCCCATGCTGCATGG
C312A_Bottom	CCATGCAGCATGGGGGGTGGCGATGAGGTTGGGTGC
C134A_Top	AGACGGCCGACTCGACGCTGGCCCACATCCTGAACCTGTACCG
C134A_Bottom	CGGTACAGGTTCAGGATGTGGGCCAGCGTCGAGTCGGCCGTCT
C237A_Top	AGCGACTGCGTGACCCTGCACGCCGGCCTCAACGAGCACAACCA
C237A_Bottom	TGGTTGTGCTCGTTGAGGCCGGCGTGCAGGGTCACGCAGTCGCT
C350A_Top	ATCCCAGACAGCCTGAAGAACGCTGTCAACAAGGACCATCTGAC
C350A_Bottom	GTCAGATGGTCCTTGTTGACAGCGTTCTTCAGGCTGTCTGGGAT
CtBP1-Q161C-top	ACGAGTCCAGAGCGTCGAGTGCATCCGCGAGGTGGCGTCC
CtBP1-Q161C-bottom	GGACGCCACCTCGCGGATGCACTCGACGCTCTGGACTCGT
CtBP1-R266A-top	CCTGGTGAACACAGCCGCAGGTGGCCTGGTGGATG
CtBP1-R266A-Bottom	CATCCACCAGGCCACCTGCGGCTGTGTTCACCAGG
CtBP1-A166C-top	AGCAGATCCGCGAGGTGTGTTCCGGAGCTGCCAGGATCCGCG
CtBP1-A166C-bottom	CGCGGATCCTGGCAGCTCCGGAACACACCTCGCGGATCTGCT
CtBP1-S158C-top	TGCGGGAGGGCACTCGAGTCCAGTGCGTCGAGCAGATCC
CtBP1-S158C-bottom	GGATCTGCTGACGCACTGGACTCGAGTGCCCTCCCGCA
CtBP1-I162C-top	AGTCCAGAGCGTCGAGCAGTGCCGCGAGGTGGCGTCCGGCG
CtBP1-I162C-bottom	CGCCGGACGCCACCTCGCGGCACTGCTCGACGCTCTGGACT
CtBP1-V159C-top	TGCGGGAGGGCACTCGAGTCCAGAGCTGCGAGCAGATCCG
CtBP1-V159C-bottom	CGGATCTGCTCGCAGCTCTGGACTCGAGTGCCCTCCCGCA
CtBP1-E164C-top	TCGAGCAGATCCGCTGCGTGGCGTCCGGAGCTGCCAGGATCC
CtBP1-E164C-bottom	GGATCCTGGCAGCTCCGGACGCCACGCAGCGGATCTGCTCGA

Figure 3.1 (i) – *Krüppel*-Promoter: Two-dimensional representation of *Krüppel* promoter region including 7.2 kb of endogenous promoter including Central Domain 1 (CD1) and Central Domain 2 (CD2) as mapped by Hoch et al. 1990 (Left); *Drosophila* CtBP: Two-dimensional representation of *dCtBP* wild type and mutant cDNA constructs including sites of mutations and FLAG epitope tag (Right)

(ii) – Two dimensional representation of *Krüppel*-GAL4 driver line transgene (Left); Two dimensional representation of UAS-*dCtBP* transgene

(iii) – Stage 5 embryo from male *Krüppel*-GAL4 transgenic fly crossed with female wild type UAS-*dCtBP* transgenic fly; probed with mouse anti-FLAG antibody, anti-mouse-HRP secondary antibody, and Tyramide-568 Alexa Fluor, visualized on Confocal microscope with 561nm DPSS laser.

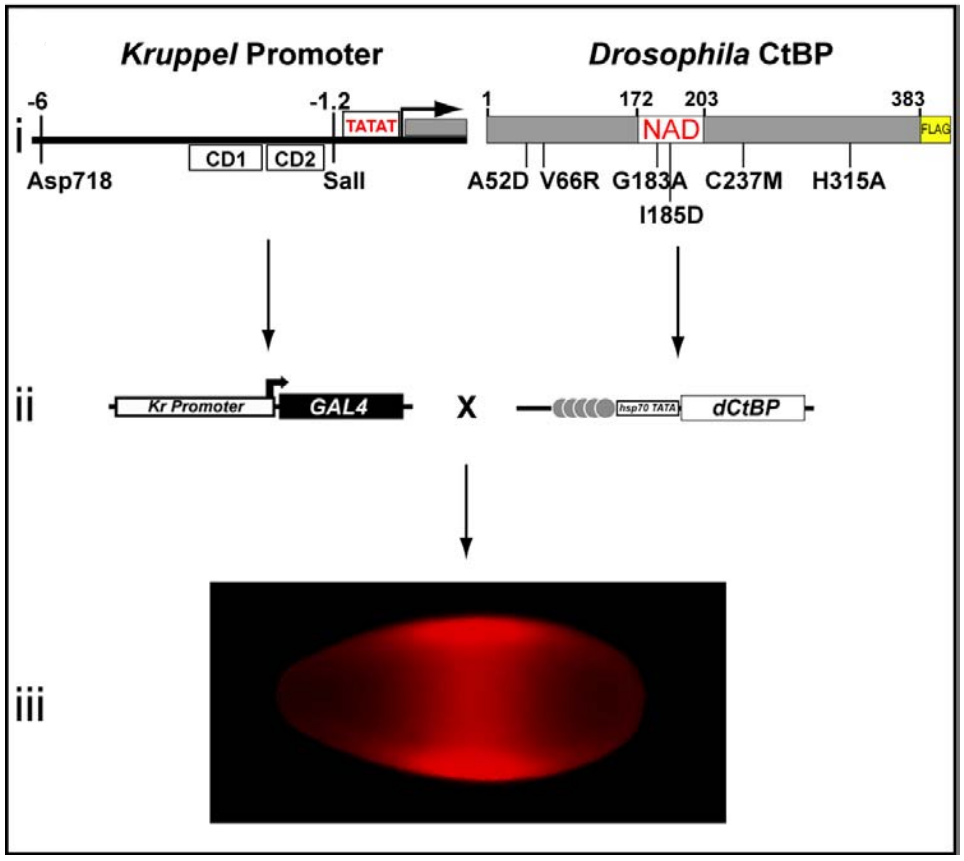

Figure 3.2 – *Eve* in situ probe: A. dCtBP +/+ staged embryo probed with DIG-labeled *eve* RNA probe, sheep anti-DIG-HRP antibody, Tyramide Alexa Fluor 488, imaged on Confocal Microscope using 457/488/514nm Argon laser

B. dCtBP -/- embryo *eve* expression, probed with DIG-labeled *eve* RNA as describe in Figure 3.2 A

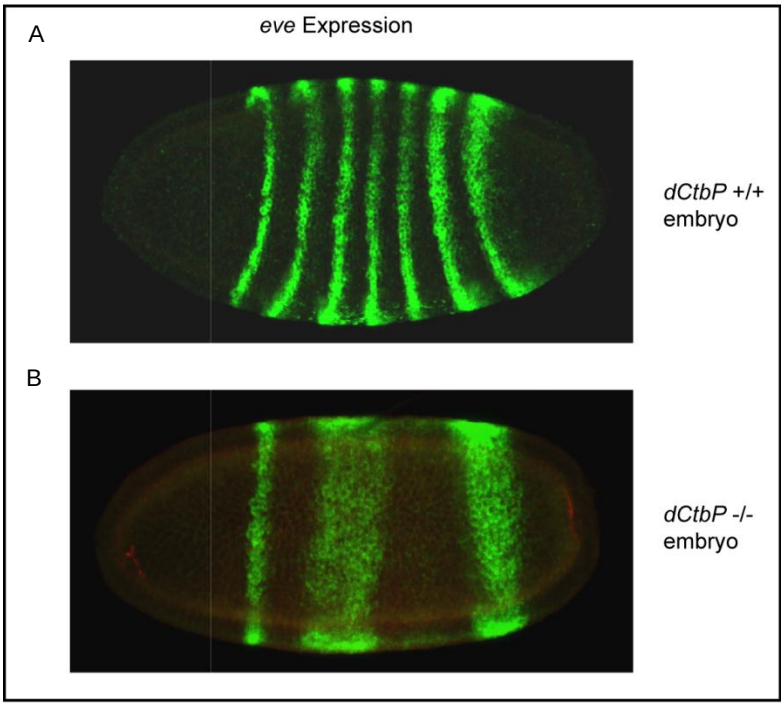

Figure 3.3 – Western Blot of embryos expressing FLAG epitope tagged UAS-*dCtBP* transgenes: Crushed embryos from GAL4 UAS screen corresponding to wild type or mutant transgenes, *yw* embryos, and FLAG tagged protein control.

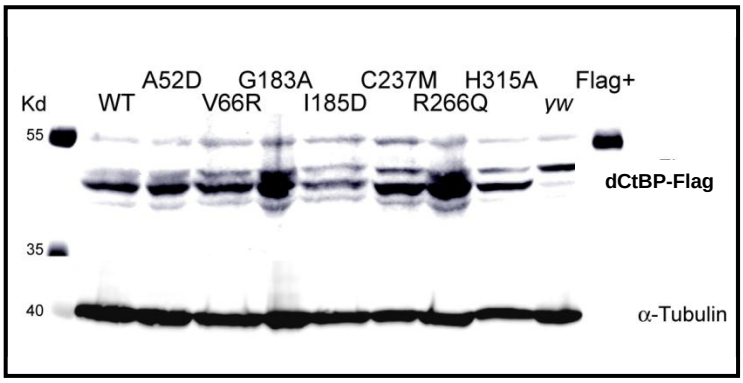

Figure 3.4 – Confocal images of dCtBP null embryos stained for UAS-FLAG epitope tagged transgene (red) and *eve* mRNA transcript (green): (A) wild type UAS transgene, partial rescue of *eve* stripes 3 and 4 (see arrows) when compared to dCtBP -/- (H); (B) A52D mutant UAS transgene, no *eve* stripe 3 or 4 rescue; (C) V66R mutant UAS transgene, no *eve* stripe 3 or 4 rescue; (D) G183A mutant UAS transgene, no *eve* stripe 3 or 4 rescue; (E) I185D mutant UAS transgene, no *eve* stripe 3 or 4 rescue; (F) C237M mutant UAS transgene, no *eve* stripe 3 or 4 rescue; (G) R266Q mutant UAS transgene; partial rescue of *eve* stripes 3 and 4; (H) H315A mutant UAS transgene; partial rescue of *eve* stripes 3 and 4; (I) *dCtBP* -/- stage 5 embryo; (J) Summary of results from two screens per genotype.

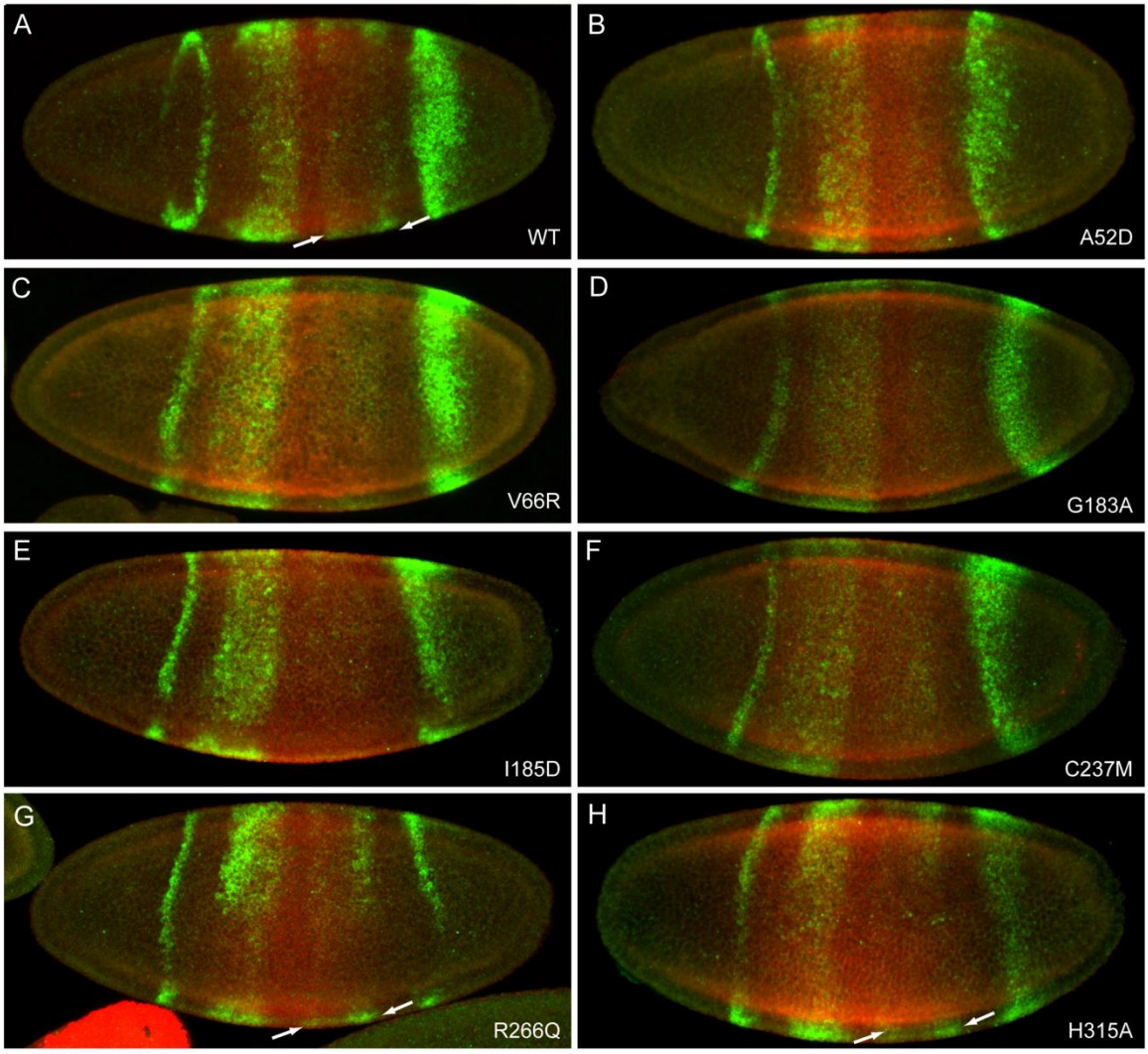

J

Transgene	Embryos/Rescue*	% Rescue
WT	53/32	60
A52D	48/0	0
V66R	45/0	0
G183A	49/0	0
I185D	47/0	0
C237M	56/0	0
R266Q	60/37	62
H315A	75/48	64

* sum of two transgenic lines per genotype

Chapter 4. The role *Drosophila* C-terminal Binding Protein functional domains play in short-range transcriptional repression – Locus transgene

Damian E. Curtis[1], Sarah M. Smolik[2], and James R. Lundblad[3]

[1]*Dept. of Biochemistry and Molecular Biology, Oregon Health Sciences University*

[2]*Dept. of Cell and Developmental Biology, Oregon Health Sciences University*

[3]*Dept. of Medicine, Oregon Health and Sciences University*

Abstract

Drosophila Carboxyl-terminal Binding Protein (dCtBP) is an essential transcriptional repressor during normal embryogenesis. The work described in this chapter examines the roles of target binding, dinucleotide binding, and dehydrogenase activity in short-range repression of the *eve* locus introducing the entire *dCtBP* locus including all endogenous regulatory elements and potential for encoding each isoform. Through these experiments we determined that dinucleotide binding is essential for this process, dehydrogenase activity does not appear to play a role in short-range repression, and different *dCtBP* isoforms could potentially play different and separable roles in normal embryogenesis.

Introduction

Chapter 3 describes an *in vivo* assay for monitoring exogenously expressed wild type and mutant *dCtBP* transgenes in a *dCtBP* null embryo. From this we concluded that *dCtBP* mutants which can't bind dinucleotide do not properly coordinate short-range *eve* repression via the target gap protein *Knirps*, and dehydrogenase mutants rescued *eve* stripes 4 and 5 at a similar frequency as wild type. One of the advantages of the GAL-UAS expression system established in Chapter 3 was tightly controlled regulation of the expression of our transgene. This was powerful because we created a system in which we could express our transgene of interest in a specified domain and at a specified level. The level of expression was determined mostly by the endogenous *Krüppel* promoter fused to the GAL4 protein. One of the rationales for using this region of the promoter, described in Chapter 3, was proper endogenous expression and this was an important facet of the experimental design. A common experimental practice within the CtBP field of research is to overexpress either CtBPs or other biological molecules in the biological pathway. When working with transcription factors that, by their very nature, have a multitude of complex binding partners, have pleiotropic effects on cellular biology, and whose activities are often concentration dependent, it is important to design experiments that replicate endogenous expression levels. The GAL4-UAS *in vivo* model attempted to do that. Another way to ensure endogenous expression levels is by using the endogenous dCtBP promoter region.

In this chapter we describe a set of experiments, again using an *in vivo* assay, which examined some of the same biological questions in a slightly different manner. Instead of using transgenic flies which contain UAS-responsive transgenes, we generated

flies which have a transgene containing the entire *dCtBP* locus. The entire locus not only contains the coding sequence for all isoforms, but it also has all the endogenous regulatory elements which ensure normal transcription, splicing, and translation of *dCtBP*. First we generated *dCtBP* null germline clones as we did in Chapter 3, briefly, we cloned out the entire 14 kb dCtBP locus including all endogenous regulatory elements and coding regions, inserted an epitope tag to the construct, inserted point mutations, and generated transgenic flies for each mutant construct. Using a set of wild type locus transgenes lines, a dinucleotide mutant transgene line, and three different dehydrogenase mutants, we evaluated the regulation of *eve* transcription by wild type and mutant *dCtBP* in null embryos. The only dCtBP protein made in these embryos is derived from our FLAG-epitope tagged transgenes and therefore any short-range repression activity utilizes our exogenous constructs. This *in vivo* assay provided more compelling evidence that dinucleotide binding plays an essential role in dCtBP coordination of short-range repression at the *eve* locus. In addition, by using the entire *dCtBP* locus, we were able to include all *dCtBP* isoforms.

Materials and Methods

Construction of dCtBP wild type and mutant locus-transgene constructs

The entire *dCtBP* locus was cloned by PCR from the Bacterial Artificial Chromosome BACRP98-17F05 obtained from Children's Hospital and Research Center at Oakland (5700 Martin Luther King Jr Way Oakland, CA 94609). The locus was subdivided into three fragments (Figure 4.1) and cloned separately from BAC plasmid DNA purified using Qiagen Plasmid Maxi Prep Kit (QIAGEN Valencia, CA 91355). PCR cycling conditions for all *dCtBP* locus fragments: 1.75 ul of 1:10 dilution of BAC DNA, 1 ul of 10 uM Forward PCR primer, 1 ul of 10 uM Reverse PCR primer, 8.0 ul of Takara Primestar dNTPs, 5 ul of Takara Primestar 10 X Buffer, 0.5 ul of Takara Primestar enzyme, brought to 50 ul with 37.75 ul of molecular grade H_2O. PCR cycling conditions: 94ºC for 1 minute, 30 cycles of 94ºC for 30 seconds, 68ºC for 1 minute, 68ºC for 7 minutes, 72ºC for 10 minute (Table 2.1).

Fragment #1 cloning: The 5' end of fragment #1 (5.735 kb) began at a naturally occurring BamHI restriction enzyme site just downstream of the most proximal loci to the *dCtBP* locus and contained promoter region and 5' UTR of *dCtBP* up to a naturally occurring EagI restriction enzyme site. Fragment #1 PCR amplicon was gel purified as described in Chapter 2 Materials and Methods, digested with BamHI and EagI, ligated to BamHI/EagI prepped pCDNA3 vector, confirmed by Sanger sequencing with T7 and SP6 primers. The entire fragment was sequenced to confirm that no errors were introduced during PCR amplification.

Fragment #2 cloning: The 5' end of fragment #2 (5.6 kb) begins at the endogenous EagI site used as the 3' anchor of Fragment #1. Fragment #2 encompasses

virtually all of the *dCtBP* 5'UTR as well the entire coding region for all *dCtBP* isoforms except isoform E (*dCtBP (l)*) whose coding region continues into fragment #3. The 3' end of fragment #2 is a unique XbaI site in the 3'UTR just downstream of the termination site for all isoforms except E. Fragment #2 PCR amplicon cloned into EagI/XbaI prepared pBSKS vector and sequenced to ensure no PCR introduced nucleic acid changes.

A 2xFLAG epitope tag was inserted in-frame just upstream, of the termination codon by subcloning the 3' end of Fragment #2 (Fragment #2.1) into pBSKS plasmid vector using a unique PstI restriction enzyme site and the XbaI site at the 3' end. Following verification of PstI-XbaI fragment, unique XhoI and BamHI sites were inserted at the termination codon using site-directed mutagenesis. Restriction sites confirmed by sequencing, and a 2xFLAG double stranded oligo with a 5' XhoI and 3' BamHI (sites abolished following insertion into Fragment #2.1) compatible ends was ligated to XhoI/BamHI prepped Fragment #2.1. Fragment #2.1 containing 2xFLAG epitope tag digested out of pBSKS with PstI and XbaI and ligated to PstI/XbaI prepped Fragment #2. A unique Asp718I restriction site was inserted into Fragment #2 with 2xFLAG epitope tag using site-directed mutagenesis (see Chapter 2 Materials and Methods), just upstream of the start codon.

Fragment #3 cloning: Fragment #3 (4.7 kb) is anchored at the 5' end with the unique XbaI restriction enzyme site at the end of Fragment #2. The entire 3' UTR as well as two exons from *dCtBP* isoform E is contained in Fragment #3 which ends just upstream of the most proximal loci downstream of the *dCtBP* locus and is anchored with a unique NotI site inserted during PCR amplification. Fragment #3 PCR amplicon

digested with XbaI and NotI, cloned into NotI/XbaI prepared pCDNA3 vector, and Sanger sequenced to confirm. The entire fragment was sequenced to ensure no nucleic acid changes were introduced during PCR amplification.

The entire wild type *dCtBP* locus was reconstructed in two stages by ligating Fragment #1 (BamHI to EagI) and the EagI to Asp718I portion of Fragment #2 into BamHI/Asp718I prepped pCDNA3 vector (Fragment #1_2.5). The Asp718I to BglII end of Fragment #2, containing the 2xFLAG epitope tag, was ligated with Fragment #3 (BglII to NotI) to Asp718I/NotI prepped pcDNA3 vector (Fragment #2.5_3). Fragment #1_2.5 (digested from pCDNA3 with BamHI and Asp718I) and Fragment #2.5_3 (digested from pCDNA3 with Asp718I and NotI) were ligated to BamHI/NotI prepped pCASPER3 p-element containing vector. *dCtBP* wild type locus pCASPER3 plasmid DNA was purified using CsCl protocols and sent to BestGene Inc. for creation of transgenic flies.

CsCl purified *dCtBP* wild type locus plasmid DNA was used as template DNA for subcloning of the mutation cassette between the Asp718I and BglII restriction sites into an Asp718I/BglII prepared pBSKS plasmid vector. Site-directed mutagenesis used to insert single point mutations into the coding sequence corresponding to Alanine 52 to Aspartic Acid (A52D), Glycine 183 to Alanine (G183A), Isoleucine 185 to Aspartic Acid (I185D), Arginine 266 to Glutamine (R266Q), Glutamic Acid 295 to Alanine (E295A), and Histidine 315 to Alanine (H315A) (Table 2.1). Each individual mutant was confirmed by Sanger sequencing and subcloned back into Asp718I/BglII prepped wild type locus construct in pCASPER3 vector. Mutant locus pCASPER3 plasmids were purified using CsCl protocols and sent to BestGene Inc. for creation of transgenic flies.

Construction of wild type and mutant locus-transgene fly stocks

dCtBP-locus wild type and mutant fly stocks constructed in the same manner as the *UAS-dCtBP* fly stocks described in Chapter 3 Materials and Methods. The following genotype (*w'/w;dCtBP-locus/dCtBP-locus;dCtBP*^{03463}*/TM-2R3)* were constructed for all of the wild type, R266Q, E295A, and the I185D locus transgenes. Constructed the H315A mutant locus stock (*w'/w;Sp/CyO;dCtBP*^{03463}*/TM-2R3;dCtBP-locus/dCtBP-locus)*. The *TM-2R3* marked stock was provided by Dr. Smolik and was constructed by transposon hopping the *Krüppel*-GAL4 driver transgene from Chromosome II described in Chapter 2 Materials and Methods onto a UAS-DsRed containing chromosome III. This marker expresses DsRed within the endogenous *Krüppel* expression domain including the central domain in developing embryos. The presence of a DsRed fluorescent signal in stage 5 embryos indicates that these embryos contain a wild type *dCtBP* locus on the third chromosome and serves as a control for flipase induced recombination event required for the creation of *dCtBP* maternal and zygotic null embryos. All fly stocks maintained as described in Chapter 3 Materials and Methods.

Construction of Heat-Shock Flipase stock

Heat shock flipase *(P{hsFLP}12, yw';Sp/CyO;TM-2/MKRS)* fly stock used for the locus experiments was the same stock used in the UAS-GAL4 experiments described in Chapter 3.

Creation of maternal and zygotic dCtBP null germline clones

Germline clones created using essentially the same protocol as used for the GAL4-UAS experiments described in Chapter 3 Materials and Methods. In place of the UAS-*dCtBP* wild type and mutant fly stocks, the locus transgene stocks, described above we used. *P{hsFLP}12, yw';Sp/CyO;TM-2/MKRS* virgins collected and crossed to Bloomington stock 2149 *(w'; P{neoFRT}82B P{ovoD1-18}3R/ TM3, Sb)* males. Male *P{hsFLP}12, yw';Sp or CyO/+; P{neoFRT}82B P{ovoD1-18}3R /TM-2 or MKRS* flies collected and crossed to virgin *w'/w;dCtBP-locus/dCtBP-locus;dCtBP^{03463}/TM-2R3* flies. Males and females combined for 3 days at 25ºC and, when vials contained mostly first instar larvae, all flies removed and vials heat shocked in a 37°C water bath for one hour twice a day for 3 days to induce heat shock-FLPase gene. Adult flies as collected as they eclose and virgin *P{hsFLP}12, yw'; dCtBP-locus/+; P{neoFRT}82B P{ovoD1-18}3R / dCtBP^{03463}* crossed to male flies from the original locus transgene stocks (*w'/w;dCtBP-locus/dCtBP-locus;dCtBP^{03463}/TM-2R3)* .

Embryo collection and fixing

Embryos collected using the same protocol used in the GAL4-UAS experiments described in Chapter 3 Materials and Methods using virgin female *P{hsFLP}12, yw'; dCtBP-locus/+; P{neoFRT}82B P{ovoD1-18}3R / dCtBP^{03463}* flies and male *w'/w;dCtBP-locus/dCtBP-locus;dCtBP^{03463}/TM-2R3* flies. Embryos stored at -20ºC following dechorionation and fixing.

Embryo in situ, immunohistochemistry and fluorescent staining

Three day in situ hybridization and fluorescent staining protocol for locus embryos was identical to that used in the GAL4-UAS experiments described in Chapter 3 Materials and Methods with one significant change. The DIG-labeled *eve* RNA probe was visualized with the Tyramide 568 Alexa Fluor and the FLAG epitope was visualized with the Tyramide 488 Alexa Fluor. This switch was made to ensure that the Alexa Fluor 568 FLAG-tag signal did not mask the DsRed emission from the TM-2R3 marker on chromosome III.

Confocal Microscopy: Image capture and analysis

Mounting, viewing, and imaging protocols the same as those used for UAS-GAL4 experiments described in Chapter 3 Materials and Methods (Figure 4.2).

Western blot of locus-transgene embryos

Western blot performed to determine the presence of FLAG tagged locus transgenes using the protocol described in Chapter 3 Materials and Methods for the UAS-*dCtBP* transgene embryos (Figure 4.3).

Results

We constructed wild type and mutant (A52D, G183A, I185D, R266Q, E295A, and H315A) transgenes containing the entire *dCtBP* locus (Figure 4.1) according to the Materials and Methods section of this chapter. The locus transgene contains all of the endogenous elements for expression of the different isoforms of *dCtBP* (isoform A and E are the predominant forms (38)) as well as a FLAG epitope tag fused to the c-terminus of isoform A exon 8. All isoforms except isoform E (*dCtBP(l)*) share the same termination site, thus all expressed proteins are FLAG-tagged with the exception of protein derived from isoform E. In addition, protein from all isoforms, including isoform E, expressed from mutant locus transgenes will contain the inserted amino acid changes.

dCtBP locus target binding mutant A52D was injected into *Drosophila* embryos for construction of transgenic flies 3 different times with two DNA sources but we were unable to obtain any transgenic flies (see Discussion for a possible explanation of this result). Dinucleotide binding mutants G183A and I185D transgenes were constructed but only I185D yielded flies expressing the transgene, albeit at very low integration rates. Flies transgenic for locus constructs containing dehydrogenase mutants, R266Q, E295A, and H315A, were isolated but also integrated at very low frequencies.

Embryos collected from the germ line clone protocol described in Chapter 2 Materials and Methods, were probed for FLAG-tagged protein and *eve* transcription was monitored. Germline clones were generated using the same protocol as was used for the GAL4-UAS screen assay except that the heat shocked female flies were crossed with males homozygous for the locus transgene and carrying a *Krüppel*-DsRed transgene on the third chromosome opposite the *dCtBP* P-element knockout. *Krüppel*-DsRed, a

Krüppel dependent fluorescent marker on a dCtBP+ chromosome III, allowed us to eliminate embryos containing a wild type *dCtBP* gene (Figure 4.2G). To ensure expression of the transgenes we lysed embryos and ran the proteins out on a SDS-PAGE gel and performed a western blot with an anti-FLAG antibody. These embryos produce FLAG tagged dCtBP protein of the appropriate size when compared to embryos collected from *yw* females (Figure 4.3). Chapter 2 Materials and Methods describes the embryo collection, processing, and staining protocol in detail; embryos processed this way have FLAG-tagged protein labeled with a green fluorescent probe (Alexa Fluor 488) and *eve* mRNA is labeled with a green fluorescent probe (Alexa Fluor 568).

Null embryos containing four different wild type Locus transgenes almost completely rescued *eve* transcription (Figure 4.2A, F). There is a slight broadening of *eve* stripe 7 when compared with a wild type embryo (Figure 3.2A), which has also been reported by Arnosti et al. Figure 6Ai (39). Embryos containing a transgene mutated for dinucleotide binding (185D) do not rescue *eve* transcription and in every embryo found *eve* transcription was further disrupted when compared to the *dCtBP* null (Figure 4.2B, F). Unlike the dinucleotide binding mutant, transgenes containing the *dCtBP* locus with mutations inserted at three different catalytic residues (R266Q, E295A, and H315A) rescued *eve* transcription much like the wild type transgene and at the same rate (Figure 4.2C,D,E, H). Within the collection of embryos for the dehydrogenase mutant transgenes, there was much greater variability of *eve* transcription compared to the wild type locus transgenes. Further broadening of *eve* stripe 7 was found as well as many embryos in which *eve* stripes 4 and 5 were barely visible or improperly regulated when compared to the wild type transgenes. The implications of this are discussed below.

Discussion

The goal of these experiments was to evaluate dinucleotide and dehydrogenase mutants generated from a locus transgene in a *dCtBP* null embryo in order to better understand how these distinct biochemical functions affect *dCtBP*-mediated short-range repression of *eve* transcription. One of the challenges we encountered while generating the reagents for these experiments was the extremely low frequency of successful transgene insertion. For all constructs except for the wild type, Dr. Smolik and I screened thousands of F1 flies. We also prepared several CsCl purified DNA preps with little success. Despite three different attempts, we were never able to collect a target binding mutant (A52D). One explanation for this is that upon insertion into the germ cells, the locus transgene (unlike the UAS-GAL4 system) would immediately be transcribed and translated. Having any of the mutant protein in the cell, especially one that can't bind to important co-repressors, could lead to a dominant negative effect by binding to the endogenous dCtBP protein and sequestering it away from normal functions. As we know from the E1A-CtBP interaction, removal of CtBP from its normal functions has profound effects on the cell. A dominant negative affect could also explain the low integration rates of the other mutant transgenes as well. If this was the case, we were very fortunate to collect an dinucleotide (I185D) binding mutant given the level of *eve* disruption.

The observation that many different wild type locus transgenes lead to normal *eve* transcription (Figure 4.2A) across the entire embryo was expected but also informative when compared to the other locus transgenes. While many of the null embryos expressing any of the three dehydrogenase mutants (R266Q, E295A, and H315A) look much like the wild type locus rescue embryos, there was a greater level of variability in the rescue

observed. Many embryos had faint or missing *eve* stripes particularly in the central domain of the embryo and noticeable widening of stripe 7, and this was not the case with any of many wild type constructs tested (data not shown). This is reflected in the rate of rescue (Figure 4.2 H) as well.

Based upon our findings as well as those recently described by the Arnosti lab (39), we concluded that, although *dCtBP* dehydrogenase activity may be important for some aspects of *dCtBP* biology, when specifically dissecting short-range repression of *eve,* disruption of dehydrogenase activity is far less disruptive than dinucleotide binding which is clearly essential to the process. Furthermore it is quite possible that the specific mutation used to disrupt each biochemical function affects the results. For instance, we described in detail how each of the distinct mutations created abolish only the desired function while leaving the other endogenous *dCtBP* activities intact, but other researchers traditionally do not evaluate their mutants in this way. For example, the catalytic mutant at Histidine 315 used by the Arnosti lab to eliminate dehydrogenase activity utilizes the bulky, polar amino acid Glutamine (39). The insertion of this amino acid could disrupt other *dCtBP* functions more so than a small non polar amino acid such as Alanine. We also find the dinucleotide binding mutant utilized by the Arnosti lab to be poorly characterized within the *Drosophila* biological system. Several mutations that abolish dinucleotide binding have been extensively studied including Aspartic Acid 204, and not only did these mutants alter NAD(H) binding but they also greatly diminished target binding (27,68). We evaluated our dinucleotide mutants and found them to retain wild type like secondary structures as well as target binding ability, and unlike the D204N described by Arnosti (39) our dinucleotide binding mutant does not appear to be mostly

cytosolic (Figure 4.2 B), which could be the result of gross protein three dimensional changes in the case of the Arnosti mutation.

Based upon the results from Chapter 3 we speculated about the roles that *dCtBP* isoform A and E play in *eve* repression. One plausible explanation for the lack of repression at stripe 2 in the GAL4-UAS experiment was that each isoform regulates short-range repression of *eve* at distinct regions of the developing embryo. In the locus transgene embryos both isoforms are added back to the null genetic background, it is certainly possible that the complete rescue of all *eve* stripes observed requires both isoforms. It would be worthwhile to sort out exactly which isoform is responsible for short-range repression at each individual stripe and how that process is regulated.

Tables and figures

Figure 4.1 – Construction of wild type and mutant locus transgene: Schematic of the key steps taken to construct the wild type and locus transgene

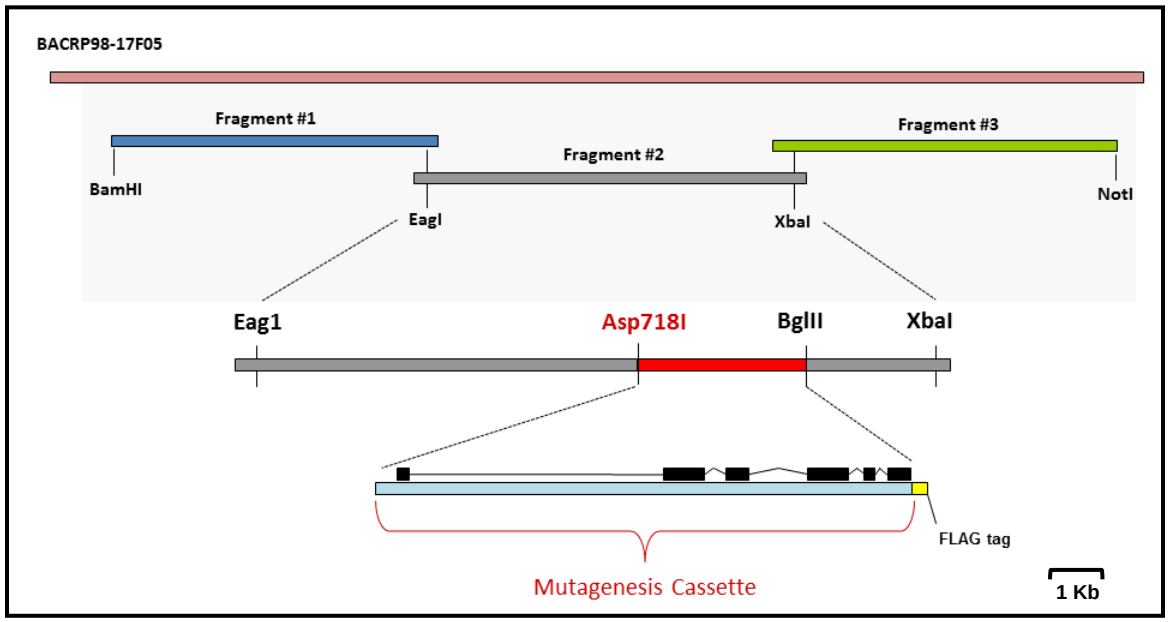

Figure 4.2 – Confocal images of *dCtBP* null embryos expression FLAG epitope tagged Locus transgenes (green) with *eve* mRNA transcript (red): (A) wild type Locus transgene, complete *eve* rescue when compared to *dCtBP* -/- (H); (B) I185 locus transgene, no rescue of *eve* transcription; (C) R266Q locus transgene, *eve* rescue; (D) E295A locus transgene, *eve* rescue; (E) H315A locus transgene, *eve* rescue; (F) *dCtBP* -/- embryo; (G) *dCtBP -/TM3Kr-dsRed* control embryo; (H) Summary table of results from locus transgene experiments.

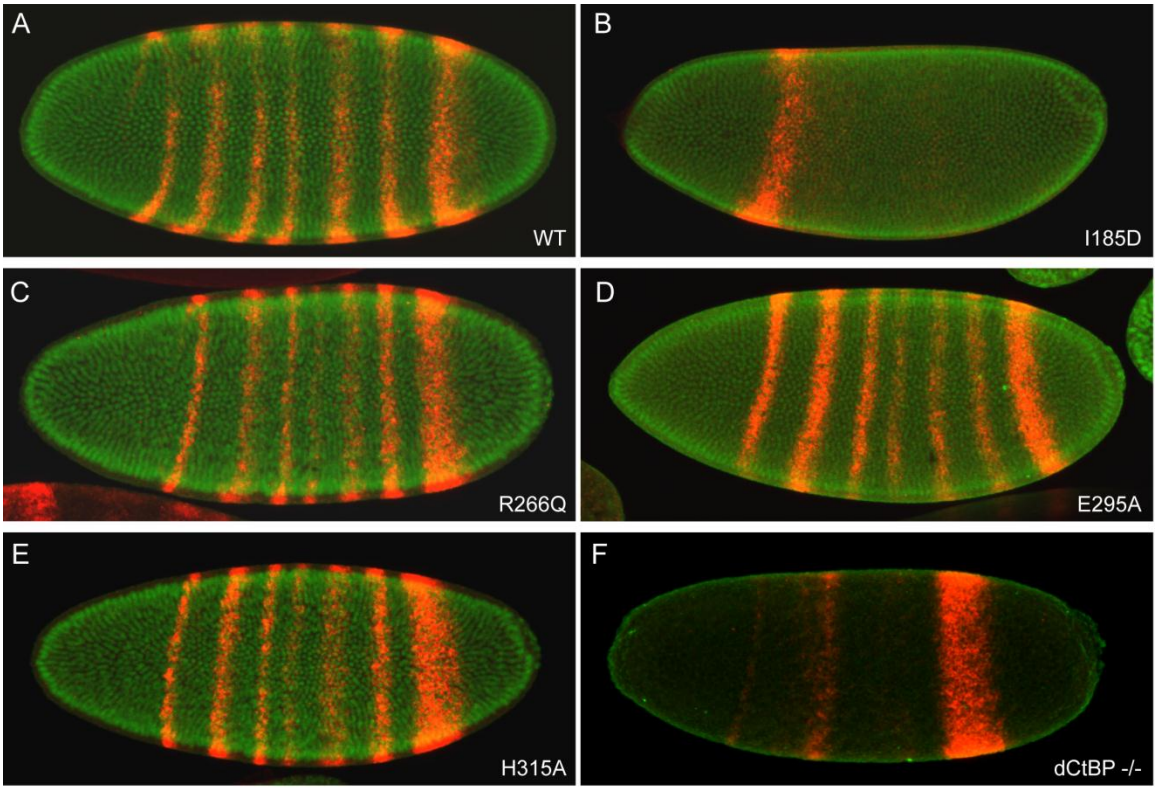

H

Locus	Embryos	% Rescue
WT*	388	84
I185D	110	0
R266Q	89	76
E295A	80	66
H315A	78	70

* sum of four transgenic lines

Figure 4.3 – Western Blot of embryos expressing FLAG tagged locus transgenes: Crushed embryos from locus germline null screen corresponding to wild type or mutant transgenes, *yw* embryos, and FLAG tagged protein control

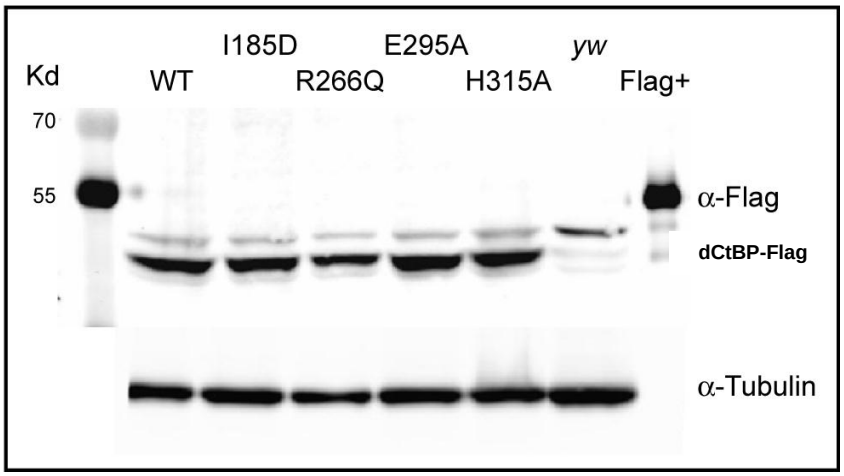

Chapter 5. NAD binding and dimerization in human C-terminal Binding Protein 1 (CtBP1)

Damian E. Curtis[1] and James R. Lundblad[2]

[1]*Dept. of Biochemistry and Molecular Biology, Oregon Health Sciences University*

[2]*Dept. of Medicine, Oregon Health and Sciences University*

Abstract

Human Carboxyl-Terminal Binding Proteins (hCtBP) have been identified as important regulators in several human cancers. Their role in transcriptional regulation of key pro-apoptotic genes as well as tumor suppressors is being examined by many researchers. Based upon this area of CtBP research it has become clear that a useful research tool, and possibly clinical tool, would be a CtBP inhibitor. Using our structural knowledge of CtBP and its coenzymes and co-repressors, we initiated a method for screening for small molecule inhibitors of CtBP based upon the disruption of a key aspect of its biology. Described in this chapter are the first steps towards fluorescent monitoring of NAD induced dimerization.

Introduction

In Chapter 1 we discussed CtBPs role in suppression of the epithelial to mesenchymal transition in tumor cells; the functions of the CtBP target, E-cadherin in this process; as well as the role that NAD(H) mediated dimerization could play in this process. Unpublished data from our lab indicates that CtBP co-repressor complexes affect DNA methylation of the E-cadherin promoter in cell lines derived from cancer patients and this observation suggests that a small molecule antagonist of CtBP could have clinical utility in the treatment of epithelial cancers.

In this chapter we report the beginning steps towards the construction of a medium throughput small molecule CtBP dimerization inhibitor screen utilizing site-directed fluorescence labeling (SDFL). SDFL would allow us to differentiate between monomeric and dimeric forms of CtBP proteins. We hope to employ one of two similar approaches to monitor the formation of dimers. The first, simpler, method would be to measure environment-induced changes of a fluorescent probe located at the dimerization interface. The second, more challenging, modality utilizes Photo-induced Electron Transfer (PET) developed by the Farrens lab here at OHSU. One advantage of PET is that it can be used for determining proximity relationships within a CtBP dimer (74,75). In this method fluorescence of extrinsic fluorophores (bimane derivatives and BODIPY 507/545 iodoacetamide) are quenched by proximity to an intrinsic tryptophan (Figure 5.2 B) (75). Both methods require the introduction of exogenous cysteines whose thiol side-chain reacts with fluorescent probes such as monobromobimane (mBBR). Due to the sensitive nature of fluorescent monitoring, a system such as this requires only a small

concentration of fluor reactive substrate and probe and measurements are simplified, compared to FRET assays, because one only has to monitor fluorescent levels.

Human CtBP1 contains eight cysteine residues. In order to create an unreactive version of CtBP1, we attempted selective replacement of all cysteine residues with an inert amino acid such as serine. Albeit there are success stories using this approach, many times the further one mutates a protein it either loses biological activity or becomes insoluble when expressed in *E. coli* protein expression systems. In light of that potential pitfall we utilized available crystal structures and attempted to predict which cysteine residues are positioned on the surface of the monomer and thus available to a reactive fluorescent probe. Based upon our analysis, C134 appeared completely surface accessible in the monomeric state and C118 also appeared to be partially surface accessible. C237 is involved in dinucleotide binding and insertion of a bulky methionine residue block binding, so it too may be located in a reactive three dimensional position. A completely cysteine-free version of CtBP1 or version with all surface accessible cysteine residues removed would allow us to monitor dimerization using the two methods described above.

In this first approach, dimerization would be monitored by environment-induced alterations of fluorescence intensity. By placing an extrinsic fluor at the dimerization interface such as mBBR (ex/em 380/470 nm), a small fluor with high quantum yield similar in size to that of tryptophan, we could monitor dimerization. Incorporation of mBBr has been shown to cause minimal structural alterations even when placed at buried sites (74) and is sensitive to changes in the polarity of the surrounding solvent. The second approach, PET, incorporates the placement of a reactive cysteine at a location within the CtBP1 monomer which would reside proximal to tryptophan 318 (W318) upon

dimerization. In a CtBP1 dimer, W318 lies close to the N-terminus of αC (residues 156 to 162) of the opposite dimer (Figure 5.1) Thus, an engineered cysteine at this position of αC could be used for labeling. Fluorescence quenching would be predicted only with dimerization and fluor proximity to W318 in the nucleotide-binding domain due to domain swapping.

The creation of a sensitive fluorescence assay for CtBP dimerization would be the first step towards screening for small molecule inhibitors of CtBPs and could potentially lead to the identification of a cancer therapeutic which exploits a new therapeutic modality.

Materials and Methods

Construction of cysteine free human CtBP

Confirmed, by Sanger sequencing, CtBP1_CT_2xFLAG provided by Dr. Lundblad as template for mutation of surface exposed cysteine residues to serine residues. Site directed mutagenesis used to insert nucleic acid changes which conferred amino acid changes at desired sites and insert new restriction sites, if possible, for easier screening. Started with Cysteine 134 to Serine mutation (C134S) followed by other mutations in succession (Cysteine 237, Cysteine 350, Cysteine 38, Cysteine 54, Cysteine 118, Cysteine 312, and Cysteine 232) using each previous mutant construct as a template. All mutations confirmed for correctness by Sanger sequencing. Manipulation of plasmid DNA, use of *E. coli* competent cells, and PCR protocols all the same as described in Chapter 3 Materials and Methods.

Mutation of all eight endogenous Cysteine residues to Alanine sequentially starting with Cysteine 134 (C134A) was performed using the same site directed mutagenesis protocol described in Chapter 3 Materials and Methods. C134A mutagenesis performed in CtBP1_CT_2xFLAG, sequence confirmed, and subcloned into pET23D protein expression vector. pET23D_CtBP1_C134A used as a template for site directed mutagenesis of Cysteine 237, Cysteine 350, Cysteine 38, Cysteine 54, Cysteine 118, Cysteine 312, and Cysteine 232 sequentially. All Cysteines converted to Alanines corresponding to the mutant constructs C134A, C2A (C134A + C237A), C3A (C2A + C350A), C4A (C3A + C38A), C5A (C4A + C54A), C6A (C5A + C118A), C7A (C6A + C312A), and C8A (C7A + C232A). All sequences confirmed by Sanger sequencing, transformed into BL21 *E. coli* competent cell, and stored as glycerol stocks at -80ºC.

Insertion of cysteine residues proximal to tryptophan 318 (W318) for labeling with bimane was accomplished using site-directed mutagenesis protocols with CtBP1_C8A as the template for mutagenesis. Residues Q161, A166, S158, I162, V159, and E164 chosen based upon structural information placing them within the necessary distance to be quenched byW318. Primers designed and ordered for converting residues to cysteines (Table 3.1) and stored at -20ºC in the Lundblad lab. All mutations require sequencing to detect correct mutation.

Protein expression and purification

CtBP1 cysteine mutants expressed and purified using the same protocol described in Chapter 2 Materials and Methods for expression and purification of the dCtBP wild type and mutant proteins. This protocol was performed using standard BL21 *E. coli* cells and ArcticExpress cells from Stratagene. Cell pellets collected and protein purified using protocols described in Chapter 2 Materials and Methods. Prior to dialysis into storage buffer, ion exchange column fractions concentrated using Millipore Centricon centrifugal filter devices. Proteins dialyzed, quantified, and stored at -80ºC.

Bimane labeling

Proteins dialyzed into Bimane labeling buffer (50mM MOPS, 50mM Tris, 1mM EDTA, pH 7.6) overnight prior to labeling. Protein diluted to 5 uM in Bimane labeling buffer and incubated with 10X molar (50uM) excess Bimane, dissolved in DMSO, at 4ºC with rocking for more than 4 hours. Reaction stopped with 1mM DTT and samples run out, along with non-labeled samples, on a 10% SDS-PAGE gel at 120 volts for 1 hour.

Gel removed and visualized on a BioRad GelDoc system using a UV light box. Gel stained overnight with Coomassie Blue and destained to compare protein concentration.

GST pulldown experiments

GST pulldowns performed as described in Chapter 2 Materials and Methods using GST-E1A protein provided by Dr Lundblad. GST-E1A contains the C-terminal, PxDLS containing, portion of E1A fused to GST. GST-E1A protein expressed and purified using the protocol described in Materials and Methods Chapter 2.

Results

In order to construct a version of human CtBP1 which has no surface accessible Cysteine residues which can be labeled by the small fluorescent probe monobromobimane (mBBr) (Figure 5.2), we mutated cysteine 134 and cysteine 237 to the amino acid serine. Based upon analysis of three-dimensional CtBP structures, these two cysteines are two of the most surface accessible out of the eight cysteines present in human CtBP1. Conversion of these two cysteines to non-reactive serine residues did not affect bimane labeling (Figure 5.3) when compared to wild type CtBP1 or either single cysteine mutant protein. We then mutated some of the other cysteines using the C134S/C237S backbone and found that by mutating C350 to serine (C350S) we were able to eliminate virtually all labeling by bimane. This protein (C3S) was relatively straightforward to express in *E. coli* and mostly soluble. We performed GST-E1A pulldown experiments with the C3S protein and it bound to target with similar affinity as CtBP1 (Figure5.3 B).

Unfortunately future attempts to repeat these data failed many times and several different preparations of C3S protein reacted with bimane in follow-up experiments (data not shown). We became convinced that one must remove all cysteines to completely abrogate bimane labeling. Next we continued sequential mutation of the 5 remaining cysteine residues but as each new mutation was constructed the protein became very difficult to express and formed insoluble inclusion bodies.

According to personal communication, a cysteine to alanine replacement is much less disruptive to overall protein folding compared to replacement with a serine. In light of this observation, we attempted to make soluble CtBP1-cysteine free mutant protein by

mutating all 8 (Cysteine 237, Cysteine 350, Cysteine 38, Cysteine 54, Cysteine 118, Cysteine 312, and Cysteine 232 sequentially) cysteine residues to alanine residues (C8A construct) and express and purify this protein two different *E. coli* protein expression cells (BL21 and ArcticExpress). We successfully expressed and purified a small amount of the C8A CtBP1 mutant protein, and showed that it was not labeled by bimane but retained binding to GST-E1A (Figure 5.4).

Discussion

The notion of inhibiting CtBP function has been bandied about pretty much since it was identified as a binding partner of E1A and as we gain a greater understanding of this multifaceted transcriptional regulator the idea gathers more and more steam. Whether inhibiting CtBPs with a small chemical inhibitor, an antibody, and peptide mimetic it is generally agreed upon that we need a more complete grasp of the "inhibit-able" functions of this protein. Our lab and others have identified dimerization as a jumping off point for modulating CtBP activity in cells or *in vivo*. The approach outlined in this chapter is built upon our observations that dimer formation is an essential component of CtBP biology, is regulated by NAD(H), and the fact that simply having a tool to monitor dimerization would have far reaching applications in CtBP basic research.

Should our small successes lead to a sensitive fluorescence assay for dimerization, one could apply it to 96-well plate format for screening small molecules. For initial screening one could evaluate compounds from the Open Chemical Repository of the Developmental Therapeutics Program (DTP) of the National Cancer Institute (dtp.nci.nih.gov) which includes a set of 57 compounds shown to have activity in human tumor cell lines but whose mechanism of action is not known. In addition there is a Natural Products set which consists of 235 compounds selected from an open repository of 140,000 compounds. One could use a more reason based approach and screen either libraries of dinucleotide mimetics or known inhibitors of dehydrogenase enzymes which could concentrate molecules likely to interact with CtBP proteins based upon structural similarities. Using a 96-cell plate set up with a fluorescence plate reader, one could screen by monitoring fluorescence signal of a low concentration of labeled protein in

each well, and evaluation of inhibition of NAD(H) induced dimerization. This would read-out as a loss of Bimane quenching in the presence of an inhibitor.

The identification of a chemical inhibitor of CtBP could have clinical applications but would assuredly provide a valuable tool for trying to understand the complex biological functions of this important family of proteins.

Tables and figures

Figure 5.1 – Adapted from J. Lundblad 2006; CtBP1 protein structure, Tryptophan 318 and proximal residues

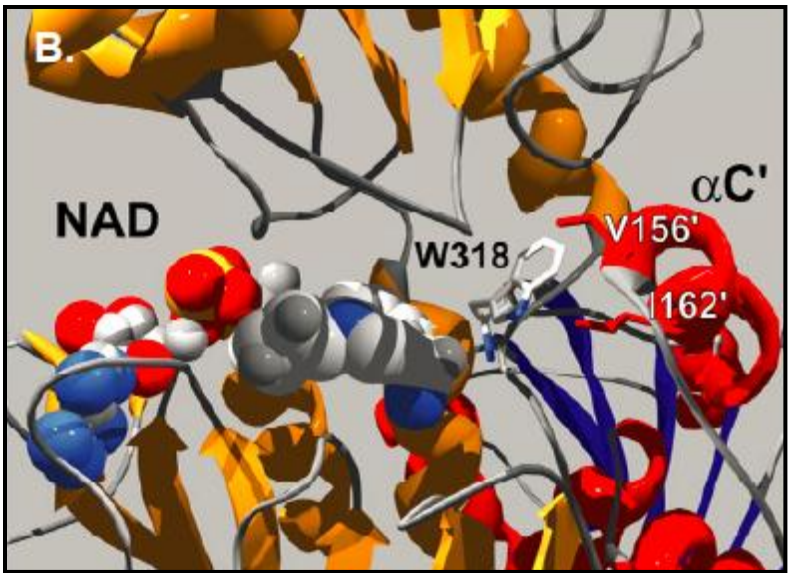

Figure 5.2 – Adapted from Mansoor SE, et al., *Biochemistry*. 2002; A. Monobromobimane structure and mode of binding and quenching affect; B. Quenching effect of proximal tryptophan

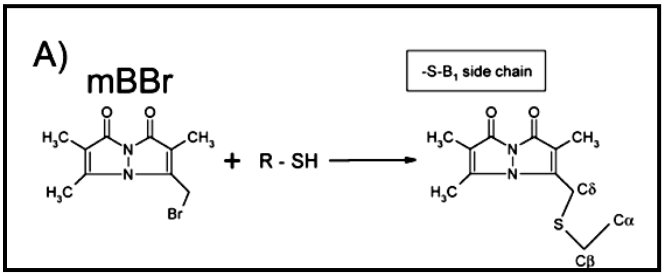

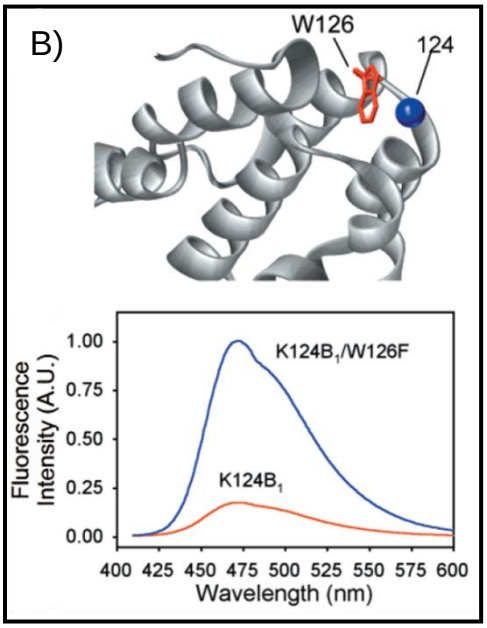

Figure 5.3 – CtBP1_C3S mutant protein analysis: A.(Top) SDS-PAGE gel of bimane labeled CtBP1 cysteine to serine mutants, and C8A purified protein, Bimane visualized on UV light box; (Bottom) Coomassie stained gel from above;

B GST-pulldown with CtBP1 wild type and C3S protein with GST-E1A and GST-E1A_DLAS

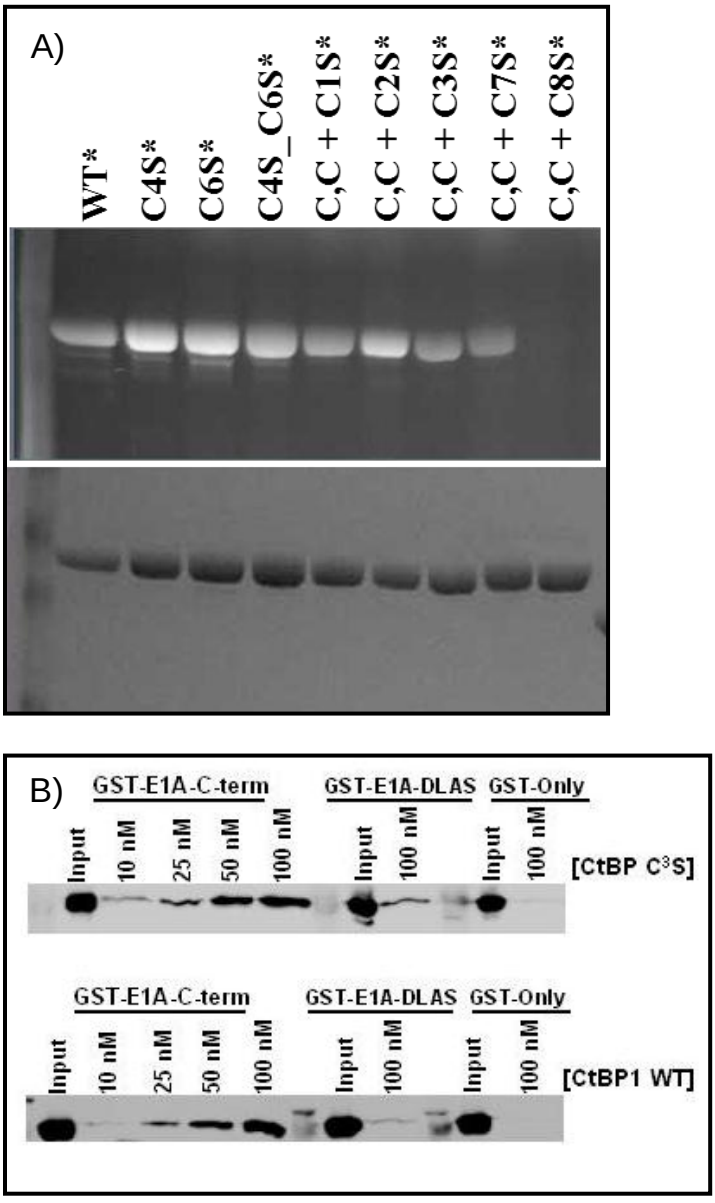

Figure 5.4 – CtBP1_C8A mutant protein analysis: A. SDS-PAGE gel of bimane labeled CtBP1 wild type, C3A, and C8A purified protein, SDS-PAGE gel with Bimane visualized on UV light box; B. GST-pulldown with C8A protein (100 uM) with GST-E1A and GST-E1A_DLAS

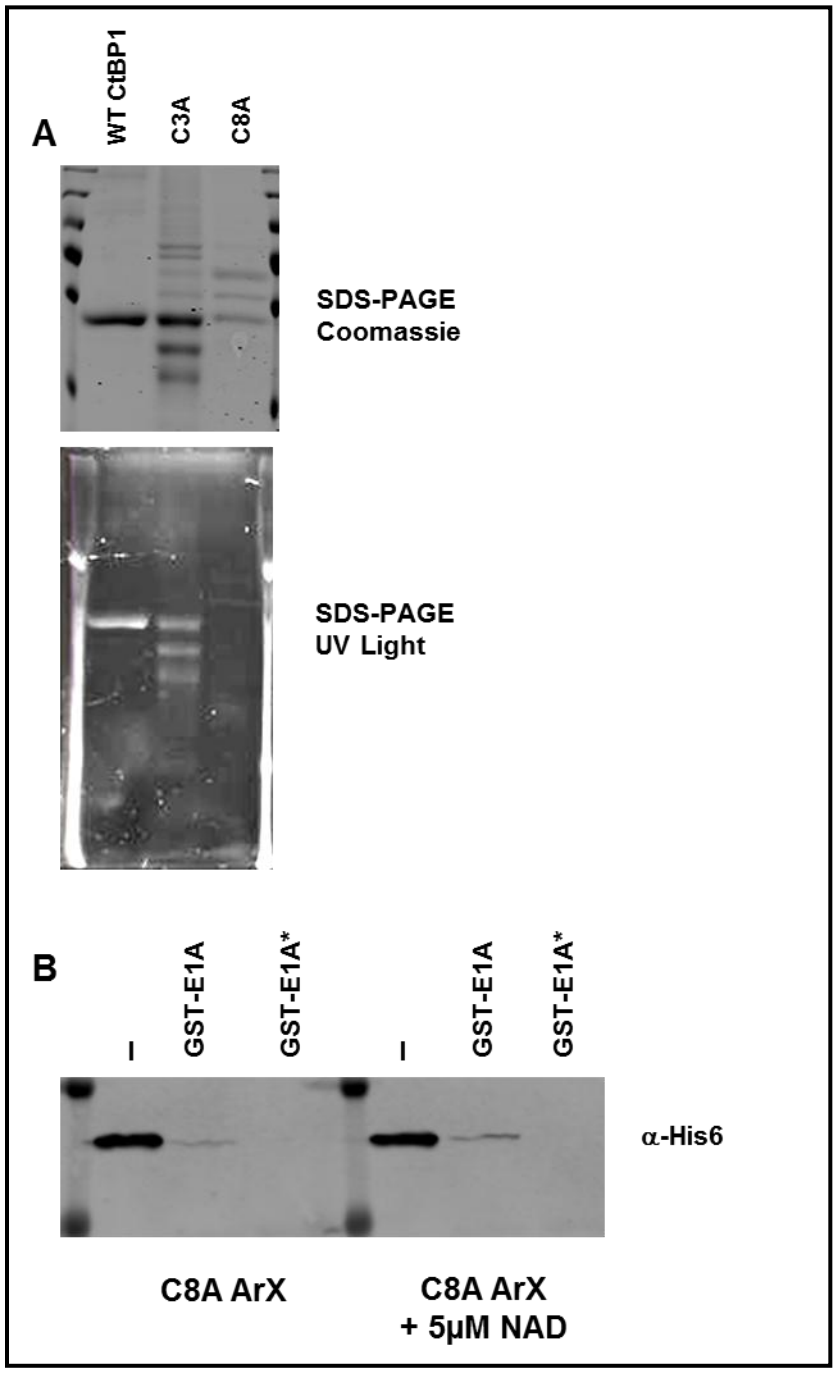

Chapter 6. Summary, Conclusions, and Future Directions

The work presented in this thesis examines the biochemical functions of Carboxyl-terminal Binding Proteins and the role these biochemical functions play in CtBP biology. In order to contribute to the understanding of this complex family of proteins, we focused primarily on the *Drosophila* CtBP form and examined it within a biologically relevant *in vivo* assay which did not utilize gross overexpression or abnormal fusion constructs. Instead we devised a way to express exogenous wild type and mutant forms at endogenous levels in the absence of endogenous CtBP expression. The fact that this worked at all, let alone in two distinct assays was quite remarkable. In addition to getting an assay like this to work, we were able to show that CtBP must retain the ability to bind dinucleotide co-factors to properly partake in short-range repression at the *eve* locus and the dehydrogenase domain is not essential for this activity. The possibility remains that mutations in the dehydrogenase domain cause less severe disruptions but in our assay that is difficult to say for sure. Unlike other CtBP labs, we used a variety of biochemical tools to show that the mutants we constructed form properly folded proteins and retain all wild type functions excepting that which was mutated away; all of which enhances the validity of our *in vivo* results.

Although other researchers recently examined the role that distinct *dCtBP* isoforms play in embryogenesis and *Drosophila* biology (39), we've also contributed to a new paradigm in which *dCtBP-eve* regulation may be more complex than previously thought and further dissecting the roles that distinct *dCtBP* isoforms play would be very interesting. Even though we cannot definitively say that *dCtBP(l)* is responsible for short-range repression involving the gap gene Krüppel and *dCtBP(s)* coordinates short-range

repression with Knirps, our data certainly suggests that as a possible explanation. Constructing a UAS-*dCtBP(l)* and repeating the GAL4-UAS experiments outlined in Chapter 3 would answer this question very nicely. One might find that in our assay UAS-*dCtBP(l)* transgene could rescue *eve* stripe 2 where UAS-*dCtBP(s)* did not. If this were the case, examination of the differences conferred by the C-terminal extension in *dCtBP(l)* would be very compelling and open the doors to several areas of research. Along this line of thinking, it would be very interesting to perform homology modeling and ab initio prediction with dCtBP(l) amino acid sequence and compare it to our model of the short form. Is the C-terminal extension structured as we've predicted in our model of the short form or unstructured like the vertebrate CtBPs? Another relatively straightforward and informative experiment would be to see if dCtBP(l) protein forms higher order oligomers in the presence of NAD(H) using a gel fractionation column as we did with dCtBP(s) as well as measuring self-assembly of the long form. Each of these experiments would help understand the role of the longer C-terminal portion of the dCtBP(l) molecule.

The work presented here also includes the beginning steps towards creating a screen for small molecule inhibitors of CtBP. This would be a very exciting and challenging experimental road, but one that would be very fruitful. With an inhibitor of CtBP one could begin to determine the effect of turning CtBP off in cancer cell lines which no longer make E-cadherin. Could one recapitulate complete CtBP1 and CtBP2 knockdown data performed by Dr. Dana Madison simply by disrupting CtBP dimers? Would blocking CtBP alter the DNA methylation pattern at the E-cadherin promoter or are there more complicated mechanisms at play. Could a CtBP inhibitor be an effective

treatment for leukemias which contain abnormal CtBP fusions? There are a myriad of basic and cancer biology questions one could begin to answer with a chemical inhibitor of CtBP and devising an assay to screen for one is a critical first step. Clearly a lot has to be done to get to a screen-able assay, and one huge obstacle to overcome in order to develop a dimerization based assay is efficient production of the CtBP1_C8A protein. Possible solutions to this could be optimization of the codon sequence for production in *E. coli* expression systems. Even with making modifications to the nucleic acid sequence, one could try to increase soluble expression using an inducible system in *E. coli* or a mammalian expression system, Clontech's Tet-on/off system. Efficient, robust, and reliable expression of the cys-less hCtBP1 is the next critical obstacle for construction of this important assay.

Literature Cited

1. **Schaeper U, Boyd JM, Verma S, Uhlmann E, Subramanian T, Chinnadurai G.** Molecular cloning and characterization of a cellular phosphoprotein that interacts with a conserved C-terminal domain of adenovirus E1A involved in negative modulation of oncogenic transformation. *Proc Natl Acad Sci* 1995; 92(23):10467-71.
2. **Thiery JP.** Epithelial-mesenchymal transitions in tumour progression. *Nat Rev Cancer* 2002; 2(6):442-54.
3. **Potter E, Bergwitz C, Brabant G.** The cadherin-catenin system: implications for growth and differentiation of endocrine tissues. *Endocr Rev* 1999; 20(2):207-39.
4. **Furosawa T, Moribe H, Kondoh H, Higashi Y.** Identification of CtBP1 and CtBP2 as corepressors of zinc finger-homeodomain factor deltaEF1. *Mol Cell Biol* 1999; 19(12):8581-90.
5. **Chinnadurai G.** CtBP family proteins: more than transcriptional corepressors. *Bioessays* 2003; 25(1):9-12.
6. **Chinnadurai G.** CtBP, an unconventional transcriptional corepressor in development and oncogenesis. *Mol Cell* 2002; 9(2):213-24.
7. **Spano S, Silletta MG, Colanzi A, Alberti S, Fiucci G, Valente C, Fusella A, Salmona M, Mironov A, Luini A, Corda D.** Molecular cloning and functional characterization of brefeldin A-ADP-ribosylated substrate. A novel protein involved in the maintenance of the Golgi structure. *J Biol Chem* 1999; 274(25):17705-10.

8. **Schmitz F, Konigstorfer A, Sudhof TC.** RIBEYE, a component of synaptic ribbons: a protein's journey through evolution provides insight into synaptic ribbon function. *Neuron* 2000; 28(3):857-72.
9. **Hildebrand JD, Soriano P.** Overlapping and unique roles for C-terminal binding protein 1 (CtBP1) and CtBP2 during mouse development. *Mol Cell Biol* 2002; 22(15):5296-307.
10. **Shi Y, Sawada J, Sui G, Affar el B, Whetstine JR, Lan F, Ogawa H, Luke MP, Nakatani Y, Shi Y.** Coordinated histone modifications mediated by a CtBP co-repressor complex. *Nature* 2003; 422(6933):735-8.
11. **Thio SS, Bonventre JV, Hsu SI.** The CtBP2 co-repressor is regulated by NADH-dependent dimerization and possesses a novel N-terminal repression domain. *Nucleic Acids Res* 2004; 32(5):1836-47.
12. **Verger A, Quinlan KG, Crofts LA, Spano S, Corda D, Kable EP, Braet F, Crossley M.** Mechanisms directing the nuclear localization of the CtBP family proteins. *Mol Cell Biol* 2006; 26(13):4882-94.
13. **Lin X, Sun B, Liang M, Liang YY, Gast A, Hildebrand J, Brunicardi FC, Melchior F, Feng XH.** Opposed regulation of corepressor CtBP by SUMOylation and PDZ binding. *Mol Cell* 2003; 11(5):1389-96.
14. **Barnes CJ, Vadlamudi RK, Mishra SK, Jacobson RH, Li F, Kumar R.** Functional inactivation of a transcriptional corepressor by a signaling kinase. *Nat Struct Biol* 2003; 10(8):622-8.

15. **Zhao LJ, Subramanian T, Zhou Y, Chinnadurai G.** Acetylation by p300 regulates nuclear localization and function of the transcriptional corepressor CtBP2. *J Biol Chem* 2006; 281(7):4183-9.
16. **Riefler GM, Firestein BL.** Binding of neuronal nitric-oxide synthase (nNOS) to carboxyl-terminal-binding protein (CtBP) changes the localization of CtBP from the nucleus to the cytosol: a novel function for targeting by the PDZ domain of nNOS. *J Biol Chem* 2001; 276(51):48262-8.
17. **Koipally J, Georgopoulos K.** Ikaros interactions with CtBP reveal a repression mechanism that is independent of histone deacetylase activity. *J Biol Chem* 2000; 275(26):19594-602.
18. **Koipally J, Georgopoulos K.** Ikaros-CtIP interactions do not require C-terminal binding protein and participate in a deacetylase-independent mode of repression. *J Biol Chem* 2002; 277(26):23143-9.
19. **Chinnadurai G.** CtBP Family Proteins. Landes Bioscience. Georgetown Texas. 2007.
20. **Srinivasan L, Atchison ML.** YY1 DNA and PcG recruitment require CtBP. *Genes and Development* 2004; 18(21):2506-2601.
21. **Atchison L, Ghias A, Wilkinson F et al.** Transcription factor YY1 functions as a PcG protein in vivo. *Embo J* 2003; 22(6):1347-1358.
22. **Dioum EM, Rutter J, Tuckerman JR et al.** NPAS2: A gas-responsive transcription factor. *Science* 2002; 298:2385-2387.
23. **Rutter J, Reick M, Wu LC et al.** Regulation of Clock and NPAS2 DNA binding by the redox state of NAD cofactors. *Science* 2001; 293:510-514.

24. **Ame JC, Spenlehaur C, de Murcia G.** The PARP superfamily. *Bioessays* 2004; 26:882-893.

25. **Denu JM.** Linking chromatin function with metabolic network: Sir2 family of NAD(+)-dependent deacetylases. *Trends Biochem Sci.* 2003; 28:41-48.

26. **Zhang Q, Piston DW, Goodman RH.** Regulation of corepressor function by nuclear NADH. *Science* 2002; 295(5561):1895-7.

27. **Kumar V, Carlson JE, Ohgi KA, Edwards TA, Rose DW, Escalante CR, Rosenfeld MG, and Aggarwal AK**. Transcription corepressor CtBP is an NAD(+)-regulated dehydrogenase. *Mol Cell* 2002; 10:857-869.

28. **Balasubramanian, PL, Zhao J, Chinnadurai G**. Nicotinamide adenine dinucleotide stimulates oligomerization, interaction with adenovirus E1A and an intrinsic dehydrogenase activity of CtBP. *FEBS Lett* 2003; 537:157-160.

29. **Thio SS, Bonventre JV, Hsu SI.** The CtBP2 co-repressor is regulated by NADH dependent dimerization and possesses a novel N-terminal repression domain. *Nucleic Acids Res* 2004; 32:1836-1847.

30. **Nardini M, Spano S, Cericola C, Pesce A, Massaro A, Millo E, Luini A, Corda D, Bolognesi M**. CtBP/BARS: a dual-function protein involved in transcription co-repression and Golgi membrane fission. *EMBO J*. 2003; 22:3122-3130.

31. **Sutrias-Grau M, Arnosti DN**. CtBP contributes quantitatively to Knirps repression activity in an NAD binding-dependent manner. *Mol. Cell Biol*. 2004; 24:5953-5966.

32. **Nardini M, Valente C, Ricagno S, Luini A, Corda D, Bolognesi M**. CtBP1/BARS Gly172-->Glu mutant structure: impairing NAD(H)-binding and dimerization. *Biochem Biophys Res Commun.* 2009 Mar 27;381(1):70-4.

33. **Li S, Chen PL, Subramanian T, Chinnadurai G, Tomlinson G, Osborne CK, Sharp ZD, Lee WH**. Binding of CtIP to the BRCT repeats of BRCA1 involved in the transcription regulation of p21 is disrupted upon DNA damage. *J. Biol. Chem.* 1999 274:11334-11338.

34. **Nibu Y, Zhang H, Levine M**. Interaction of short-range repressors with Drosophila CtBP in the embryo. *Science* 1998; 280:101-104.

35. **Poortinga G, Watanabe M, Parkhurst SM**. Drosophila CtBP: a Hairy-interacting protein required for embryonic segmentation and hairy-mediated transcriptional repression. *EMBO J* 1998; 17:2067-2078.

36. **Drysdale RA, Crosby MA, Gelbert W et al.** Flybase: Genes and gene models. *Nucleic Acid Res* 2005; 33(Database issue); D390-395.

37. **Hamada F, Bienz M**. The APC tumor suppressor binds to C-terminal binding protein to divert nuclear beta-catenin from TCF. *Dev. Cell* 2004; 7:677-685.

38. **Mani-Telang P, Arnosti DN.** Developmental expression and phylogenetic conservation of alternatively spliced forms of the C-terminal binding protein corepressor. *Dev Genes Evol* 2007; 217(2):127-35.

39. **Zhang Y, Arnosti DN.** Conserved Catalytic and C-terminal regulatory domains of the C-Terminal Binding Protein Corepressor fine-tune the transcriptional response in Development. *Mol. Cell. Biol. 2011*; 31: 375-384.

40. **Weigmann K, Klapper R, Strasser T, Rickert C, Technau G, Jäckle J, Janning W, Klämbt**. FlyMove – a new way to look at development of *Drosophila.Trends Genet* 2003; 19, 310.

41. **Gray S, Levine M**. Transcriptional repression in development. *Curr Opin Cell Biol* 1996; 8(3):358-364.

42. **Fujioka M, Emi-Sarker y, Yusibova GL et al.** Analysis of an even-skipped rescue transgene reveals both composite and discrete neuronal and blastoderm enhancers, and multi-stripe positioning by gap gene repressor gradients. *Development* 1999; 126(11):2527-2538.

43. **Nibu Y, Zhang H, Bajor E, Barolo S, Small S, Levine M**. dCtBP mediates transcriptional repression by Knirps, Kruppel and Snail in the Drosophila embryo. *EMBO J*. 1998; 17(23):7009-7020.

44. **Frisch SM, Screaton RA.** Anoikis mechanisms. *Curr Opin Cell Biol* 2001; 13(5):555-562.

45. **Frisch SM, Mymryk JS.** Adenovirus-5 E1A: Paradox and Paradigm. *Nat Rev Mol Cell Biol* 2002; 3(6):441-452.

46. **Grooteclaes ML, Frisch SM.** Evidence for a function of CtBP in epithelial gene regulation and anoikis. *Oncogene* 2000; 19:3823-3828.

47. **Grooteclaes ML, Deveraux Q, Hildebrand J, Zhang Q, Goodman RH, and Frisch SM**. C-terminal-binding protein corepresses epithelial and proapoptotic gene expression programs. *Proc. Natl. Acad. Sci. USA* 2003; 100(8):4568-4573.

48. **Ferreira R, Ohneda K, Yamamoto M et al.** GATA1 function, a paradigm for transcription factors in hematopoiesis. *Mol Cell Biol* 2005; 25(4):1215-1227.

49. **Turner J, Crossley M.** Cloning and characterization of mCtBP2, a co-repressor that associates with basic Kruppel-like factor and other mammalian transcriptional regulators. *EMBO J.* 1998; 17(17):5129-5140.

50. **Katz SG, Cantor AB, Orkin SH.** Interaction between FOG-1 and the corepressor C-terminal binding protein is dispensable for normal erythropoiesis in vivo. *Mol Cell Biol* 2002; 22(9):3121-3128.

51. **Deconink AE, Mead PE, Tevosian SG et al.** FOG acts as a repressor of blood cell development in Xenopus. *Development* 2000; 127(10):2031-2040.

52. **Turner J, Nicholas H, Bishop D et al.** The LIM protein FHL3 binds to basic Krüppel-like factor/Krüppel-like factor 3 and its corepressor C-terminal binding protein 2. *J Biol Chem* 2003; 278(15):12786-12795.

53. **Georgopoulos K, Bigsby M, Wang JH, et al.** The Ikaros gene is required for the development of all lymphoid lineages. *Cell* 1994; 79(1):143-156.

54. **Izutsu K, Kurokawa M et al.** The corepressor CtBP interacts with Evi-1 to repress transforming growth factor beta signaling. *Blood* 2001; 97(9):2815-2822.

55. **Palmer S, Brouillet JP, Kilbey A et al.** Evi-1 transforming and repressive activities are mediated by CtBP corepressor proteins. *J Biol Chem* 2001; 276(28):25834-25840.

56. **Mitani K.** Molecular mechanisms of leukemogenesis by AML/EVI-1. *Oncogene* 2004; 23(24):4263-4269.

57. **Chan EM, Comer EM, Brown FC et al.** AML1-FOG2 fusion protein in myelodysplasia. *Blood* 2005; 105(11):4523-4526.

58. **Dukers DF, van Galen JC, Giroth C et al.** Unique polycomb gene expression pattern in Hodgkin's Lymphoma-derived cell lines. *Am J Pathol* 2004; 164(3):873-881.

59. **Alpatov R, Munguba GC, Caton P et al.** Nuclear speckle-associated protein Pnn/DRS binds to the transcriptional corepressor CtBP and relieves CtBP-mediated repression of the E-cadherin gene. *Mol Cell Biol* 2004; 24(23):10223-10235.

60. **Hamada F, Bienz M.** The APC tumor suppressor binds to C-terminal binding protein to divert nuclear beta-catenin from TCF. *Dev Cell* 2004; 7:677-685.

61. **Bellamacina, CR.** The nicotinamide dinucleotide binding motif: a comparison of nucleotide binding proteins. *FASEB J*. 1996; 10(11):1257-69.

62. **Berger F, Ramirez-Hernandez MH, Ziegler M.** The new life of a centenarian: signaling functions of NAD(P). *Trends Biochem. Sci.* 2004; 29(3):111-8.

63. **Schuller, DJ, Grant GA, Banaszak LJ.** The allosteric ligand site in the Vmax-type cooperative enzyme phosphoglycerate dehydrogenase. *Nat. Struct. Biol*. 1995; 2(1):69-76.

64. **Zheng L, Baumann U, Reymond JL.** An efficient one-step site-directed and site-saturation mutagenesis protocol. *Nucl. Acids Res*. 2004 32:115.

65. *Guide to Equilibrium Dialysis*. 2009. **Harvard Apparatus;** 84 October Hill Road, Holliston, Massachusetts 01746, USA

66. **Fu X, Masayori I, Shinde U**. Folding pathway mediated by an intramolecular chaperone. The inhibitory and chaperone functions of the subtilisin propeptide are

not obligatorily linked. *The Journal of Biological Chemistry*. 2000; 275:22:16871-16878.

67. **Kim DE, Chivian D, Baker D**. Protein structure prediction and analysis using the Robetta server. *Nucleic Acids Res*. 2009 32 Suppl 2:W526-31 (WEB SERVER ISSUE)
68. **Kuppuswamy M, et al.** Role of the PLDLS-binding cleft region of CtBP1 in recruitment of core and auxiliary components of the corepressor complex. *Mol. Cell. Biol.* 2008; 28:269–281.
69. **Nibu Y, Zhang H, Bajor E, Barolo S, Small S, Levine M.** dCtBP mediates transcriptional repression by Knirps, Krüppel and Snail in the Drosophila embryo. *EMBO J.* 1998; 17(23):7009-20.
70. **Maniatis T, Fritsch EF, Sambrock J.** 1982. Molecular Cloning. A Laboratory Manual. 488. Cold Spring Harbor Laboratory. USA: 86-96.
71. **Spradling AC.** P element-mediated transformation. In Drosophila*: A Practical Approach,* (ed. D. B. Roberts) pp. 175-197, Oxford, England: IRL Press. 1986.
72. **Lécuyer E, Parthasarathy N, Krause HM.** Fluorescent *In Situ* Hybridization Protocols in *Drosophila* Embryos and Tissues**.** *Methods in Molecular Biology:* Drosophila: *Methods and Protocols* Edited by: C. Dahmann © Humana Press Inc., Totowa, NJ
73. **Tyramide Signal Amplification Kits** – Product Manual; Molecular Probes May 18, 2010.
74. **Mansoor SE, McHaourab HS, and Farrens DL**. Determination of protein secondary structure and solvent accessibility using site-directed fluorescence

labeling. Studies of T4 lysozyme using the fluorescent probe monobromobimane. *Biochemistry* 1999; 38:16383-16393.

75. **Mansoor SE, McHaourab HS, Farrens DL**. Mapping proximity within proteins using fluorescence spectroscopy. A study of T4 lysozyme showing that tryptophan residues quench bimane fluorescence. *Biochemistry* 2002; 41:2475-2484.
76. **Gill SC, von Hippel PH**. Calculation of protein extinction coefficients from amino acid sequence data. *Analytical Biochemistry* 1989; 182:319-326.